Further Development and Evaluation of Remote Sensing Products for Characterization and Monitoring of Features in Landscapes

Dissertation

der Mathematisch-Naturwissenschaftlichen Fakultät

der Eberhard Karls Universität Tübingen

zur Erlangung des Grades eines

Doktors der Naturwissenschaften

(Dr. rer. nat.)

vorgelegt von

Sebastian Goihl

aus Dissen am Teutoburger Wald

Tübingen

2025

Gedruckt mit Genehmigung der Mathematisch-Naturwissenschaftlichen Fakultät der Eberhard Karls Universität Tübingen.

Tag der mündlichen Qualifikation:	14.10.2025
Dekan:	Prof. Dr. Thilo Stehle
1. Berichterstatter/-in:	Prof. Dr. Peter Dietrich
2. Berichterstatter/-in:	Prof. Dr. Volker Hochschild

Contents

List of Figures

List of Tables

List of publications

Manuscript 1 **Goihl, S.** (2023a). Mapping overwintering grain stubbles using machine-learning methods and image compositions for CAP-control and Water Framework Directive connected activities. *Journal of Applied Remote Sensing.* Vol. 17 (1). https://doi.org/10.1117/1.JRS.17.014515.

Manuscript 2 **Goihl, S.** (2023b). Determining the usefulness of the Copernicus High-Resolution Vegetation Phenology and Productivity Product (HR-VPP) with official agricultural data on cropland in case of the 2018 drought in the Federal State of Saxony, Germany. *Journal of Water and Climate Change* 14 (11). https://doi.org/10.2166/wcc.2023.501.

Manuscript 3 **Goihl, S.** (2025). Tillage direction analysis in agricultural fields from Digital Orthophotos and Sentinel-2 imagery. *Remote Sensing Applications: Society and Environment*. https://doi.org/10.1016/j.rsase.2025.101486.

Abstract

The European Space Agency's (ESA) Copernicus program has also provided free access to satellite remote sensing data, making it an attractive option for public institutions. Government institutions are currently evaluating and identifying use cases for satellite imagery. Agricultural administration stands to benefit particularly, with the potential uses being substantial, especially in this area. This is primarily driven by two factors: (1) legal requirements within the framework of the Common Agricultural Policy (CAP), and (2) the substantial proportion of agricultural land within the total land cover in a mid-european study area. In the domain of agriculture and environmental discourse, there are a variety of applications for agricultural remote sensing in the context of providing a data base for decision makers within the agricultural administration.

This thesis examines three different use cases of agricultural remote sensing from the perspective of public administration. The requirement for accuracy of the data products for administrative use is explicitly addressed. The use cases, which include "overwintering stubble" as an independent land cover class, the reanalysis of the agricultural drought in Saxony in 2018, and the determination of the direction of cultivation of agricultural land, offer insight into the versatility of agricultural administration.

The administration's activities are connected with the careful handling of the created geodata products, depending on the data requirements and the uncertainties inherent in the products as a result of the creation process. Government institutions have high accuracy requirements for the products they use to make decisions. In this regard, this thesis examines the factors that influence the informative value of agricultural remote sensing products and proposes possible solutions based on the case studies. This was followed by the general handling of product uncertainties and the possibilities of communicating these in a targeted manner.

The objective of this thesis was to assess the potential and limitations of applications by remote sensing data from the point of view of the agricultural administration, based on the three publications that have been published.

Zusammenfassung

Dank des Copernicus-Programms der Europäischen Weltraumagentur (ESA) wurde die Nutzung von Daten der Satellitenbildfernerkundung, auf Grund der kostenfreien Datenverfügbarkeit, auch für öffentliche Einrichtungen zu einer attraktiven Option der Datengewinnung. Die staatlichen Einrichtungen sind seither bestrebt, Anwendungsfälle zu identifizieren und die Nutzbarkeit der Satellitenbilddaten zu evaluieren. Gerade im Bereich der landwirtschaftlichen Verwaltung ergeben sich vielfältige Nutzungsmöglichkeiten. Diese Entwicklung wird einerseits durch rechtliche Vorgaben im Bereich Gemeinsamer Agrarpolitik (GAP) begünstigt, andererseits sind landwirtschaftlicher Flächen durch ihren hohen Flächenanteil an der Gesamtfläche als attraktives Untersuchungsobjekt prädestiniert. Insbesondere im Spannungsfeld Landwirtschaft und Umwelt ergeben sich eine Vielzahl von Anwendungsfällen für die landwirtschaftliche Fernerkundung im Kontext als Datengrundlage für Entscheidungsträger innerhalb der landwirtschaftlichen Fachverwaltung.

Diese Arbeit untersucht drei verschiedene Anwendungsfälle der landwirtschaftlichen Fernerkundung aus der Sichtweise der öffentlichen Verwaltung. Hierbei wurden explizit die Anforderungen an die Genauigkeit der Datenprodukte für den Einsatz durch die Verwaltung adressiert. Die Anwendungsfälle der „überwinternden Stoppeln" im Monitoring als eigenständige Landbedeckungsklasse, der Reanalyse der landwirtschaftlichen Dürre im Jahr 2018 in Sachsen und der Feststellung der Bewirtschaftungsrichtung landwirtschaftlicher Flächen geben einen Einblick in die Vielseitigkeit der Anwendungsfälle in der landwirtschaftlichen Verwaltung.

Mit dem Verwaltungshandeln verknüpft ist ein achtsamer Umgang mit den erstellten Geodatenprodukten (im Hinblick auf den jeweiligen Datenbedarf) sowie die Unsicherheiten, die den Produkten aufgrund ihres Erstellungsprozesses immanent sind. Staatliche Einrichtungen haben hohe Genauigkeitsansprüche an die Produkte, welche diese zur Entscheidungsfindung nutzen. Aus diesem Grund wurden innerhalb dieser Arbeit einerseits die Einflussfaktoren auf die Aussagekraft der landwirtschaftlichen Fernerkundungsprodukte diskutiert und anhand der Fallbeispiele Lösungsmöglichkeiten vorgeschlagen. Zusätzlich wurde der Umgang mit Produktunsicherheiten, sowie die Möglichkeiten einer zielgerichteten Kommunikation dieser Risiken, erörtert. Das Ziel dieser Arbeit bestand darin, die Möglichkeiten und Grenzen der landwirtschaftlichen Fernerkundung aus Sichtweise der Verwaltung anhand der drei veröffentlichen Publikationen zu evaluieren.

1 Introduction

1.1 Definitions and scope of the work

Remote sensing facilitates the quantitative and qualitative investigation and monitoring of a wide variety of land use and land cover types on the earth's surface (Lillesand et al., 2015). It is therefore necessary to narrow down the scope of this thesis, entitled: "Further development and evaluation of remote sensing products for characterization and monitoring of features in landscapes".

The focus of this thesis will be the development and application of remote sensing data from the perspective of public authorities for the agricultural sector. The communication and evaluation of data uncertainties of these products from the perspective of the public data user is also linked to this. The present dissertation is built upon the findings of three publications concerning agricultural remote sensing. These publications explicitly address the level and task performance of the agricultural state administration of the federal state of Saxony, administered by the State Office for Environment, Agriculture and Geology (LfULG). It is important to note that the present study is limited to a specific regional context, and thus, it cannot draw definitive conclusions about the interplay between administration and agriculture in other geographical areas. The remote sensing data utilized in this study comprise aerial photographs (DOP) and Sentinel-2 images from the Copernicus program. Nevertheless, it is acknowledged that the findings of the publications can be extrapolated to other regions. The administration generally deals with other land cover classes and their characteristics than agriculture. This is accompanied by specialist fields for which the administration has to fulfil legal tasks and for which remote sensing can in principle be used as a data source. The specialist field of soil, water and nature conservation serve as examples of this. This paper presents a selection of these subject areas, with the aim of delineating the fundamental initial problem. Features in landscape are to be understood as spatially clearly definable objects. These can include forest areas, bodies of standing water or, in the context of this work, agricultural areas at field level, or their regional aggregations.

1.2 Current situation of stakeholders in agricultural remote sensing

The monitoring of agricultural areas using remote sensing data and methods is of great interest to a wide variety of stakeholder groups. Remote sensing must serve group-

specific information needs. According to Jewiss et al. (2020), the information requirement is structured spatially hierarchically. The hierarchy of information needs differs according to specific stakeholder groups, beginning at the field level with farmers and extending to governments and state institutions at various regional and agro-structural levels (Jones et al. 2016). Depending on the specific state tasks, the interest of state institutions sometimes also extends to the field level, for example in Europe. The "Area Monitoring System" through remote sensing (European Union 2021a) as part of the Integrated Administration and Control System (IACS) with mandatory monitoring of the individual field (Navarro et al. 2021, Triebnig et al. 2024) by state actors is applicable to all EU states.

According to Jewiss et al. (2020), the various interest groups can be divided into farmers, the state, non-governmental organizations (NGOs), science and the private sector. Farmers have a natural interest in having as much knowledge as possible about their fields. While the state utilizes remote sensing data, in particular, to implement legal requirements, the private sector also demonstrates interest in such data, including agricultural consultants, insurance companies, and global agricultural traders (Jewiss et al. 2020). However, in addition to product utilization, companies are also able to provide precision farming services for sale, based on their own calculations, for example as application maps for farmers (Bach & Mauser 2018).

In contrast to the groups mentioned above, the primary goal of science and research is not the operational use of remote sensing data, but rather the acquisition of knowledge and methodological development. Science is both a data consumer and a data producer. The spatial-hierarchical classification according to Jewiss et al. (2020) can therefore only be regarded as an orientation, as there are fluid transitions between the interest groups and their needs. This thesis deals in particular with the relationship between the state and agricultural land via remote sensing. The farmer as a person directly affected by government measures and decisions cannot be excluded from the analysis. The stakeholder groups NGOs, science and business are not considered in detail below.

Satellite images are frequently utilized in the agricultural sector as a source data product for precision farming applications (Khanal et al. 2020, Ferguson & Rundquist 2018, Bach & Mauser 2018). The application of precision farming products, usually delivered via application maps, is associated with economic (Griffin et al. 2018) and environmental benefits (Joy et al. 2018). These maps are used for the targeted

application of seeds, fertilizers and pesticides (Bach & Mauser 2018). Furthermore, satellite data has been shown to provide additional information, including yield estimates (Stumpe et al. 2024, Hara et al. 2021, Khlif et al. 2023, Probst et al. 2018, Zhao et al. 2020, Ali et al. 2022) or to contribute to water management (Probst et al. 2018). As Khanal et al. (2020) showed, remote sensing can, in principle, be used holistically with different applications from pre-season planning to harvesting.

The products offered by remote sensing should enable the farmer to save on operating resources or to achieve greater efficiency on the available land. The products serve as decision support and primarily generate economic costs (information costs, data processing costs, management adaptation costs, learning costs) (Sonntag et al. 2022, Guetschow & Fuchs 2024). Due to increasing mechanization and digitalization, farmers are already using opportunities to independently create and evaluate remote sensing images using unmanned aerial vehicle (UAV) systems and integrate them into operational processes (Bitkom Research 2024).

In addition to the farmers themselves, the administration has a significant interest in the use of remote sensing data, e.g. to check agricultural land for compliance with subsidy guidelines (Sarvia et al. 2022, Villanueva et al. 2024, van der Velden et al. 2024, Schulz et al. 2021). In Europe, this is primarily due to the Common Agricultural Policy (CAP) (European Union 2021a). European farmers receive fixed area payments from the EU for the cultivation of their land. In addition, national subsidies supplement the range of possible support measures. In Germany, these national measures are implemented by the federal states and can therefore be specifically adapted to regional conditions.

The EU member states are responsible for implementing funding and sanctioning any violations. To this end, the EU has mandated member states to adopt remote sensing data as the method of field control (European Union 2021a). Satellite image-based determination of the cultivated crop type (Navarro et al. 2021, Luzano-Tello et al. 2021) can be used to check the application data by comparing it with the areas applied for by the farmer. As both a large number of areas and large sums of money are linked to this procedure, the requirements for the reliability of the results are high. Agricultural funding constitutes a substantial portion of the annual EU budget. In 2023, the CAP in the EU budget amounted to approximately €57.5 billion (European Commission 2025). Germany accounted for about €6.9 billion of this in 2023 (BMEL 2024). In 2024,

Saxony, a federal state within the EU, allocated around €205 million in direct payments to farmers (SMUL 2024).

The utilization of remote sensing data has the potential to yield benefits for both farmers and the state. In contrast to the past approach of conducting inspections on a limited subset of agricultural land, the state now has the capability to conduct comprehensive assessments. In an ideal system, the digitalization of control processes would significantly reduce the bureaucratic burden on farmers, as on-site inspections would be substantially reduced.

The CAP (European Union 2021b) also establishes a connection between farmers' compliance with the so-called "conditionalities" and their participation in the CAP. These conditions ensure good agricultural and environmental conditions (GAEC), which are fundamental prerequisites for eligibility for agricultural subsidies. The verification of land cover classes in extensive areas, such as the ban on plowing up grassland (GAEC 8) (Mardian et al. 2021), continuous land cover (GAEC 6) (Goihl 2023a, Gao et al. 2020, Schulz 2021), and the ban on burning stubble fields (GAEC 3) (Chawala & Sandhu 2020), can be achieved through remote sensing.

Administrative decisions can have a direct impact on farmers, as illustrated by the scenario in which remote sensing data results in the nonpayment of CAP-payments. In this domain of conflict, the necessity for high-quality data is crucial. Conversely, farmers' reactions to the threat of sanctions can vary significantly, depending on the initial situation. Significant protests are to be anticipated if an arable crop specified in the application is erroneously classified by remote sensing, thereby obstructing the payment. Conversely, if the misclassification occurs for a crop declared in the application that is not actually grown in the field, there are unlikely to be any protests from farmers.

In addition to the stringent requirements for reviewing application data, the administration has expressed interest in other monitoring tasks beyond the scope of the CAP. The utilization of remote sensing data can facilitate the establishment of a comprehensive database, which is instrumental in a variety of tasks within the agricultural administration, e.g. for the testing and evaluation of new cultivation methods, as a data basis for agricultural water protection (e.g. degree of soil cover throughout the year, type of soil cover) or for yield estimation. Furthermore, remote sensing data can be utilized to prepare or evaluate own support measures. Given the limited attention this subject area receives outside the CAP, this work will focus on it.

2 Remote sensing data in administration: Balancing usability and practical application

2.1 Challenges for agricultural remote sensing

The primary challenges associated with agricultural remote sensing include the traditional shortcomings of remote sensing systems (e.g. cloud cover, spatial resolution), which are common to all remote sensing applications in all disciplines. Phenological and site-specific effects, caused by weather conditions, arable farming measures, and the influence of pathogens, introduce significant uncertainties into the recording of agricultural areas. Additionally, regulatory constraints exist, as the administration is legally obligated to adhere to stringent data collection criteria. Table 1 offers a comprehensive overview of the factors influencing agricultural remote sensing, as seen from the perspective of the administration.

The phenological development of an arable crop at a specific location is ultimately influenced by weather conditions, soil characteristics, and management decisions made by the farmer. The substantial number of input variables gives rise to considerable variation in crop types across the year under consideration and in comparison with different years. However, the unique characteristics of each land cover class, influenced by the specific vegetation period within a region, can lead to ambiguous class delineations and uncertain boundaries with other classes. This can, in turn, result in misclassifications. To mitigate these challenges, various methodologies have been proposed to reduce these pixel-based disturbance variables, also referred to as noise, including approaches by Nyborg et al. (2022) and Zeng et al. (2020).

As demonstrated in Table 1, a multitude of factors exert influence on the domain of agricultural remote sensing. Temporary and field-related local uncertainty factors (No. 8-31, 35-41) can be determined using the time series analysis or the total area. However, if these uncertainties exist for a specific area at a precisely determinable point in time and if, for example, payouts are linked to this for the farmer, then these uncertainty factors take on immense significance for the individual case. However, for classification or monitoring purposes, the absence of retrospective, suitable, cost-effective data for validation poses a significant challenge.

The in-situ data situation in agricultural remote sensing is very limited in terms of mapping the aforementioned uncertainty factors (No. 8-31, 35-41). It is virtually

impossible to verify the results of a calculation for these uncertainty factors if area-wide monitoring is to be carried out. Given the multitude of influencing factors (Table 1), a favorable in-situ data situation can be reasonably anticipated if the field boundaries, crop type, and cultivation period are known.

As illustrated in Table 1, the presence of uncertainty factors contributes to the imprecision observed in the classification and monitoring outcomes of remote sensing. Uncertainty sources were the data, the user and the process (Chow & Kar 2017). This complicates the comparison of results at this spatial level. This prompts questions regarding the general benefits and practical applications of remote sensing approaches in general. Conversely, regional approaches exhibit enhanced resilience due to the effects of smoothing. Nevertheless, established methodologies exist for the exclusion of remote sensing uncertainties, including cloud and cloud shadow masking, snow masking, and atmospheric correction. For other uncertainties, it is rational to incorporate supplementary data in the calculation, such as soil maps or climatic information. However, the information content of such products for the direct stroke level must be critically examined due to different initial spatial resolutions. Field-level considerations are characterized by a greater degree of uncertainty compared to regional considerations, where error factors tend to be mitigated by the number of study areas and classes examined (Venter et al. 2022).

Administrative limitations also include legal requirements and regulations that arise from a context other than remote sensing and therefore may not harmonize with the properties of remote sensing data (No. 32+33). Consequently, a predetermined calendar date assumes greater significance than the actual condition of the object under investigation. This does not negate the administration's capacity to assess the usability of existing remote sensing products (Goihl 2023b), explore its own developments for monitoring legal requirements (Goihl 2023a, Goihl 2025)

Concurrently, the data situation and use case were so specific that new scientific value was created for each process in the absence of suitable literature on these issues. According to Thomson et al. (2005), there are nine general categories of uncertainties. These are accuracy/error, precision, completeness, consistency, lineage, timing, credibility, subjectivity and interrelatedness respectively quality (MacEachren et al. 2005). According to Werther & Burggraf (2023), a focus on uncertainties leads to more accurate and reliable results, as new perspectives on the product are generated and decision-making in management is based on more information.

Table 1: Challenges for (agricultural) remote sensing. The numeration system is not subject to any hierarchical order. The table pertains to common remote sensing applications, including classification and monitoring.

#	Uncertainty sources	Explanation, Example of the effect as an uncertainty factor	Consequence for the RS results	Solution approach & Gaps	Reference
	Ordinary Remote Sensing				
1	Cloud cover	Monitoring obscured by clouds at the crucial time, e.g. mowing event	Overlapping of crucial times for monitoring, shortening and thinning of analysis time series, no data available	Subsequent interpolation of index values, masking of clouds and cloud shadows	Lakso 2022, Goihl 2023a, Sudmanns et al. 2020, Baetens et al. 2019
2	Ground resolution	Mixed pixels, edge effects, examination object smaller than recording geometry	No recording of the object of investigation possible	No processing of too small objects, exclude mixed pixels from further analysis in pre- or post-processing, masking out objects that are too small; Pansharpening the original image	Goihl 2023a, Goihl 2025, Nazeer et al. 2021, Schröder et al. 2024, Povey & Grainger 2015, Zhang & Mishra 2012
3	Orbit	Different viewing angles, e.g. due to the orbits of Sentinel-1 (SAR), lead to various distortion effects	Shadowing, distortion effects	Use of orbit correction data and height models, masking of shadowed areas	Van Zyl 1993. Löw et al. 2024
4	Atmospheric correction	Methodical approaches vary, which means that the pre-processing generates different data for further processing	Can lead to deviations in the results in further processing, despite using the same classification method	Selection of a powerful correction method, consistent use of the same method within a time series or when comparing data products	Nazeer et al. 2021
5	Radiometry	Sensor systems are not radiometrically standardized. For optical systems, central wavelength (CWL) and full width at half maximum (FWHM) for comparability	Results will not be identical between different satellite systems using the same methodology	Harmonization; Avoid direct mixing/comparisons	Nazeer et al. 2021, Claverie et al. 2018, Povey & Grainger 2015
6	Ground truth, In-Situ-data	Validation data unevenly or unfavorably distributed in space, training data insufficient for classification, some classes also very rare or temporary in reality (e. g. open ground, construction sites); subjective perception of the data collector distorts the mapping result	Higher classification accuracy of overrepresented classes, spatially varying intra-class accuracies, too low information density for individual classes	Adapted data collection, sensible selection from existing data sets, large amounts of data required for AI and ML approaches, incomplete validation	Rustamov & Hasanova 2014, Goihl 2024, Schmidt et al. 2024, Schröder et al. 2024, Teucher et al. 2022, Mirpulatov et al. 2023, Ray & Burgman 2006
7	Illumination variation	Shadows and/or coverage by objects or topology lead to misclassification or non-detection of the object under investigation	Lower classification accuracies at the affected locations	Interpolation by time series data, masking of non-monitoring areas	Van Zyl 1993
	Phenology				
8	Phenological stage	Superordinate, determined by many influencing factors (e.g. No. 9-29): The same type of crop can be at different stages of development at the same time and in close proximity	High variability within individual crop types, both spatially and temporally, softening of class boundaries and temporal patterns, increased chance of incorrect classifications	Many influencing factors. Targeted solutions difficult to implement. Consideration of agri-structural regions, regional classifications preferred over national ones; e.g. noise fitting, thermal encoding, data smoothing	Goihl 2023a, Goihl 2023b, Goihl 2025, Wu et al. 2023, Nyborg et al. 2022, Zeng et al. 2020, Bormann et al. 2023, Löw et al. 2024
9	Nutrient supply	Biomass varies despite the same crop type and location, depending on water availability, location and fertilization	Like number 8	Cannot be reasonably collected on site, indirect approximation via soil types/soil communities, small-scale N measurement	Wu et al. 2023
10	Stress response	Biomass reduced, locally or regionally, e.g. due to drought or pests	Declining vitality compared to the usual course of the time series of a fruit species	Inclusion of weather and soil data in the classification	Goihl 2023b
11	Diseases, Pests	Local biomass reduction	Declining vitality compared to the usual course of the time series of a fruit species	No practical area-wide mapping possible. Spot checks or UAV deployment	Wu et al. 2023

#	Uncertainty sources	Explanation, Example of the effect as an uncertainty factor	Consequence for the RS results	Solution approach & Gaps	Reference
12	Weed pressure	Additional vegetation signals, for example, are measured after the ripening of wheat	Change in vitality compared to the usual course of the time series of a crop species on an area	No practical area-wide mapping possible. Spot checks or UAV deployment	Ronay et al. 2022, Kerimkhulle 2021
	Management				
13	Fertilization	The type and quantity of fertilizer used influences plant development and thus affects the measurable values. Affects number 9	Like number 8	Comparison with management data, integration into the classifiers. However, this data is generally not available and would have to be procured at great expense	Wu et al. 2023
14	Precision Farming	Compensation vs. exploitation strategies. Cultivation adapts strongly to the site conditions and can thus influence growth in the fields in various ways.	Fields become more homogeneous or heterogeneous by the farmer's decision. Remote sensing can falsely indicate homogeneous soils or nutrient deficiencies	Like number 13	Khanal et al. 2020, Ferguson & Rundquist 2018, Bach & Mauser 2018
15	Irrigation	Vital biomass compared to non-irrigated areas increases the range of possible input signals for the sensor	Increased local variability compared to other fields of the same crop type. Like number 8	Like number 13. Additional RS data on irrigation locations may be available.	Wu et al. 2023, Gao et al. 2018, Ozdugan et al. 2010
16	Tillage methods, Sowing method	Variation of the background signal (soil), e.g. whether to sow on fallow land or use no-till methods	Influencing of the optical measurement by the background signal of the ground. Interferes with the clarity of the signals and leads to an increase in class boundaries	Like number 13	Martins et al. 2021
17	Sowing date, Harvest date	Regional differences, disadvantageous for holistic model approaches, also dependent on No. 20	Regional and local differences between start and end of season on the individual fields. Increase the temporal diversity of the classes and thus lead to more uncertainties in the classification	Like number 13; inclusion of additional remote sensing products. Use of knowledge of agri-structural regions with comparable soil management	Nyborg et al. 2022, Franch et al. 2022, FAO 2025, SLfL 1999
18	Crop rotation	Annual change of crop type at the location	No annual comparisons of remote sensing values can be made on the same area, only possible for grassland	Like number 13. Mapping in the field. Additional information on crop types needful, e. g. CAP-data.	Goihl 2023b
19	Herbicide application	Sudden death of vegetation compared to reference area without treatment	Unsystematic measurements within the same land cover class	Like number 13	Pause et al. 2019
20	Sort type, Seed mix	Characterization of variety-specific properties e.g. freezing vs. non-freezing catch crops (class terms, early potatoes vs. late potatoes)	Like number 8. Different phenological progression for the same land use class	Like number 18	Schmid & Maidl 2005, Schulz et al.2021
21	Variety selection	Variety-specific differentiation within the same crop type ("Which early potatoes are to be cultivated") in the spectral reflection	Consequences for spectral separability from a remote sensing perspective: Reduces the uniqueness of the spectral profile, increases the chance of misclassification	Like number 13	Schmid & Maidl 2005, Schulz et al. 2021
22	Farm orientation: organic or conventional	Organic farms less productive in the same crop type, productivity is also mapped via yield and vegetation	Like number 8	Like number 13. Data on application data available if organic farms are additionally supported	Martins et al. 2021, Denis et al. 2020
23	Livestock on grassland	Unsystematic or proportional change in the spectral properties of a test surface	Disadvantageous for Object-Based Image Analysis (OBIA) approaches	Training data/Validation data must include information on livestock units/ha and time period	Numata et al. 2007, Castro et al. 2020
24	Mowing, partial mowing	Unsystematic changes depending on intensity of use, weather, etc.; proportional change in spectral properties of a study area	Disadvantageous for Object-Based Image Analysis (OBIA) approaches	Training data/Validation data requires corresponding information, post-processing	Schwieder et al. 2022
	Biophysical parameters				
25	Soil properties	Permanent background signal. Variability of soil types within a field. Leads to differences in phenology due to nutrient and water supply. Variable but also between regions.	Like numbers 8 and 16	Comparison with soil information, e.g. Soil Quality Rating; integration into the classifiers. Use of soil-adjusted vegetation index (SAVI) or comparable data, but sufficient accuracy for field level questionable	Martins et al. 2021, Richardson & Wiegand 1977, Qi et al. 1994, Xue & Su 2017, BGR 2025
26	Harmful soil changes	Erosion spots or soil compaction affect yields. Has a negative effect on phenological development. Other	Like numbers 8 and 16	As number 25, but depending on the type of disturbance factor, it may not be possible to map the entire area.	Wang et al. 2023, Khanal et al. 2020

#	Uncertainty sources	Explanation, Example of the effect as an uncertainty factor	Consequence for the RS results	Solution approach & Gaps	Reference
		damaging factors are salinization, desertification, and contamination		Inventory by remote sensing. Comparison with soil information and soil cadastre	
27	Weather conditions	Key factor influencing the phenology	Like number 8	Comparison with weather and climate data, integration into the classifiers.	Wu et al. 2023, Goihl 2024
28	Mikroclimate	Together with weather conditions (No. 27), an important factor influencing phenology	Like number 8; Explains and causes local variability	Only integration of local sensors at field level, integration of digitial elevation model, weather and climate data; but spatial resolution mainly too imprecise here	Wu et al. 2023, Goihl 2024, Kuntzman & Brom 2025, Tian et al. 2020
29	Soil moisture	Background signal, depending on the weather and irrigation, varies with the weather, soil discoloration	Like numbers 8 and 16	Areal data products not available, approximation via model data	Wu et al. 2023, Tollerud et al. 2020
	Agricultural structure				
30	Field size	Minimum size required to be detected by certain satellite systems	No recording of the objects under investigation possible	Change of sensor system, exclusion of these areas from the classification	Goihl 2023a, Goihl 2025
31	Field shape	The less complex the shape, the greater the possibility of detection by satellite images; object shape error (topological inconsistency)	No recording of the objects under investigation possible; incorrect input data for analysis	Change of sensor system, exclusion of these areas from the classification	Goihl 2023a, Goihl 2025, MacEachren et al. 2005
	Legislative factors				
32	Legislative requirements	Funding directives can contain rigid deadlines (e.g. restrictions on use, date-related). Due to cloud cover or non-daily overflights, it is not possible to check whether exactly this limit is adhered to, e.g. date of first mowing not before a fixed date; parameters cannot be determined by remote sensing	Existing and available sensor systems do not fit the requirements of legal texts	Use of other data collection methods	European Union 2021a, European Union 2021b, Goihl 2023a, Samarinas et al. 2023, Rinke et al. 2023
33	Subsidies, support programs	Support programs can prescribe management measures that differ from non-supported cultivation in the same land cover class and thus generate different signals (e.g. “overwintering stubble“, fixed time periods)	As for numbers 8, 19 and 32; Actual status less important than the calendar date of a funding guideline	Comparison and integration of data from the funding programs in classification or post-processing	Goihl 2023a, Goihl 2023b
34	Undocumented activities	Some data sources does not cover the entire agricultural area. Voluntary measures are not recorded, but can take place and be interpreted as misclassification (e.g. “overwintering stubble“)	Like numbers 8 and 19	Like number 33	Goihl 2023a, Goihl 2023b
	Temporal, Hazards				
35	Flooding	Detection of the object of investigation not possible or only possible to a limited extent as it is covered with water. May have a distorting effect as part of a time series analysis, image composites, etc.; Can also affect an area in the long term or be recurring.	Temporary covering of the object under investigation	Classification of flooded areas by means of remote sensing, masking, on-site mapping, not practical to implement on a large scale for small-scale and short-term events, water level information is also important	Notti et al. 2018, Büttig et al. 2018
36	Game browsing, feeding damage	Temporary local changes in the vegetation signal	(Temporary) destruction of the object under investigation. See number 8 and 19.	A cost-efficient on-site survey is not universally available; therefore, UAV mapping is performed as close in time to the satellite image as possible.	Kuželka et al. 2018
37	Rodent damage in grassland	Temporary local changes in the vegetation signal up to complete damage to an area (often mice in grassland)	(Temporary) destruction of the grassland under investigation. See number 8 and 19.	Like number 36	Andreo et al. 2019, Dong et al. 2023
38	Temporary storage	Used as a temporary storage area (e.g. manure, hay bales). Recording of the object of investigation not possible or only possible to a limited extent, as it is covered. As part of a time series analysis, image composites etc. distorting effect.	Temporary covering of the object under investigation	Like number 36	-
39	Fire damage	Abrupt change in the spectral properties of a test area as a result of the effect of fire	Damage/destruction of the object under investigation. As number 8 and 19	Like number 36. Identification and masking of burnt areas using remote sensing	Roteta et al. 2021
40	Hailstorm damage	Abrupt change in the spectral properties of a study area as a result of hailstorms	Like number 39	Cost-efficient on-site survey not available across the board. Hailstorm data in spatial detail missing	Singh et al. 2017

#	Uncertainty sources	Explanation, Example of the effect as an uncertainty factor	Consequence for the RS results	Solution approach & Gaps	Reference
41	Snow	Observation of the object of investigation not possible or only possible to a limited extent as it is covered with snow. May have a distorting effect as part of a time series analysis, image composites, etc. Can also affect an area in the long term or be recurring	Temporary covering of the object under investigation	Identification and masking of snow using remote sensing, formation of the Normalized Difference Snow Index (NDSI)	Hall et al. 1995, Härer et al. 2018
	Product and interpretation uncertainties				
42	Indices	Continuous values or normalized index. The entire numerical range of the data product is provided to the user	Data product delegates the interpretation of the index values to the user, no further explanation, benefit depends on the user's knowledge	Documentation (see number 50), provision of interpretation aids, overview of possible and meaningful limit values, provision of additional quality management products Classification instead of continuous individual values → like number 44	Rivera-Marin et al. 2022
43	Predicted values	For example, the predictions of yields, soil moisture or soil carbon. Are all based on prediction probabilities of the respective model for the corresponding pixel/object	Data product shows pixels/objects with a specific value within a closed product, even if the probability of this value is very low	Like number 42	Mirpulatov et al. 2023
44	Classification, Semantics	Various options for creating or grouping classes, e.g. of land cover and land use, soil moisture, etc.; classification error	Finished data products do not allow any conclusions to be drawn about class formation. Choice of the right methodology is questionable; bad labeling for usage	Like number 42	Venter et al. 2022, Devos et al. 2020, MacEachren et al. 2005
45	User	Subjective knowledge and the user's perception lead to misinterpretation, visual interpretation of aerial images	Misinterpretation or incorrect further use of the data by the user	Like number 42	Brus et al. 2018
	Structural uncertainties				
46	Choice of method, no known method	Affects class sizes or number of classes; not the ideal method chose; no ideal method available	Other methods achieve higher accuracies, results (No. 42-44) or chosen methods do not meet the user's requirements	Optimization of the method, e.g. in relation to the user's requirements, comparison of methods via quality metrics, await progress of research	Goihl 2023a, Scholand & Schmalz 2024, Paasche et al. 2020, All case studies
47	Length of available time series	Trend analyses strongly affected by short time series, comparisons on the same agricultural area under the influence of a multi-year crop rotation not possible	Limited informative value of short time series, low comparability	Choice of other methods, wait for a longer time series	Goihl 2023b
48	Non monitorable aspects	No monitoring of desired parameters possible with remote sensing	No detection using remote sensing data and methods or the favored satellite system due to monitoring parameters or geometry (see number 29)	Choice of other methods	Devos et al. 2020
49	Misregistration	Spatial displacement of two scenes by several pixels due to incorrect geolocalization	Limitations in the usability of incorrectly localized satellite scenes. No monitoring possible, deviation between different satellite systems (geolocalization, resolution), change detection errors	Manual registration of required images, exclusion of incorrectly registered images from the evaluation	Storey et al. 2016, Jiao et al. 2016
50	Metadata	E.g. data without indication of date or data status	Possibly outdated data used within this product	Metadata management	Koedel et al. 2022
51	Systematic weakness	Differences between the chosen description of the environment and reality	Reality cannot be described using data and models	Make adjustments to the selected description	Povey & Grainger 2015
52	Technical defects	Defects and failure of sensors	Sudden interruption of the data series, impairment of the time series, disruption of individual bands	Error Correction Methods, changing the remote sensing system	Adiyaman et al. 2025
53	Time	Effects arising when data from different time periods are used	Useful for time series analysis and change detection, but not every use case, therefore consider targeted data selection	Control Metadata (No. 50), Ground Truth (No. 6) and choice of method (No. 46)	MacEachren et al. 2005

The uncertainty factors mentioned in Table 1 are categorized as follows. Firstly, epistemic uncertainty is defined as "unknown unknowns, systematic errors" (Povey & Grainger 2015, Harken et al. 2019). Secondly, aleatory uncertainty is defined as "known unknowns, unsystematic errors" (Harken et al. 2019). For number 46, the ontological uncertainty of an inappropriate methodology also applies (Paasche et al. 2020). The product uncertainties mentioned above (numbers 42-44), however, are an essential part of all data. On the one hand, uncertainties can be employed to effectively communicate strengths and weaknesses to the user; on the other hand, they serve as a metric for the descriptive description and comparison of data (Povey & Grainger 2015; see Chapter 5.4). According to Koedel et al. (2022), three aspects are crucial for the trustworthiness of data: data consistency, validity, and data origin. In an ideal scenario, the results, or the usable products, are influenced only by the natural variability of the recorded parameters (Harken et al. 2019). However, as illustrated in Table 1, this can only be wishful thinking in view of the large number of influencing factors (No. 1-41, 46-49). A multitude of factors exhibit a degree of interconnection, more or less systematic, e.g. drought stress (No. 10) can weaken a crop and make it susceptible to disease (No. 11). The subsequent examples illustrate the consequences of the above-mentioned effects of uncertainties for users:

Practical example no. 1 - Detection of mowing dates on grassland

The technical reality of remote sensing does not necessarily correspond to the reality of fixed funding guidelines. For instance, guidelines are linked to fixed dates, such as grassland management and its mowing dates. In order to ensure the preservation of meadow flora and fauna, the initial mowing is prohibited prior to a predetermined date. Farmers who adhere to these measures and comply with the relevant requirements receive a compensation payment. However, the temporal discrepancy between satellite revisit times and the actual mowing dates poses a challenge in the application of remote sensing for this purpose. This results in a time window between satellite overflights during which mowing activities could potentially be detected (Schwieder et al. 2022). The imprecision of this temporal span hinders the ability to ascertain violations with the precision required to implement subsequent sanctions. Consequently, a complaint would have a good chance of success because it cannot be proven beyond doubt that the mowing took place at the end of the time window. Therefore, only the remote sensing data source is specified for the verification of crop

types for direct payments (European Union 2021a), but not the methodology or mandatory classification accuracies.

Practical example no. 2 - Impact of precision farming management decision

Assuming that state institutions seek to promote precision farming technologies more strongly, it is necessary to inventory the heterogeneity of agricultural land in the administrative area using remote sensing images. A farmer employs precision farming methodologies. The farmer must decide whether to pursue a compensation or an exploitation strategy. The compensation strategy involves the homogenization of cultivation in the field, while the exploitation strategy increases cultivation in the most productive areas and reduces production in the least productive areas (lower seed density, less fertilizer). In case of the compensation strategy: The satellite image, through the use of vegetation indices, will demonstrate a more homogeneous cultivation pattern. Consequently, the state might reach the conclusion that precision farming is not necessary for farmers who employ compensation strategies, given the homogeneous measurement signals. Conversely, the state could ascertain a high demand for the farmer who utilizes the exploitation strategy. However, the state would need to have access to additional information to reach a comprehensive understanding of the situation.

Practical example no. 3 - Freedom of interpretation of the indices

A considerable number of remote sensing products grant users the liberty to interpret data according to their own discretion. This is exemplified by index values (Table 1, No. 42), such as the NDVI, where a distinct delineation value is employed to ascertain a particular class, depending on the scientific study (Rivera-Marin et al. 2022). It is noteworthy that novice users (Table 1, No. 45) may encounter challenges in comprehending such definitive determinations when left to their own devices. In instances where the product manufacturer has conducted a classification in advance using such threshold values, the decision-making process for class formation becomes obscured within the product itself. Consequently, an experienced user (Table 1, No. 45) might have doubts about the correctness of the classification based on his subjective perception.

2.2 Opportunities for governmental remote sensing

Government agencies that are responsible for monitoring activities in the sectors of agriculture and the environment have a growing need for remotely sensed information. This necessity is generally shared by all administrative units related to land (agriculture, environment, geodesy, local authorities, statistical offices, etc.). The dense time series provided by remote sensing also make such products interesting for official use, as does the free availability of data from the European Space Agency (ESA) (Rinke et al. 2023). Beyond the fundamental necessity for high-resolution geodata in terms of both space and time, two additional fundamental criteria must be considered when assessing the information content: Reliability and incorporation into legal provisions (Chapter 2.1, Rinke et al. 2023) or use as a supplementary and additional data source. Employees in administration, for instance, have access to the product portfolios of space organizations. These offer a wide range of data sets, for example the Copernicus Land Monitoring Service (CLMS 2025) with almost 200 products (as at 24.01.2025). The fundamental challenge with these products is that they are rarely tailored to the specific needs of the administration and therefore cannot cover the necessary data requirements. Consequently, authorities are compelled to develop their own products or initiate fundamental suitability studies in order to meet their requirements (Büttig et al. 2022, Schmidt et al. 2024, Goihl 2023a, Goihl 2023b, Goihl 2025). Authorities at municipal, state and federal level have had remote sensing applications developed or developed them themselves for a wide variety of specialist areas, e.g. water bodies (Schmidt et al. 2024, Schröder et al. 2024, Kuhwald et al. 2024), climate and climate impacts (Kuhwald et al. 2024, Lehmler et al. 2023), agriculture (Reitz 2024) or nature conservation.

The potential of remote sensing products is contingent upon their provision to users in readily accessible formats. The continuous placement of remote sensing experts within authoritative agencies is unrealistic, which means that barrier-free use must be guaranteed for non-remote sensing experts. This "last mile" is a critical component in the transition from research to practice. Laue et al. (2025) have developed exemplary service models for the interfaces between satellite data and state environmental agencies in the field of water monitoring. These models vary according to the dependency on external service providers. According to Wang et al. (2018), comprehensive product validations are necessary for the user, divided into three parts:

the description of relevant uncertainties, the quantitative results and the qualitative assessment taking into account user needs.

The challenges and opportunities identified in the use of remote sensing data in administration highlight the need for targeted methodological approaches. The subsequent chapter will present the specific research objectives of this thesis.

3 Objectives

The objective of the study was to ascertain the informative value of geoinformation and remote sensing products with regard to the issues and needs of agricultural administration. In addition to the informative value, the primary objective was to determine the possibilities and limitations of such products in application, and to identify and communicate potential for improvement and uncertainties. The findings of this study were used to assess the conditions under which such products could be used for each application. The objectives of this study were achieved by

- Implementation of application-related in-house developments to support expert questions (1, 3) for soil-conserving land cover (stubble) and cultivation direction of agricultural fields
- Interpretation of existing products in the transfer case of science to practice (2)
- Control of processing efforts with input data minimization through image compositions and feature engineering (1)
- Demonstration of possibilities for minimizing uncertainty in pre- and post-processing (1, 2, 3) and the associated increase in usability
- Impact analysis of spatial differentiation and evaluation of vegetation parameters (2)
- The following analysis and interpretation of products is to be conducted against the background of the significance and associated uncertainties as a technical application from the perspective of the authorities in the field of agriculture (1, 2, 3)

This resulted in a number of notable features of the research work. Specifically, products for specific administrative issues were developed or investigated. These product developments included detailed questions that had not yet been scientifically investigated in this form and with this level of data availability, and therefore had a high novelty value (Goihl 2023a, Goihl 2023b, Goihl 2025). The core content of this work

focused on the practical applicability of results, the communication of uncertainties, the testing of improvement options, and the follow-up assessments for agricultural administration, generating additional new scientific value.

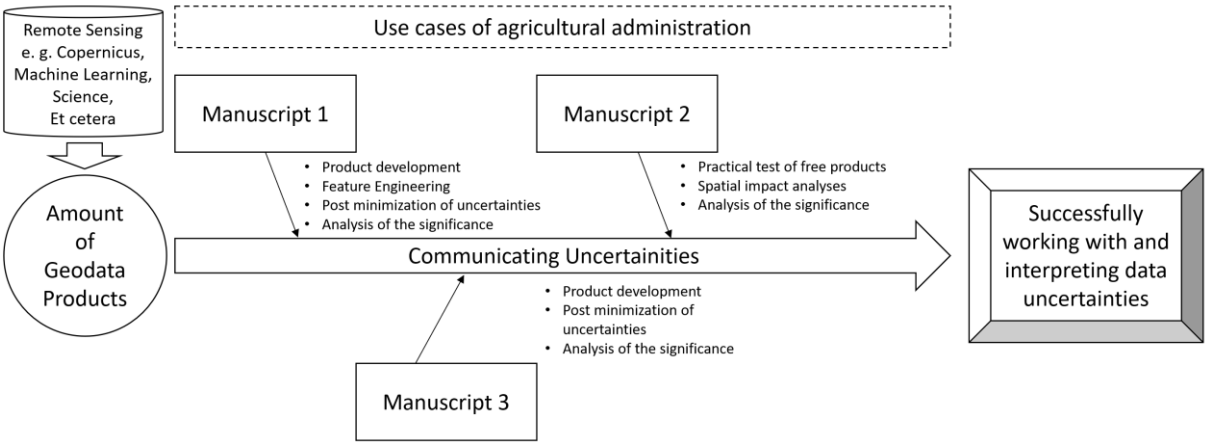

Figure 1: Interaction of the individual components of the dissertation to fulfill the overall objective.

In order to achieve the above objectives, possible use cases were created through in-house development or tested using third party product offerings. On the one hand, use cases were based on the verification and monitoring of specific land cover types and conditions. This aspect is of particular importance given the highly dynamic nature of agricultural land throughout the year and in comparison to previous and subsequent crops. Consequently, the investigation of these detailed questions was only possible for a comparatively short period of time within the agricultural utilization phase.

The mapping of "overwintering stubble" (SMEKUL 2017) was carried out as an in-house development, a measure from the area of agri-environment and climate services (AUKM), which is funded by the state of Saxony (Goihl 2023a). The primary uncertainty categories (Table 1) for Goihl (2023a) derive mainly from in-situ data (No. 6), phenology (No. 8), funding regulations (No. 33), application data vs. voluntariness (No. 34), snow (No. 41), cloud cover (No. 1), field size (No. 30), and field shape (No. 31). Utilizing contemporary cloud technology from Google Earth Engine (GEE) (Gorelick et al. 2017) in conjunction with image compositions and machine learning algorithms (Tassi & Vizzarri 2020), a robust development environment was employed. Image composites were created for multi-month management periods of the measure, which made it possible to reduce the influence of phenology, clouds, and snow, especially in the fall and winter months.

A geographic information system (GIS) was utilized to evaluate the results, and various post-processing approaches were employed to enhance the outcomes. This was

achieved, for example, by integrating additional knowledge on previous and subsequent crops, or by using and testing usable pixels without mixing effects according to field geometry. As this research project progressed through its iterative phase, some uncertainty factors only became apparent in the course of the analysis, such as the influence of strict calendar specifications from the funding guideline and the associated application data as a data basis (No. 8, 33, 34). In post-production, the application of thresholds per field has also been identified as a strategy to minimize uncertainties. If the classification indicated that more than 65% of the area of a field corresponded to the searched class, all pixels of this object were transferred to the target class (Yulianto et al. 2021). It is important to note that such thresholds are typically arbitrary and must be adapted to the user's confidence level.

Subsequent enhancement of the results was also realized in the determination of the main cropping direction of the fields (Goihl 2025). The primary uncertainty categories (Table 1) for Goihl (2025) derive mainly from ground resolution (No. 2), crop type and variety selection (No. 20), crop rotation (No. 18), field size (No. 30) and field shape (No. 31), in-situ data (No. 6), and phenological stage (No. 8). In this study, Digital Orthophoto (DOP) and Sentinel-2 images were utilized to ascertain the compass direction of cultivation for individual fields, with the objective of leveraging this information for future applications, such as addressing issues related to erosion. While the technical feasibility of the approach was successfully demonstrated, the Sentinel-2 survey covered a much smaller area than the DOP approach. This phenomenon can be attributed to the varying spatial resolutions of the images, as well as the disparate developmental patterns of the crop types during the vegetation period, which occurred at a specific point in time during the satellite image acquisition. Depending on the crop type, the patterns of the direction of cultivation were accordingly better or worse. This phenomenon can be attributed to the varying spatial resolutions of the images, as well as the disparate developmental patterns of the crop types during the vegetation period, which occurred at a specific point in time during the satellite image acquisition. The direction of cultivation exhibited distinct patterns, contingent on the specific crop type. An independent in-situ data collection was carried out in the form of digitization. The utilization of these findings led to the identification of beneficial crop types, thereby enhancing the reliability of the study area's results by excluding unfavorable crop types (Goihl 2025). In addition to the issue of crop types, the uncertainties in the DOP were

increased by not considering the turning area (negative buffer into the field), while this had a worsening effect on the satellite image.

In addition to the establishment of small-scale study areas for the purpose of application development, the agricultural administration generally aims to be active throughout the entire state. In 2018, Saxony was affected by a severe agricultural drought. The Copernicus Land Monitoring Service (CLMS) provides a suite of products focused on vegetation, including the High Resolution Vegetation Phenology and Productivity Index (HR-VPP). This product's unique characteristics make it particularly well-suited for reanalysis of drought events. While the results enabled spatial and crop-specific differentiation, the practical benefits were found to be limited (Goihl 2023b). The primary uncertainty categories (Table 1) identified by Goihl (2023b) derive mainly from in-situ data (No. 6), phenology (No. 8), weather (No. 27), microclimate (No. 28), stress responses (drought) (No. 10), crop rotation (No. 18), irrigation (No. 15), subsidies/support programs (No. 33), and indices (No. 42).

On the one hand, HR-VPP products were only available approximately one year after the calendar year under review, which limited the study to a reanalysis of the events. Consequently, active management of a drought event, including timely impact assessment (policy advice), is not possible with this product. Additionally, the data was not sufficiently disaggregated to differentiate between drought aid applicants and non-applicants. This situation was made even more difficult by the fact that applicants for drought aid submitted their applications without specifying the affected areas, which meant that it was not possible to locate particularly affected areas on the spot, and this was ruled out as a source of validation. However, this would have been an important aspect for recognizing and using patterns in the context of policy advice in order to communicate emerging needs for drought aid in advance. Additionally, there were further uncertainties regarding crop rotation and the comparison of farms. The development of a custom comparative indicator has the potential to address a significant number of the uncertainty factors mentioned above. However, due to the nature of crop rotation, direct comparisons between the VPP index values of the drought year and the reference years (with the exception of grassland) could not be made on a site-specific basis. This was due to the necessity of comparing different crop types with each other. The dissemination of results was found to be challenging due to the absence of a discernible correlation between yield data and VPP values. This is further compounded by the fact that yield-generating plant parts do not

inherently encompass the entire plant (e.g., as in the case of grassland and silage maize). Additionally, the units of the VPP datasets are dimensionless index values, which limited their communicability to a stakeholder (Goihl 2023b).
The synthesis of diverse methodologies and research inquiries in these studies contributes to a comprehensive investigation of the uncertainties inherent in data products, thereby enhancing our understanding of these factors in future studies (see Table 1). This comprehensive overview can support future decisions for administrative activities and connect expectations of remote sensing products with reality.

4 Material and Methods

The following section presents the data sources, methods, and analytical approaches relevant to this work. These are based on three publications (see appendix), which address the central aspects of usability and uncertainty in agricultural remote sensing with the aim of administrative activities. As the publications do not build on each other in terms of the subject of the study, reference is made to the relevant chapters of these publications for a deeper understanding the respective state of research.

4.1 Application of machine learning and image compositions for mapping the soil cover “overwintering stubble” in the agricultural landscape (Manuscript 1)

The study was based on data from the agri-environmental and climate measure "Overwintering Stubble" in Saxony (SMEKUL 2017). The objective of this study was to investigate the monitoring potential of this land cover class using satellite imagery. The concept of "overwintering stubble" is designed to provide animals with habitat and sustenance during winter months, while contributing to soil protection, as stubble fields may no longer be cultivated after the harvest until February 15 of the following year. This also resulted in a possible study period with the end of season for cereals (Franch et al. 2022), here using the example of winter wheat, in July and August in Central Europe and the date from which a field was allowed to be cultivated again. The geographical area under consideration was situated in the southwestern region of the federal state of Saxony, encompassing the Sentinel-2 tile 33UUS. The selection of this region was predicated on the presence of the most abundant training data for the target class. Subsequently, the trained models were applied to a smaller sub-area within the investigated area.

The arable land from the agricultural subsidy on which the "overwintering stubble" measure was carried out at the turn of the year 2019/2020 served as ground truth data. As no additional ground truth data regarding land cover was available, nor could it have been obtained efficiently for this brief study period, Corine Land Cover data was employed (CLC 2021). In this data set, the stubble fields were updated using a Geographic Information System (GIS) tool. The training and test points were then derived from this data set (5,000 points, 500 points), and machine learning (Random Forest, Support Vector Machine) was subsequently performed. The selection of these machine learning methods was informed by their prior efficacy in LULC classification, as evidenced by previous studies (Tassi & Vizzari 2020).

The methodological implementation was executed on the Google Earth Engine (GEE) as a processing platform. The study methodically investigated the existence of particularly suitable combinations of input data for the models. This involved a suitable selection of Sentinel-2 bands and statistical parameters from the NDVI, BSI, NDMI, and SNDTI indices. The study period was divided into three subsections, classified according to management and phenology, thereby effectively tripling the amount of input data. The bands and indices were then stacked on top of each other, resulting in so-called image composites (Tassi & Vizzari 2020, Phan et al. 2020). These composite images constituted the original data set for the training and test data generated above. After the model training, particularly high accuracy and low accuracy data sets were selected for a detailed examination of the results and validation using the application data from the AUKM for winter 2019/2020.

Furthermore, the implications of the classification outcomes for potential stubble fields that were not applied for funding by the farmer, but may have been present as land cover, were investigated. Finally, the potential for minimizing uncertainties in the results was explored by establishing limit values, considering the influence of field size, and incorporating the concept of crop rotation.

4.2 Evaluation of Copernicus HR-VPP product usefulness in case of the year 2018 drought in Saxony (Manuscript 2)

Utilizing the High Resolution Vegetation Phenology Product (HR-VPP) (Smets et al. 2021), a comprehensive, crop species- and region-specific reanalysis of the agricultural drought that occurred in 2018 was conducted (Beillouin et al. 2020). To this end, the data sets for the years 2017 to 2020 (time series available at the time of the study) were evaluated in conjunction with the Integrated Administration and Control

System (IACS). As part of the preliminary investigation of the VPP datasets, their effect on land cover data from Corine Land Cover (CLC) was evaluated. Finally, the correlation between the VPP data and the application data of farmers for drought aid in Saxony 2018 was investigated. The primary objective was to search for patterns and rules that would support the prediction of possible future drought aid amounts for policy advice.

The HR-VPP products are representing the length and intensity of the vegetation period. These area-wide data sets, characterized by a high spatial resolution (HR = 10 m), were obtained for the whole of Saxony for the years 2017 to 2020. A preliminary test using CLC data and the GIS tool "zonal statistics" was conducted to investigate the detectability of effects in the VPP index in the land cover classes "cropland" and "grassland" for the drought year 2018. This test also served to determine whether further use of the data would be unsuccessful. The preliminary test revealed a significant decline in the reference years for agricultural land (cropland, grassland), especially for 2018. To determine the mean VPP values for the entire national area for different crop types, significance tests were also used. The reference years 2017, 2019, and 2020 were then compared with the drought year of 2018. The findings revealed that the data for 2018 exhibited significant deviation from that of the reference years.

Subsequently, the area data concerning agricultural subsidies were subjected to analysis, with the analysis distinguishing between crop types and considering spatial location. The objectives of this analysis were twofold: first, to identify regional variations in the impact of drought on crop productivity in 2018; and second, to examine the specific impact of drought on different crops within the region. The spatial evaluation encompassed various spatial levels, including district, municipality, and farm. The farm was defined as the smallest spatial unit, and its examination in a final step aimed to determine whether farms that applied for drought aid also generally exhibited poorer performance within the VPP values for their fields. The only link between the application for drought aid and the specific agricultural fields was the individual farm identifier. The extent to which individual farm fields were specifically affected was not documented in the application. These applications only contained economic information.

A further obstacle was the comparability of the drought impact between different farms and their economic orientation, geographical location, and cropping structure. Due to

limitations in the data set, including a short time series of only four years and the fact that crops are rotated, it was not possible to compare VPP values on the same plot of land. Consequently, the "VPP-based Farm-Level Temporal Comparison Indicator (VPP-FLTCI)" was developed. This indicator took into account crop-specific VPPs and their regional differences on the basis of the municipality, and compared these with the farm's own VPP values on an area-weighted basis. Consequently, a dimensionless FLTCI value was obtained for each farm, enabling the comparison of the drought effect between farms, despite their geographical differences and the diversity of their crop types. Subsequently, a comparison was made between FLTCI values of farms that had and had not applied for drought aid, and it was investigated whether the values were sufficient to map the drought aid application process with remote sensing data. To comprehensively assess the performance of the farm in relation to the drought event itself, a baseline was determined using the same methodological approach. By replacing the VPP values for the drought year 2018 with the mean value of the reference years per farm, crop type and municipality, the general performance of the farm was recorded in a regional comparison with other farms, measured by the VPP index.

4.3 Tillage direction analysis from DOP and Sentinel-2-images (Manuscript 3)

The primary objective of the data processing was to extract the line structures (= tillage direction) contained in the remote sensing images (Sicre et al. 2014, Scholand & Schmalz 2024) of the field management from the raster data using GIS methods in such a way that lines were created as vector data. The study utilized Digital Orthophotos (DOP), Sentinel-2 Satellite Image, Agricultural field data (IACS), and self-generated validation data. These lines were to follow the line structures in the fields, for example the tractor tracks in the DOP. The main direction of cultivation was then derived from the large number of lines within an agricultural area. The Linear Directional Mean (LDM) tool of ArcGIS was employed to determine the average compass orientation of an area over the lines within it. The utilization of medium resolution satellite data (Sicre et al. 2014) posed a distinctive challenge and had not been executed with Sentinel-2 data yet.

The study area covers the Saxon part of an 8 km x 12 km area in the Meerane region, Saxony. The study area was selected because it is a hilly area in which agricultural yields are particularly at risk from water erosion (LfULG 2023).

The lines for the LDM tool were determined using established GIS methods. For instance, the high pass filter proved effective in detecting the edges of tractors' lanes against a homogeneous vegetation background. With a spatial resolution of 20 cm x 20 cm for the DOP and a lane width of approximately 80 cm, the DOP provided sufficient pixels to perform such differentiation. The filter's output was then reclassified into three distinct classes: "Tractor lane", "Tractor lane borders", and "vegetation". Following this classification, the data was cropped to align with the specific characteristics of each field. The raster data was transformed into polygons and the extracted target class "tractor lane" was converted into polylines. Subsequent to this, artifacts were eliminated, and the vector data were intersected with the field data to assign the information to which agricultural area the lines can be assigned and which crop type was cultivated on this area. A similar method was used to process the Sentinel-2 images. Given the 10-meter spatial resolution of the images, row structures that were visually recognizable on the cropland in the satellite image were used for this purpose (Li et al. 2022). Segmentation into two classes was achieved through the implementation of a high-pass filter. Due to the reduced spatial resolution, additional steps such as smoothing and polygon to centerline conversion were necessary and were implemented. Validation data was digitized manually from both the DOP and the Sentinel-2 image. Out of 977 plots in the study area, validation data was collected from the DOP for 519 and from the satellite image 219 for fields.

Furthermore, a comparison was conducted between DOP and Sentinel-2, using the additional information on crop type (IACS) to draw conclusions on the most efficient calculation methods for future research.

5 Results and Discussion

5.1 Application of machine learning and image compositions for mapping the soil cover “overwintering stubble” in the agricultural landscape (Manuscript 1)

In the case of the selected datasets, which were subjected to a detailed analysis, the Support Vector Machine (SVM) achieved superior results in comparison to the Random Forest (RF). An isolated analysis of the target class indicated that the SVM yielded superior results by a margin of 8 to 10 percentage points. Within the datasets, however, there were only minimal deviations (84.2% to 83.8%) when using the same method (SVM). The pixel-based classification process invariably leads to the "salt and

pepper" effect of satellite imagery. To enhance the confidence in the presence of "overwintering stubble" in a specific field, a threshold value of minimum pixels per field was implemented. Once an area contained 65% or more of the overwintering stubble class pixel, the result was considered reliable enough to assign the entire area to the overwintering stubble class. The implementation of this post-processing method resulted in an immediate and positive impact on the outcomes. Consequently, a maximum of 92.6% of the target areas were identified as stubble fields (see Table 2). However, it should be noted that this corresponded to only 74.6% of all individual plots for which this land cover was known. The analysis indicated that large agricultural regions were particularly benefited by the implementation of a threshold value. Conversely, small areas or those with intricate geometric configurations proved more challenging to discern through remote sensing methods, thus not deriving any benefit from post-processing.

The aforementioned mixed pixels and edge pixels in the periphery of the agricultural areas presented a promising avenue for further enhancement, as these pixels were inherently responsible for the classification fuzziness. In principle, smaller areas stand to benefit from this post-processing, as it leads to a reduction in the relative proportion of mixed pixels in the total area and a shift in focus toward the core of the agricultural area. In practice, the proportion of correctly classified fields also improved to a very good 96.1% (-10 m buffer) and 96.5% (-20 m buffer) at a threshold value of 65% (Table 3). However, this enhancement was not observed in the results for small agricultural areas. Instead, it was due to the automatic exclusion of these areas, as they were completely buffered out. While approximately one-seventh of all plots were excluded by this method, these fields constituted a mere 0.1% (-10 m buffer) and 0.4% (-20 m buffer) of the total area excluded from the analysis (Table 3). This highlights the high applicability of the method to the entire study area, but at the same time requires early communication that a significant portion of the (smaller) individual fields must be surveyed using other methods in order to conduct a holistic approach.

Table 2: Classification improvements using a negative buffer in the target fields. Detailed analysis of dataset 1 and SVM (best case) and the influence of threshold on classification results (Goihl 2023a).

Parameter	Dataset 1 SVM		
Buffer in m	0	-10	-20
Number of fields	71	62	60
Total stubble field area in ha	679.85	581.82	491.66
Stubble field area found in classification (ha)	572.72	519.99	449.99
Share of correct found area	0.842	0.894	0.915
Improve results by	0	0.052	0.073
Share of stubble field area at threshold 0.5	0.956	0.962	0.984
Share of stubble field area at threshold 0.65	0.926	0.961	0.965
Share of stubble field area at threshold 0.75	0.785	0.800	0.880

Table 3: Classification improvements using a negative buffer in the target fields at the best scenario (Dataset 1 SVM). Comparison between different ranges of negative buffer. Number of fields total: n = 71 (Goihl 2023a).

Dataset 1 SVM	Method: Buffer -10 m	Method: Buffer -20 m
Correct stubble classification	0.894	0.912
Share of fields with >65 % correct classified stubble	0.871	0.867
Share of field area with >65 % correct classified stubble	0.961	0.965
No. of fields excluded from evaluation by buffering	9	11
No. of fields remaining	62	60
Stubble area total with excluded fields	679.85 ha	679.85 ha
Stubble area of excluded fields	1.21 ha	2.96 ha
Area share of excluded stubble fields	0.0016	0.004

In certain cases, however, farmers may have left stubble on their land without applying for subsidies (in which case no validation data is available). Conversely, areas of stubble outside the fields to be validated were also detected. To obtain a comprehensive understanding of the land cover class, it was imperative to examine the possibly "voluntary" practices. A comparison with the previous and subsequent crop showed that it would only have been possible to leave over-wintering stubble in approximately 50% of cases. This finding led to the failure to map such areas outside the control areas, as this accuracy was too error-prone for government applications.

The main findings were that the use of Corine Land Cover (CLC 2021) as a classification proxy is a cost-effective method of training data acquisition (Demir et al. 2013), but the classification results remained comparable to other studies (Tassi & Vizarri 2020). Removing edge and mixed pixels while applying majority filters (from 65% share) led to the mapping of more than 90% of the target area size, but also excluded about 25% of the smaller areas from the analysis. By setting the threshold value of the majority filter, it was possible to clearly illustrate the dependency between the certainty of the results and the remaining need for examination (Table 2). The setting of the threshold value is highly dependent on the task to be processed and the significance of the data set for decision-making for the user.

5.2 Evaluation of Copernicus HR-VPP product usefulness in case of the year 2018 drought in Saxony (Manuscript 2)

The HR-VPP data proved to be a suitable resource for reanalyzing the 2018 drought at both the spatial and crop-specific levels. The spatial level revealed significant heterogeneity in the results, particularly evident at the municipal scale, highlighting the presence of small-scale variations (Figure 2). However, by expanding the spatial level to encompass district-level analysis, the pronounced variations observed at the municipal level were largely averaged out, leading to a more averaged view of the drought's characteristics (Figure 3). Nevertheless, detectable differences between the

respective districts and crop types remained (Figure 3). Figure 3 emphasizes the percent deviation of the VPP mean values between the drought year (2018) and the reference years (2017, 2019, and 2020). Across all regions and most crop types, a further decline in VPP productivity due to the impact of drought was observed. The various forms of grassland use (clover grass, field grass, meadow, mowing pastures, pastures) or the Görlitz region were particularly affected (Figure 3).

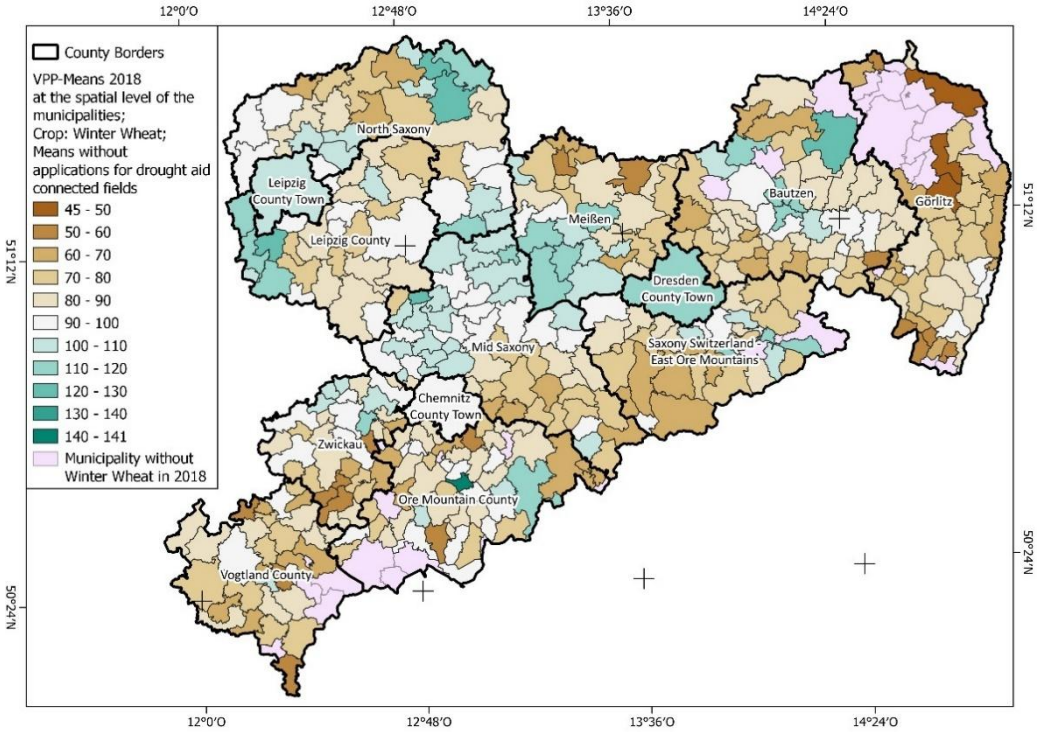

Figure 2: This map shows the VPP mean values for winter wheat in 2018 at the municipality level. There is a high variability between municipalities within the same county (see Meißen, Mid Saxony or North Saxony). Reference System: WGS 84 (Goihl 2023b).

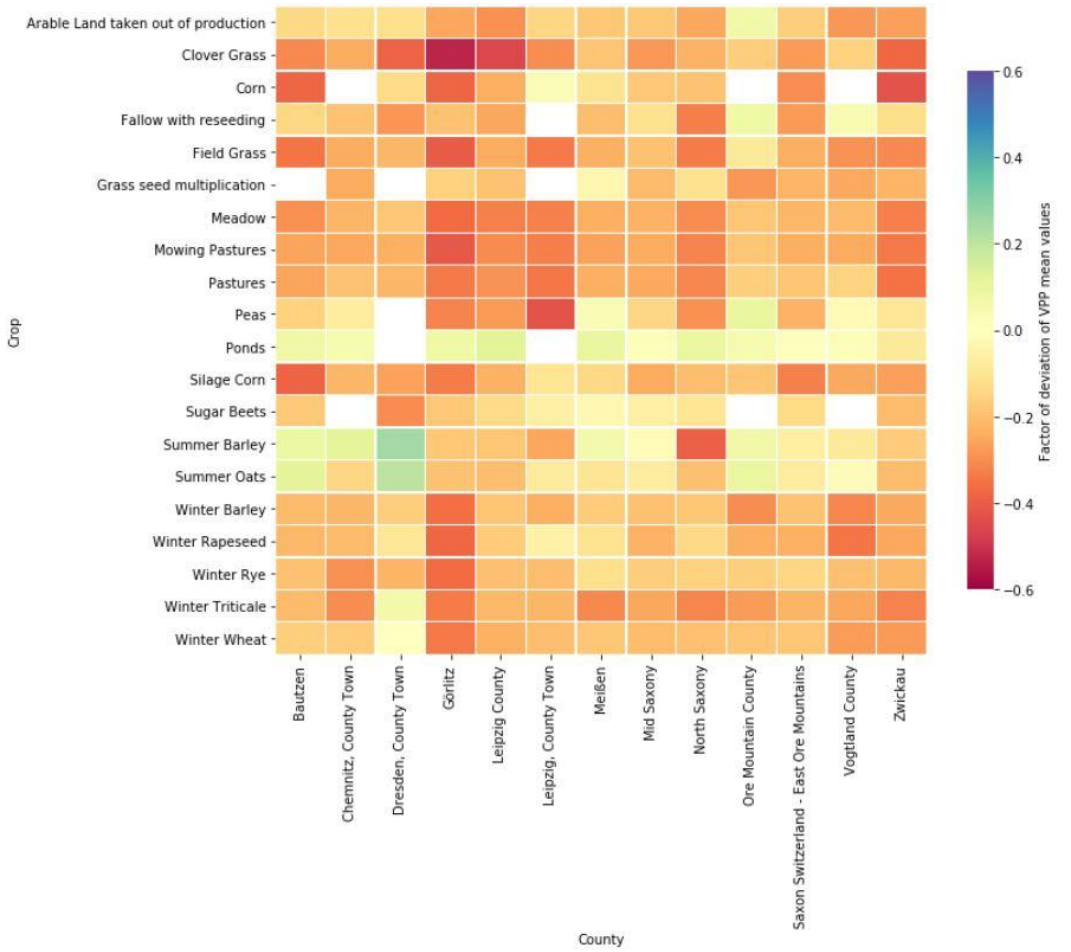

Figure 3: Percent deviation of VPP mean values per crop and county in Saxony in 2018 compared to reference years (mean from 2017, 2019 and 2020). Presented at this point: All farms without a drought relief application (Goihl 2023b).

The evaluation of the "VPP-based Farm-Level Temporal Comparison Indicator" (FLTCI) values, as outlined in section 4.2, revealed that the application status of the farms in question had no discernible impact on their performance in relation to drought aid. According to the VPP productivity values per district and crop type, the applicants once again performed measurably weaker than the non-applicants. However, this disparity did not hold when considering the farm level. Instead, Figure 4 clearly shows that applicants and non-applicants are located in the same areas in the matrix and that no clear distinction between the clusters was possible.

This discrepancy can be attributed to the application's foundation on accounting results. However, given the absence of spatial data on individual fields, the application's overall representation is constrained to the level of a single farm. In instances where a neighboring farm with analogous fields did not submit an application due to its superior economic standing, the formation of a cluster based on the FLTCI values was not feasible. The presence of numerous subjective factors influencing the application for drought aid has resulted in a lack of objective patterns in the remote

sensing data. However, the identification of such patterns would have been valuable in order to be able to predict warning signs and possible damage amounts for the purposes of policy advice. In the context of future drought events, the FLTCI will play an important role in the comparative descriptive statistics of the reanalysis.

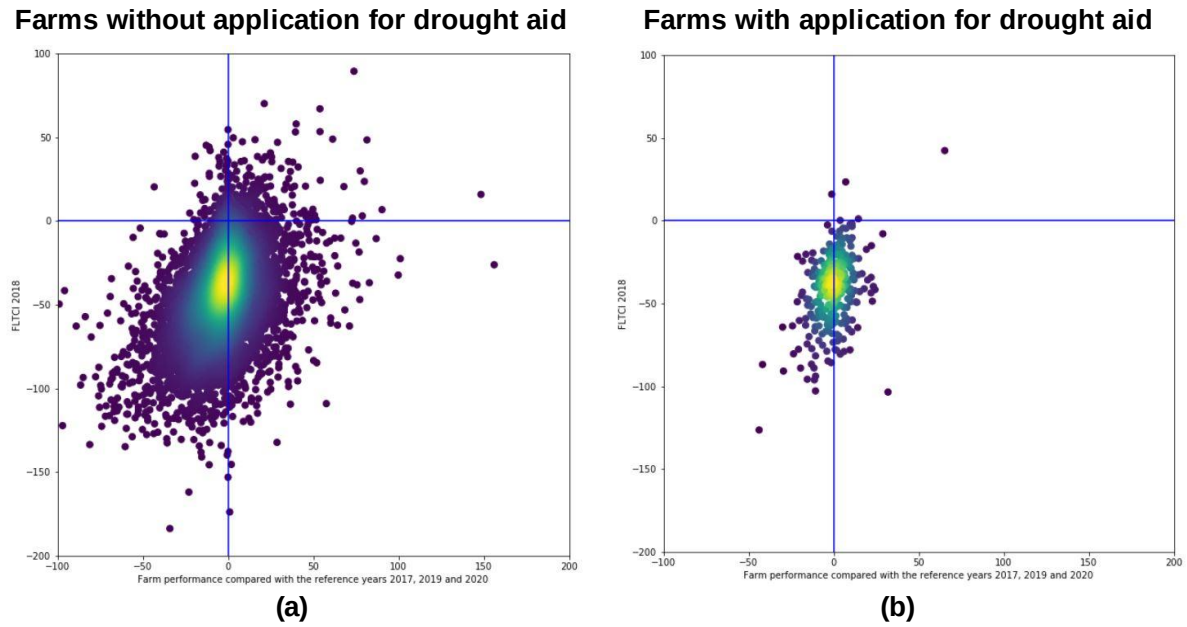

Figure 4: VPP-based Farm-Level Temporal Comparison Indicator performance. The zero lines divide the graphs a) and b) into four fields each. The square in the upper right-hand corner contains the farms that came through the 2018 drought year with higher productivity (y-axis) than in the comparison and that had higher VPP productivity than in the productivity of the reference years (x-axis). Accordingly: bottom right square: worse productivity in drought year 2018 + better than reference years; bottom left square: worse productivity in drought year 2018 + worse than reference years; top left square: better productivity in drought year 2018 + worse than reference years (Goihl 2023b).

For decision-makers in politics and agriculture, the VPP values also imply a communication problem because, unlike yield data (StaLa 2018), they are not easy to understand. These values, by their very nature, require an understanding that extends beyond that of the expert, and a direct translation into yield data has not been possible. The VPP is derived from the intensity and duration of the vegetation period within each pixel; however, yield generation takes place partially below ground (e.g. sugar beet, potato), in a part of the plant (e.g. cereals, oilseeds), or as a whole plant (e.g. corn, grass), depending on the crop type. The HR-VPP, however, was not designed to deal with this variability. The 2018 VPP exhibited the closest approximation to the reference for rapeseed and silage maize, while the yield losses in grassland were inadequately recorded and underestimated by up to 20 percentage points.

5.3 Tillage direction analysis from DOP and Sentinel-2-images (Manuscript 3)

The results are structured analogously to the initial data used (DOP and Sentinel-2). The great dependence on phenology, time of recording and spatial resolution of the systems applied equally to both methodological approaches. For the DOPs, the exclusion of grassland (which has an erosion-protective effect and therefore did not need to be considered in depth) and the turning zones already meant a large potential for improvement (Figure 5). This reasoned approach already increased the R^2 from 0.379 to 0.703 (Figure 5). By identifying and reducing the crop types to those that could be analyzed phonologically at the time of the study, the R^2 could be improved to 0.867 (Figure 6, Table 4).

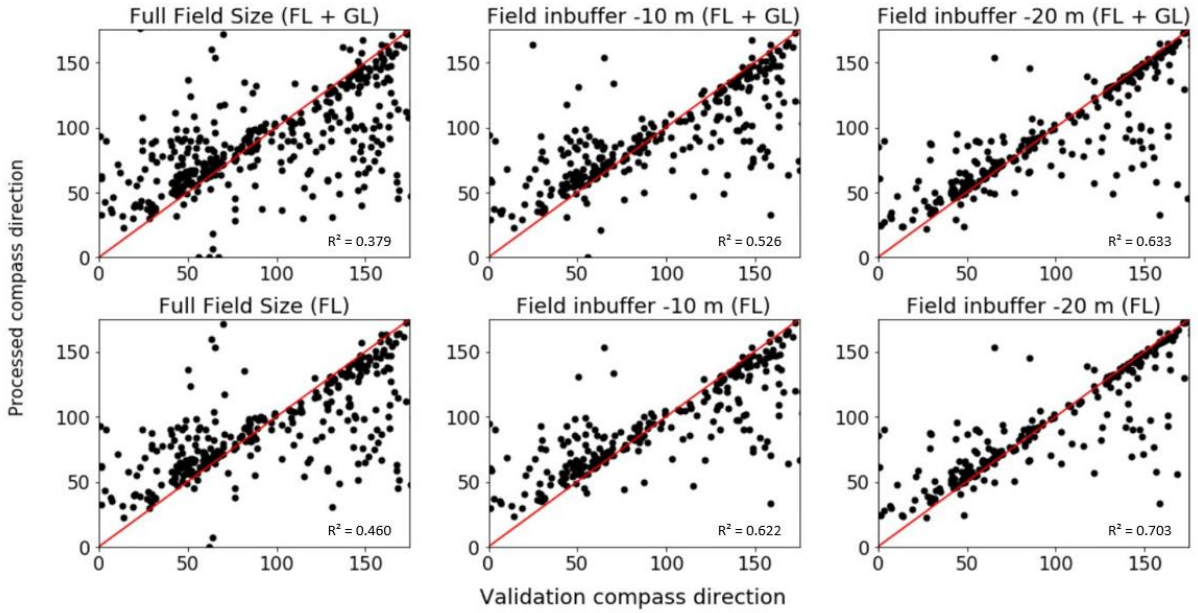

Figure 5: Scatterplots comparing the DOP-validation compass direction to the DOP-processed compass direction for each field which had validation data. Special consideration of edge effects (negative buffer in m) and differentiation between farmland (FL) and grassland (GL) (Goihl 2025).

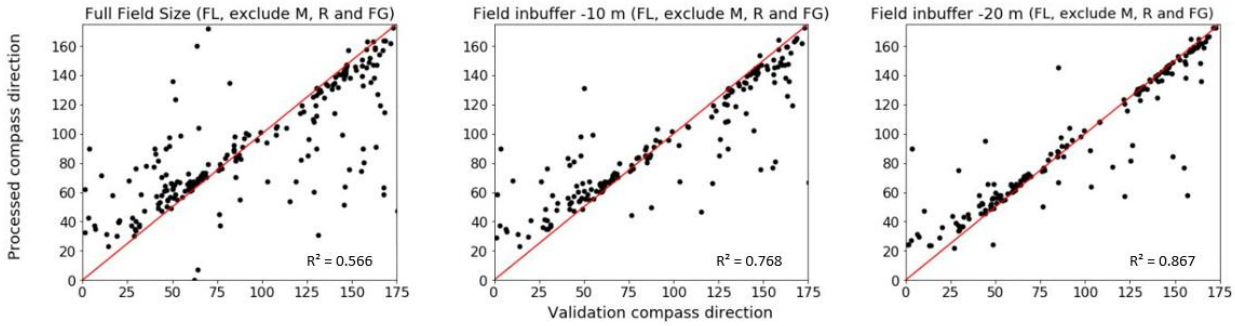

Figure 6: Scatterplots for Farmland (FL) comparing the DOP-validation compass direction to the DOP-processed compass direction for each field which had validation data. Special consideration is paid to edge effects (negative buffer in m) and the selection of particularly suitable crop species (M = Maize, R = Rapeseed, FG = Field Grass). (Goihl 2025).

In the study area, which encompassed 519 fields with a total area of 5,374 hectares, a maximum of 400 fields with an area of 4,967 hectares could be documented. However, the analysis revealed only a low correlation of $R^2 = 0.379$. Table 4 systematically illustrates the enhancements achieved by excluding uncertainty factors such as crop classes and edge effects. The most significant enhancement was attained by incorporating arable land, excluding maize, rapeseed, and field grass within a buffer of -20m. Consequently, R^2 demonstrated a notable enhancement, reaching 0.867. The exclusion of crop types was a direct result of the DOP recording date and the phenological development in the fields of the study area.

Table 4: Results and properties of the DOP analysis (Goihl 2025).

Total:	Number of fields in Validation dataset Field Area Sum in ha	519 5.374	Number of fields in AOI Field Area Sum AOI in ha	977 5.911
Land Use Classes		**Buffer = 0 m**	**Buffer = -10 m**	**Buffer = -20 m**
Farmland & Grassland	**Description**	All Agricultural Land, also erosion protecting grassland, turnaround area and field boundaries included	All Agricultural Land, also erosion protecting grassland, turnaround area partly included	All Agricultural Land, also erosion protecting grassland, turnaround area removed
	Number of fields	400	301	276
	Field Area Sum in ha	4.967	4.285	4.086
	R^2	0.379	0.526	0.633
Farmland	**Description**	All Agricultural Land, turnaround area and field boundaries included	All Agricultural Land, turnaround area partly included	All Agricultural Land, turnaround area removed
	Number of fields	323	267	255
	Field Area Sum in ha	4.703	4.160	4.002
	R^2	0.460	0.622	0.703
Farmland without Maize (M), Rapeseed (R) and Field Grass (FG)	**Description**	Farmland excluding R, M and FG, turnaround area and field boundaries included	Farmland excluding R, M and FG, turnaround area partly included	Farmland excluding R, M and FG, turnaround area removed
	Number of fields	214	177	**170**
	Field Area Sum in ha	3.051	2.718	**2.687**
	R^2	0.566	0.783	**0.867**

In the evaluation of Sentinel-2 images, only 219 fields were recorded. Analogous to the DOP evaluation, the influence of the turning zones, phenology, and monitorable crop types at the time of satellite image acquisition was investigated once more. The quality metrics for the validation data ranged from $R^2 = 0.646$ to 0.833, depending on the combination. The optimal result, $R^2 = 0.833$, was achieved without buffering, only considering arable land (only wheat (W), maize (M), potatoes (P) and legumes (L)). This analysis involved the consideration of a total of 141 fields, encompassing an area of 1,875 hectares, which constitutes slightly less than a third of the total study area. It was also determined that the tolerance level for Sentinel-2 images in medium spatial resolution must be adjusted in comparison to the DOP. Rather than a maximum

deviation of 10° in compass angle, as previously defined, the focus was extended to a maximum deviation of 20° from the validation data to be considered a usable result. As illustrated in Figure 7, the orientation of the validation lines (a) is depicted alongside the orientation of the processed lines (b) for the Sentinel-2 image. The result (c) was found to be very heterogeneously distributed in the map image.

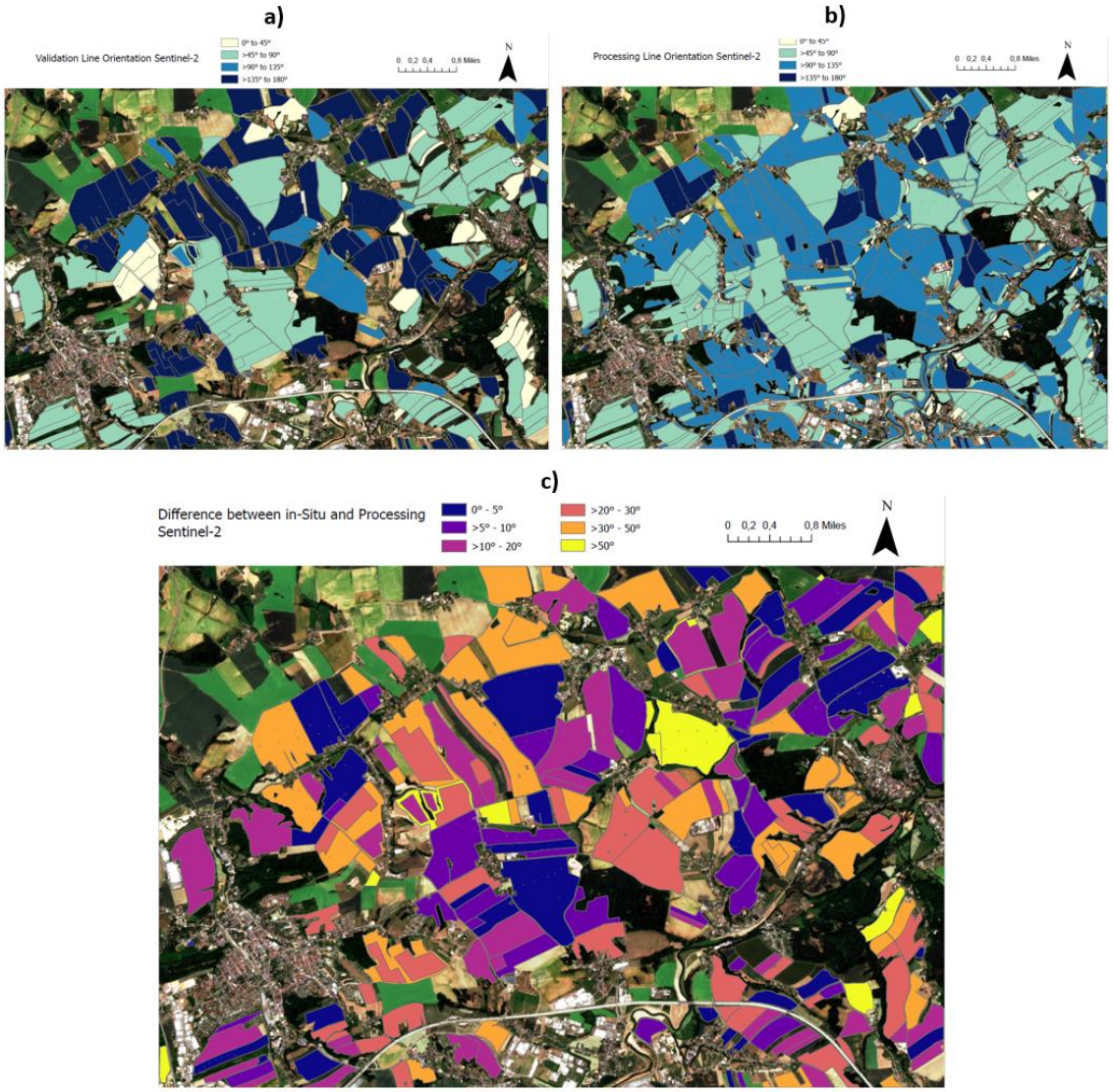

Figure 7: Processed and validated tillage directions at the area of interest. (a) Tillage Direction of the field after evaluation of the Sentinel-2 validation lines, (b) Tillage Direction of the field after evaluation of the Sentinel-2 processing results, (c) Difference between Sentinel-2 in-situ validation tillage directions and processing tillage direction from well matching results in dark blue to poor matches in yellow (Goihl 2025).

5.4 Dealing with and communicating uncertainties

Dealing with uncertainty had two main aspects: The initial aspect was to determine the application-specific acceptance level of uncertainties in the products used by the users themselves. The second aspect is further product development and the associated analysis of the main sources of uncertainty and their active reduction at all stages of product generation. It is imperative that completed products be communicated in terms

of their possibilities and limits of use. Quality metrics (Chow & Kar 2016) can be employed for this purpose. The validation of research outcomes and products using corresponding quality metrics is a common practice.

For the initial aspect previously mentioned, Harken et al. (2019) developed two critical inquiries that decision-makers in the domain of agricultural administration must pose to themselves based on model outcomes:

"How much uncertainty is acceptable?

How does one obtain the necessary information for such an acceptable level of uncertainty?"

Despite the inability to provide a comprehensive response to the initial inquiry, the optimal approach for addressing it entails a balanced consideration of the trade-off between the financial resources involved and the consequences of using/not using these products (Harken et al. 2019). For instance, the availability of cost-free satellite imagery (Sentinel-2) leads to extraordinary cost advantages compared to other remote sensing systems (Sentinel-2 at 0.20 €/ha vs. multirotor UAV at 5.52 €/ha) (Guetschow & Fuchs 2024).

The second inquiry is contingent on the specific application. An approach to this question in relation to the introductory stakeholder analysis (Chapter 1.2) leads to the derivation of Table 5. The acceptable level of uncertainty, depending on the use case and spatial scale, ranges from low to very high.

*Table 5: Decision and accuracies by farmers and government based on information derived from satellite remote sensing. AoI = Area of Investigation. Derived from Jewiss et al. 2020. *Theoretical use case: Determining eligibility for aid in extreme events (e.g. drought, flood), high accuracy needed.*

User	Farmer		National/Regional Government	
Scale	**Application**	**Accuracies needed**	**Application**	**Accuracies needed**
Field	Crop Management; Efficiency	good	CAP - Crop Monitoring - Control	Very high
Farm	Farm Decision Making; resources management/planning	moderate	-*	-*
Regional	-	-	AOI - Mapping the current situation; Monitoring, Trend analysis	moderate
National	(expected) Market Situation; Import/Export	low	AOI - Mapping the current situation; Monitoring, Trend analysis	moderate
Global	(expected) Market Situation; Import/Export	low	-	-

The studies presented (Goihl 2023a, Goihl 2023b, Goihl 2025) also had to deal intensively with these above questions. In their proof-of-concept status they served primarily as a guide for determining and dealing with uncertainty factors (Chapters 2 to 5), as well as for addressing the fundamental issue of transferring remote sensing data to administrative applications. The core problem for the government user is the

confidence in the data, especially when decisions are to be made based on remote sensing data that have direct consequences for third parties. It is a well-established fact that uncertainties have the capacity to influence decision making (MacEachren et al. 2005). To what extent does an object, a pixel, or a measurement correspond to reality? Did the user accurately select the area that is a misclassification? What security mechanisms are in place and how are the risks of the application reduced? The fewer misclassifications in the system, the higher the acceptance by the user, the stakeholders and the persons affected. Depending on the use case (Table 5), the accuracy is crucial for the usage.

Additional methods could be established to validate the methodology when the remote sensing results contain too many uncertainties. For example, a traffic light system could be used to categorize fields according to the certainty of the modeling results (OPEKEPE 2020). For example, these cases could be then clarified by timely geotagged field surveys (Wu et al. 2023, European Union 2022). This could contribute to a cascading assurance of product quality. At this point, an extension of the mentioned questions can be derived according to Harken et al. (2019):

How much contradiction is acceptable?

This issue deals specifically with the consequences of the application and requires an estimate of the number of objections, the associated resource expenditure compared to the previous procedure and the development of rule-based administrative acts for dealing with objections, e.g. via the above-mentioned traffic light system with subsequently triggered on-site inspections. This is always linked to the latent question of what could happen in the worst case when a user uses this official government data. In this case, the data user can be the state itself or, for example, a citizen via access to open data portals, depending on the product.

The second aspect of dealing pertains to the iterative process of product development. Aleatory sources of error (see Chapter 2.1) can be mitigated by enhancing observational accuracy and precision (Paasche et al. 2020). Addressing epistemic sources of error necessitates increasing the return of experimental information (Paasche et al. 2020). However, this approach requires additional effort, e.g. by expanding the recording parameters for in-situ mapping (known unknowns) or additionally expanding the data with UAV recordings (Table 1). However, it should be noted that a comprehensive cost-efficiency comparison to the added value cannot be guaranteed for these efforts (Guetschow & Fuchs 2024). Additionally, in-situ data

collection is not immune to errors (Ray & Burgman 2006), suggesting that an increase in recording parameters may also lead to an additional source of error.

Quality management and the associated optimization are holistic processes within the generation of remote sensing products. The range of potential interventions includes data selection, in-situ data collection, method selection (Werther & Burggraf 2023, Safonova et al. 2023), post-processing (Goihl 2023a, Goihl 2025) and the supply of the final product (Triebnig et al. 2024) and additional information (Table 6).

The establishment of remote sensing as a reliable and operational data source must be carried out in the awareness of data users. To this end, transparent communication regarding the capabilities and limitations of remote sensing is strongly recommended. It is essential to manage expectations, acknowledging the limitations mentioned in Table 1. Table 6 presents a range of communication methods that are available to both producers and users of remote sensing products to increase transparency. It is necessary to communicate not only the uncertainties, but also the risks of the application (Harken et al. 2019). Povey & Grainger (2015) highlight the need for close communication with users and suggest that the following information is specifically important: an error budget that outlines quantified sources of error, a description of available quality control information and its physical significance, and known weaknesses in the data that are not represented by the uncertainty.

Table 6: Selection of practices for communicating and visualization of uncertainties.

Communication medium	Communication medium	Impact	Reference
Documentation	User manuals, validation studies, quality assurance labels and/or measurements of the level of maturity of the product	Fulfilling the user's information needs through reporting	Povey & Grainger 2015
Quality metrics	Like error, BIAS, RSME, MSE, R^2, user and producer accuracy, box plot, violin plot, histogram, scatter plot	Description of different kinds of model accuracy	Chow & Kar 2016, all case studies
Masking	Masking maps: Cloud, Shadow, Snow, Ice, Resolution (masks out areas/objects that cannot be geometrically detected with remote sensing)	Exclusion of erroneous pixels, incomplete results, bad pixels, Investigation focuses on recordable geometries	Sudmanns et al. 2020, Hall et al. 1995, Härer et al. 2018, Mueller-Warrant & Whittaker 2015, Lakso 2022
Quality flag map, error map	General error map, can combine several error sources	Additional map, uncertainty areas shown	MacEachren et al. 2005, Chow & Kar 2016
Cloud flag mapping	Shows how often pixels were covered by clouds, e.g. for time series analysis, image composites	Additional map, usable data basis in addition to possible data	Ernst et al. 2018
Pixel confidence map; Probability map; Purity estimator	Confidence of the classifier per pixel, multiple classes with their confidence per pixel (fuzzy logic)	Additional map, areas with high and low uncertainties shown	Mirpulatov et al. 2023, Devos et al. 2020, Murmu & Biswas 2015, Serra & Pons 2015
Voting map; Uncertainty map	Confidence of the pixel over several classification runs	Additional map, areas with high and low uncertainties shown	Beekhuizen & Clarke 2010, Cui et al. 2018

Communication medium	Communication medium	Impact	Reference
Traffic light system	Marks results according to quality	Users can immediately differentiate between good and bad results and initiate targeted additional measures	OPEKEPE 2020, Schulz 2021

As demonstrated in Table 5, there is no universally optimal approach for representing uncertainty (MacEachren et al. 2005). A significant proportion of the methods under discussion were of a visual nature, and communication was frequently constrained to the case studies. Consequently, there is a need to understand how uncertainty communication affects decision-making and how multiple uncertainty factors can be represented efficiently (MacEachren et al. 2005). Government users must also deal with the challenge of applying uncertainty in accordance with the legislative basis for decision making.

Koedel et al. (2022) point out that the secondary user of a product will not be able to understand the significance, accuracy and limitations of such a map if they do not have comprehensive background information on the product. For example, areas can already be assigned to a class in classifications if the relatively highest proportion of area determines this (Devos et al. 2020). With a high class density, the relative proportion can be very low, but the user of the product only sees the classification result and considers this to be final. In the absence of the means of communication enumerated in Table 6, the accuracy of products is questionable without further elucidation.

Chow and Kar (2016) underscored the distinctive characteristics of geospatial data and scale. Due to their specific nature as point, line, or area objects, spatial data already bring special properties to analyses that make it difficult to compare or reuse a methodology. The correlation between spatial objects is also more or less strong depending on the distance, and the correct selection of an interpolation method for spatial data is a challenge, but a source of error (MacEachren et al. 2005).

One obstacle to communication is the variety of information involved. In the absence of integration within the data product (masks), users are required to use several products simultaneously in order to interpret the main product. This reduces the attractiveness of the main product, especially the more additional products there are, and the more expert knowledge is required. To increase the state agency user's sense of certainty, usage categories could be used in which responsibility for the products is transferred to specialized service providers to various degrees (Laue et al. 2024).

However, this approach increases the dependency on these service providers and the challenge of continuing to guarantee data protection and information security. Consequently, the government also loses sovereignty over the holistic process.

6 Conclusion and outlook

The central objectives of this thesis were to study and develop products of remote sensing for their informative value specifically for questions and needs of agricultural administration. The presented studies systematically analyzed various aspects of this extensive topic, encompassing several properties, including the impact analysis of spatial differentiations, the identification of opportunities for minimizing uncertainty in the products, and the interpretation of the products from the perspective of the authorities for the technical application. In addition to the development of products, the study encompassed the testing of products from the Copernicus service. This involved the comparison of different algorithms and the examination of the spatial effects of the results. Furthermore, various options for minimizing uncertainties in post-processing were tested.

The first publication investigated the monitoring capability of the temporary land cover "overwintering stubble". In this study, the classifiers Random Forest (RF) and Support Vector Machines (SVM) were evaluated on various combinations of image composite. The SVM emerged as the most suitable classifier and achieved good classification results for the investigated land cover. The employment of a majority filter, coupled with the exclusion of edge effects, enabled the identification of substantial areas classified as "overwintering stubble". However, this approach also led to the exclusion of small areas, which, although having a small total area size, contributed a relatively large number of areas. Areas without validation data, but which could have had this land cover and which were also classified as stubble, could not be adequately determined. In summary, this study offers promising approaches for future monitoring of this land cover, to verify government-aided measures.

The second publication examined the HR-VPP product of the Copernicus Land Service for its usability in analyzing and evaluating the 2018 drought event in the agricultural sector. Geographical information system (GIS) methodologies were employed for this objective. Additionally, an evaluation was conducted to ascertain whether the applications for drought aid in the HR-VPP product were also reflected in the data compared to non-applicants. While the product demonstrated general capability in

identifying spatial and crop-specific variations between the comparison years (2017, 2019, 2020), significant challenges emerged at the farm level. The limited time series of the data and the influence of crop rotation severely limited comparisons, necessitating spatial aggregation and the development of a separate comparison index. General differences between applicants and non-applicants for drought aid could not be identified. The index values were also found to be a major obstacle, as these values are difficult to communicate to stakeholders. The index values were found to be outside the range of conventional units such as dt/ha, which further compounded the challenge of interpretation due to their dimensionless nature.

The third publication developed and compared the possibility of deriving the main cultivation direction of a field (compass direction) from the DOP and Sentinel-2 data sources. While the tractor tracks could be used for the DOPs, the analysis of the Sentinel-2 data had to be based on spatial patterns that had developed through the regular cultivation of the fields. The data was processed using GIS methods to extract the direction of cultivation. The validation data was digitized manually from the data sources. The analysis revealed comparable and good peak results from both DOP and Sentinel-2. To this end, it was essential to ascertain the influences of boundary effects, phenology, and associated crop types. This information was used to exclude poorly mappable crop types at the respective time of investigation. This post-processing approach led to a substantial enhancement in the accuracy of the results, though it reduced the number of fields that could be monitored and the absolute area of the total study area. The utilization of Sentinel-2 data, with its medium resolution, in this context represented an innovation, as it had never been used for such a question before.

The practical relevance of this thesis is notable, as it investigates very administration-specific use cases that were outside the scope of previous research. The novelty value of this thesis was particularly evident in the fact that little comparative literature was available to discuss the results. A distinguishing feature of all three publications was their examination of the discrepancy between research and practical application, with a subsequent promotion of methods to bridge this gap (Goihl 2023a, Goihl 2023b, Goihl 2025). The methods selected generally produced good results on which future applications could be based (Goihl 2023a, Goihl 2025). However, the data examined (Goihl 2023b) also clearly showed their weaknesses and limited future usability to some specific documentary aspects.

The use of satellite remote sensing data in government agencies must always be considered in the context of the legal requirements to be fulfilled. The strengths of remote sensing in the spatiotemporal monitoring of objects under investigation were contrasted by fixed parameters, investigation dates and the monitoring capability of the object under investigation itself. Furthermore, remote sensing methods were in direct opposition to established terrestrial methods. The potential for remote sensing to become an established method in agricultural administration is most likely to be found in legal requirements. These requirements may include a) defining the satellite system as a source of data or b) specifying tasks that can only be performed cost-effectively by remote sensing methods. Achieving this objective would depend on opening up the parameters to be recorded to the extent that they can be met by standard satellite systems (time windows, points in time, recording parameters, spatial resolution).

However, as the further development of legal requirements takes time and remote sensing experts are generally not involved in this process. Remote sensing methods will be slow to establish themselves in the agricultural governmental sector outside the CAP (European Union 2021a, European Union 2022). In addition, public authorities do not have the human and IT resources to process remote sensing data with the necessary expertise and efficiency.

In summary, the present thesis demonstrated the possibility of agricultural remote sensing to achieve high quality results for specific governmental issues, despite the various uncertainty factors (Table 1). These proof-of-concept studies were necessary to strengthen future confidence in these methods, which are still new to many users, and thus provided an important link between research and practice. It is also necessary that all publications openly address the possibilities and limitations of remote sensing data and methods in order to support the basis for an honest, fact-based discourse on the use of remote sensing in public administration.

References

Adiyaman, H., Emre Varul, Y., Bakırman, T., & Bayram, B. (2025). Stripe Error Correction for Landsat-7 Using Deep Learning. *PFG* 93. https://doi.org/10.1007/s41064-024-00306-x

Ali, A.M., Abouelghar, M., Belal, A.A., Saleh, N., Yones, M., Selim, A.I., Amin, M.E.S., Elwesemy, A., Kucher, D.E., Maginan, S., & Savin, I. (2022). Crop Yield Prediction Using Multi Sensors Remote Sensing (Review Article). *The Egyptian Journal of Remote Sensing and Space Sciences*, 25(3). https://doi.org/10.1016/j.ejrs.2022.04.006.

Andreo, V., Belgiu, M., Brito Hoyos. D., Osei, F., Provensal, C., & Stein, A. (2019). Rodents and satellites: Predicting mice abundance and distribution with Sentinel-2 data, *Ecological Informatics* 51, https://doi.org/10.1016/j.ecoinf.2019.03.001.

Bach, H., & Mauser, W. (2018). Sustainable Agriculture and Smart Farming. – In: *Earth Observation Open Science and Innovation. ISSI Scientific Report* 15. Mathieu, P.-P., Aubrecht, C. (Editors). pp. 261-270. https://doi.org/10.1007/978-3-319-65633-5. Springer, Cham.

Baetens, L., Desjardins, C., & Hagolle, O. (2019). Validation of Copernicus Sentinel-2 Cloud Masks Obtained from MAJA, Sen2Cor, and FMask Processors Using Reference Cloud Masks Generated with a Supervised Active Learning Procedure. *Remote Sensing*, *11*(4). https://doi.org/10.3390/rs11040433.

Beekhuizen, J., & Clarke, K.C. (2010). Toward accountable land use mapping: Using geocomputation to improve classification accuracy and reveal uncertainty. *International Journal of Applied Earth Observation and Geoinformation*, 12. https://doi.org/10.1016/j.jag.2010.01.005.

Beillouin, D., Schauberger, B., Bastos, A., Ciais, P., & Makowski, D. (2020). Impact of extreme weather conditions on European crop production in 2018. *Philos Trans R Soc Lond B Biol Sci*. 26,375(1810). https://doi.org/10.1098/rstb.2019.0510.

BGR - Federal Institute for Geology and Natural Resources (2025). Ackerbauliches Ertragspotential der Böden in Deutschland. Available online: https://www.bgr.bund.de/DE/Themen/Boden/Ressourcenbewertung/Ertragspotential/Ertragspotential_node.html (accessed on 27.03.2025).

Bitkom Research (2024). So digital ist die Landwirtschaft (This is how digital agriculture is). Available online: https://www.bitkom.org/sites/main/files/2024-06/Bitkom-Charts-Pressekonferenz-Digitalisierung-der-Landwirtschaft.pdf (accessed on 17.03.2025).

BMEL - Federal Ministry of Food and Agriculture (2024). Agrarzahlungen 2023 veröffentlicht (Agricultural subsidies for 2023 published). Available online: https://www.bmel.de/DE/themen/landwirtschaft/eu-agrarpolitik-und-foerderung/direktzahlung/veroeffentlichung-eu-zahlungen.html (accessed on 11.03.2025).

Bontemps, S., Bajec, K., Cara, C., Defourny, P., de Vendictis, L., Heymans, D., Kucera, L., Malcorps, P., Milcinski, G., Nicola, L., Slacikova, J., Taymans, M., Tutunaru, F., & Udroiu, C. (2024). Sen4CAP- Sentinels for Common Agricultural Policy. System Software User Manual. Available online: https://www.esa-sen4cap.org/wp-content/uploads/files/Sen4CAP_SUM_v4.0.pdf (accessed on 23.03.2025).

Borrmann, P., Brandt, P., & Gerighausen, H. (2023). MISPEL: A Multi-Crop Spectral Library for Statistical Crop Trait Retrieval and Agricultural Monitoring. *Remote Sensing*, 15(14). https://doi.org/10.3390/rs15143664.

Brus, J., Pechanec, V., & Machar, I. (2018). Depiction of uncertainty in the visually interpreted land cover data. *Ecological Informatics*, 47. https://doi.org/10.1016/j.ecoinf.2017.10.015.

Buettig, S., Lins, M., & Goihl, S. (2022). WaterMaskAnalyzer (WMA) — A User-Friendly Tool to Analyze and Visualize Temporal Dynamics of Inland Water Body Extents. *Remote Sensing*, *14*(18), 4485. https://doi.org/10.3390/rs14184485.

Castro, M., Ameray, A., & Castro, J.P. (2020). A new approach to quantify grazing pressure under mediterranean pastoral systems using GIS and remote sensing. *International Journal of Remote Sensing*, 41(14), 5371–5387. https://doi.org/10.1080/01431161.2020.173193.

Chawala, P., & Sanhu, H.A.S. (2020). Stubble burn area estimation and its impact on ambient air quality of Patiala & Ludhiana district, Punjab, India. *Heliyon*, 6(1). https://doi.org/10.1016/j.heliyon.2019.e03095.

Chow, E., & Kar, B. (2016). 5. Error and Accuracy Assessment for Fused Data – In: *Integrating Scale in Remote Sensing and GIS*. Quattrochi, D. A., Wentz, E., Siu-Ngan Lam, N., Emerson C.W. (Editors). https://doi.org/10.1201/9781315373720-6.

Claverie, M., Ju, J., Masek, J.G., Dungan, J.L., Vermote, E.F., Roger, J.-C., Shakun, S., & C. Justice (2018). The Harmonized Landsat and Sentinel-2 surface reflectance data set. *Remote Sensing of Environment*, 219, 145–161. https://doi.org/10.1016/j.rse.2018.09.002.

CLC - CORINE Land Cover (2021). CORINE Land Cover. Available online: https://land.copernicus.eu/pan-european/corine-land-cover (accessed on 09.08.2021).

CLMS - Copernicus Land Monitoring Service (2025). Available online: https://land.copernicus.eu/en (accessed 18.03.2025).

Cui, G., Lv, Z., Li, G., Atli Benediktsson, J., & Lu, Y. (2018). Refining Land Cover Classification Maps Based on Dual-Adaptive Majority Voting Strategy for Very High Resolution Remote Sensing Images. *Remote Sensing*, *10*(8), 1238. https://doi.org/10.3390/rs10081238.

Demir, B., Minello, L., & Bruzzone, L. (2013). Definition of Effective Training Sets for Supervised Classification of Remote Sensing Images by a Novel Cost-Sensitive Active Learning Method. *IEEE Transactions on Geoscience and Remote Sensing* 52 (2), 1272-1284. https://doi.org/10.1109/TGRS.2013.2249522.

Denis, A., Desclee, B., Migdall, S., Hansen, H., Bach, H., Ott, P., Kouadio, A. L., & Tychon, B. (2021). Multispectral Remote Sensing as a Tool to Support Organic Crop Certification: Assessment of the Discrimination Level between Organic and Conventional Maize. *Remote Sensing*, *13*(1). https://doi.org/10.3390/rs13010117.

Devos, W., Luketic, N., Milenov, P., & Borio, D. (2020). Checks by Monitoring quality inspection: EU requirements and methodology. *JRC Technical Reports* (2020). Available online: https://wikis.ec.europa.eu/display/GUIDANCEANDTOOLSFORCAP/Checks+by+monitoring?preview=/86968800/86968899/CbMQA_DD_1_1.pdf (accessed on 27.03.2025).

Dong, G., Xian, W., Shao, H., Shao, Q., & Qi, J. (2023). Performance of Multiple Models for Estimating Rodent Activity Intensity in Alpine Grassland Using Remote Sensing. *Remote Sensing*, *15*(5), 1404. https://doi.org/10.3390/rs15051404.

Ernst, S., Lymburner, L., & Sixsmith, J. (2018). Implications of Pixel Quality Flags on the Observation Density of a Continental Landsat Archive. *Remote Sensing*, *10*(10). https://doi.org/10.3390/rs10101570.

European Commission (2025). GAP-Ausgaben (CAP expenditure). Available online: https://agriculture.ec.europa.eu/data-and-analysis/financing/cap-expenditure_de (accessed on 17.03.2025).

European Union (2021a). Regulation (EU) 2021/2116 of the European Parliament and of the Council of 2 December 2021 on the financing, management, and monitoring of the common agricultural policy and repealing Regulation (EU) No 2021/2116. *Official Journal of the European Union*, L 435, pp. 187–262.

European Union (2021b) Regulation (EU) 2021/2115 of the European Parliament and of the Council of 2 December 2021 establishing rules on support for strategic plans under the common agricultural policy. *Official Journal of the European Union*, L 435, pp. 1–186.

European Union (2022). Regulation (EU) 2022/1173 of the European Parliament and of the Council of 31 May 2022 on the integrated administration and control system under the common agricultural policy. *Official Journal of the European Union,* L 183, pp. 1–55.

Ferguson, R., & Rundquist, D. (2018). Remote Sensing for Site-Specific Crop Management. – In: *Precision Agriculture. Basics*. Shannon, D.K., Clay, D.E., Kitchen, N.R. (Editors). pp. 103-118. https://doi.org/10.2134/precisionagbasics. Madison.

Franch, B., Cintas, J., Becker-Reshef, I., Sanchez-Torrez, M.J., Roger, J., Skakun, S., Sobrino, J.A., van Tricht, K., Degerickx, J., Gilliams, S., Koetz, B., Szantoi, Z., & Whitcraft, A. (2022). Global crop calendars of maize and wheat in the framework of the WorldCereal project. *GIScience & Remote Sensing*, 59:1. https://doi.org/10.1080/15481603.2022.2079273.

FAO - Foreign Agricultural Service (2025). Crop Calendars for Europe. Available online: https://ipad.fas.usda.gov/rssiws/al/crop_calendar/europe.aspx (accessed on 17.03.2025).

Gao, L., Wang, X., Johnson, B.A., Tian, Q., Wang, Y., Verrelst, J., Mu, X., & Gu, X. (2020). Remote sensing algorithms for estimation of fractional vegetation cover using pure vegetation index values: A review. *ISPRS Journal of Photogrammetry and Remote Sensing*, 159, https://doi.org/10.1016/j.isprsjprs.2019.11.018.

Gao, Q., Zribi, M., Escorihuela, M. J., Baghdadi, N., & Segui, P.Q. (2018). Irrigation Mapping Using Sentinel-1 Time Series at Field Scale. *Remote Sensing*, *10*(9). https://doi.org/10.3390/rs10091495

Goihl, S. (2023a). Mapping overwintering grain stubbles using machine-learning methods and image compositions for CAP-control and Water Framework Directive connected activities. *Journal of Applied Remote Sensing.* Vol. 17(1). https://doi.org/10.1117/1.JRS.17.014515.

Goihl, S. (2023b). Determining the usefulness of the Copernicus High-Resolution Vegetation Phenology and Productivity Product (HR-VPP) with official agricultural data on cropland in case of the 2018 drought in the Federal State of Saxony, Germany. *Journal of Water and Climate Change* 14(11). https://doi.org/10.2166/wcc.2023.501

Goihl, S. (2024). Crop yield estimation uncertainties at the regional scale for Saxony, Germany. *Agronomy Journal,* 116 (6). https://doi.org/10.1002/agj2.21680.

Goihl, S**.** (2025). Tillage direction analysis in agricultural fields from Digital Orthophotos and Sentinel-2 imagery. *Remote Sensing Applications: Society and Environment,* 37. https://doi.org/10.1016/j.rsase.2025.101486.

Gorelick, N., Hancher, M., Dixon, M., Ilyushchenko, S., Thau, D., & Moore, R. (2017). Google Earth Engine: Planetary-scale geospatial analysis for everyone. *Remote Sensing of Environment,* 202. https://doi.org/10.1016/j.rse.2017.06.031.

Griffin, T.W., Shokley, J.M. & Mark, T.B. (2018). Economics of Precision Farming. – In: *Precision Agriculture. Basics*. Shannon, D.K., Clay, D.E., Kitchen, N.R. (Editors). pp. 221-230. https://doi.org/10.2134/precisionagbasics. Madison.

Guetschow, P., & Fuchs, C. (2024). The use of drones and comparison with other remote sensing methods in crop production. In: *Proceedings 24rd International Farm Management Conference in Saskatoon, Canada*, July 7-12, - Volume 1 - Academic Papers. p. 97-111.

Hall, D.K., Riggs, G.A., Salomonson, V.V. (1995). Development of methods for mapping global snow cover using moderate resolution imaging spectroradiometer data. *Remote Sensing of Environment*, 54(2). https://doi.org/10.1016/0034-4257(95)00137-P.

Hara, P., Piekutowska, M., & Niedbała, G. (2021). Selection of Independent Variables for Crop Yield Prediction Using Artificial Neural Network Models with Remote Sensing Data. *Land*, 10. https://doi.org/10.3390/land10060609.

Härer, S., Bernhardt, M., Siebers, M., & Schulz, K. (2018). On the need for a time- and location-dependent estimation of the NDSI threshold value for reducing existing uncertainties in snow cover maps at different scales. *The Cryosphere*, 12. https://doi.org/10.5194/tc-12-1629-2018.

Harken, B., Chang, C.-F., Dietrich, P., Kalbacher, T., & Rubin, Y. (2019). Hydrogeological modeling and water resources management: Improving the link between data, prediction, and decision making. *Water Resources Research*, 55. https://doi.org/10.1029/2019WR025227.

Jewiss, J.L., Brown, M.E., & Escobar, V.M. (2020). Satellite Remote Sensing Data for Decision Support in Emerging Agricultural Economies: How Satellite Data Can Transform Agricultural Decision Making [Perspectives]. *IEEE Geoscience and Remote Sensing Magazine*, 8(4). https://doi.org/10.1109/MGRS.2020.3023343.

Jiao, W., Long, T., Ling, S., & He, G. (2016). Study on modeling and visualizing the positional uncertainty of remote sensing image. *The International Archives of the Photogrammetry, Remote Sensing and Spatial Information Sciences,* XLI-B2. https://doi.org/10.5194/isprs-archives-XLI-B2-305-2016.

Jones, J.W., Antle, J.M., Brasso, B., Boote, K.J., Conant, R.T., Foster, I.A., Godfray, C.J., Herrero, M., Howitt, R.E., Janssen, S., Keating, B.A., Munoz-Carpena, R., Porter, C.H., Rosenzweig, C., & Wheeler, T.R. (2017). Brief history of agricultural systems modeling. *Agricultural Systems*, 155. https://doi.org/10.1016/j.agsy.2016.05.014.

Joy, M., Abit, M., Arnall, D.B., & Philips, S.B. (2018). Environmental Implications of Precision Agriculture. – In: *Precision Agriculture. Basics*. Shannon, D.K., Clay, D.E., Kitchen, N.R. (Editors). pp. 209-220. https://doi.org/10.2134/precisionagbasics. Madison.

Kerimkhulle, S., Kerimkulov, Z., Bakhtiyarov, D., Turtayeva, H., & Kim, J. (2021). In-Field Crop-Weed Classification Using Remote Sensing and Neural Network. *IEEE International Conference on Smart Information Systems and Technologies (SIST)*. https://doi.org/10.1109/SIST50301.2021.9465970.

Khanal, S., KC, K., Fulton, J. P., Shearer, S., & Ozkan, E. (2020). Remote Sensing in Agriculture - Accomplishments, Limitations, and Opportunities. *Remote Sensing*, *12*(22). https:/doi.org/10.3390/rs12223783.

Khlif, M., Escorihuela, M.J., Chahbi Bellakanji, A., Paolini, G., & Lili Chabaane, Z. (2023). Remotely Sensed Agriculture Drought Indices for Assessing the Impact on Cereal Yield. *Remote Sens., 15*. https://doi.org/10.3390/rs15174298.

Koedel, U., Schuetze, C., Fischer, P., Bussmann, I., Sauer, P.K., Nixdorf, E., Kalbacher, T., Wichert, V., Rechid, D., Bouwer, L.M., & Dietrich, P. (2022). Challenges in the Evaluation of Observational Data Trustworthiness From a Data Producers Viewpoint (FAIR+). *Front. Environ. Sci*., 9:772666. https:/doi.org/10.3389/fenvs.2021.772666.

Kuhwald, K., Oppelt, N., Scholze, J., & Stelzer, K. (2024). Operationalisierung von DAS-Indikatoren mit Fernerkundungsdaten (DASIF) (Operationalization of DAS indicators with remote sensing data (DASIF)). *Climate Change*, 50. https://www.umweltbundesamt.de/sites/default/files/medien/11850/publikationen/50_2024_cc_dasif.pdf.

Kuntzman, J., & Brom, J. (2025). From Fields to Microclimate: Assessing the Influence of Agricultural Landscape Structure on Vegetation Cover and Local Climate in Central Europe. *Remote Sensing*, *17*(1), 6. https:/doi.org/10.3390/rs17010006.

Kuželka, K., & Surový, P. (2018). Automatic detection and quantification of wild game crop damage using an unmanned aerial vehicle (UAV) equipped with an optical sensor payload: a case study in wheat. *European Journal of Remote Sensing*, 51(1). https://doi.org/10.1080/22797254.2017.1419442.

Lasko, K. (2022). Gap Filling Cloudy Sentinel-2 NDVI and NDWI Pixels with Multi-Frequency Denoised C-Band and L-Band Synthetic Aperture Radar (SAR), Texture, and Shallow Learning Techniques. *Remote Sensing*, *14*(17), 4221. https://doi.org/10.3390/rs14174221.

Laue, P., Blohm, W., Schmidt, S.I., Schröder, T., Kutzner, R.D., Wolf, T., Dietrich, D., Friese, K., Rinke, K. (2025). Satelliten-basierte Überwachung der Wasserqualität von Stand- und Fließgewässern in Deutschland (Satellite-based monitoring of the water quality of standing and flowing waters in Germany). *KW Korrespondenz Wasserwirtschaft,* 18 (2). https://doi.org/0.3243/kwe2025.02.001.

LfULG - Saxon State Office for Environment, Agriculture and Geology (2023). Ostthüringisches Lösshügelland (East Thuringian Loess Hill Country). Available online: https://www.natur.sachsen.de/download/33_Ostthueringisches_Loesshuegelland.pdf (accessed on 14.04.2023).

Lehmler, S., Förster, M., & Frick, A. (2023). Modelling Green Volume Using Sentinel-1, -2, PALSAR-2 Satellite Data and Machine Learning for Urban and Semi-Urban Areas in Germany. *Environmental Management*. https://doi.org/10.1007/s00267-023-01826-9.

Li, M., Shamshiri, R.R., Weltzien, C., & Schirrmann M. (2022). Crop Monitoring Using Sentinel-2 and UAV Multispectral Imagery: A Comparison Case Study in Northeastern Germany. *Remote Sens*., 14. https://doi.org/10.3390/rs14174426.

Lillesand, T., Kiefer, R. W., & Chipman, J. (2015). *Remote sensing and image interpretation* (7th ed.). Wiley.

Löw, J., Hill, S., Otte, I., Thiel, M., Ullmann, T., & Conrad, C. (2024). How Phenology Shapes Crop-Specific Sentinel-1 PolSAR Features and InSAR Coherence across Multiple Years and Orbits. *Remote Sensing*, 16(15). https://doi.org/10.3390/rs16152791.

Lozano-Tello, A., Fernández-Sellers, M., Quirós, E., Fragoso-Campón, L., García-Martín, A., Gutiérrez Gallego, J.A., Mateos, C., Trenado, R., & Muñoz. P. (2020). Crop Identification by Massive Processing of Multiannual Satellite Imagery for EU Common Agriculture Policy Subsidy Control. *European Journal of Remote Sensing,* 54(1). https://doi.org/10.1080/22797254.2020.1858723.

MacEachren, A., Robinson, A., Hopper, S.A., Gardner, S., Murray, R., Gahegan, M., & Hetzler, E. (2005). Visualizing Geospatial Information Uncertainty: What We Know and What We Need to Know. *Cartography and Geographic Information Science*. 32. https://doi.org/10.1559/1523040054738936.

Mardian, J., Berg, A., & Daneshfar, B. (2021). Evaluating the temporal accuracy of grassland to cropland change detection using multitemporal image analysis. *Remote Sensing of Environment*, 255. https://doi.org/10.1016/j.rse.2021.112292.

Martins, R.N., Fagundes Portes, M., Moraes, H.M.F., Furtado Junior, M.R., Rosas, J.T.F., & Almeida Orlando Junior, W. (2021). Influence of tillage systems on soil physical properties, spectral response and yield of the

bean crop. R*emote Sensing Applications: Society and Environment*, 22. https://doi.org/10.1016/j.rsase.2021.100517.
Mirpulatov, I., Illarionova, S., Shadrin, D., & Burnaev, E. (2023). Pseudo-Labeling Approach for Land Cover Classification Through Remote Sensing Observations With Noisy Labels. *IEEE Access*, 11. https://doi.org/10.1109/ACCESS.2023.3300967.
Mueller-Warrant, G.W., & Whittaker, G.W. (2015). Distorted spatial warping to compress large, high-resolution rasters for remote-sensing classification. *International Journal of Remote Sensing*, 36 (22). https://doi.org/10.1080/01431161.2015.1103917.
Murmu, S., & Biswas, S. (2015). Application of Fuzzy Logic and Neural Network in Crop Classification: A Review. Aquatic *Procedia*, 4. https://doi.org/10.1016/j.aqpro.2015.02.153.
Navarro, A., Silva, I., Catalão, J., & Falcão, J. (2021). An operational Sentinel-2 based monitoring system for the management and control of direct aids to the farmers in the context of the Common Agricultural Policy (CAP): A case study in mainland Portugal. *International Journal of Applied Earth Observation and Geoinformation*, 103. https://doi.org/10.1016/j.jag.2021.102469.
Nazeer, M., Olayinka Ilori, B., Bilal, M., Nichol, J.E., Wu, W., Qiu, Z., & Gayene, B.K. (2021). Evaluation of atmospheric correction methods for low to high resolutions satellite remote sensing data. *Atmospheric Research*, 249. https://doi.org/10.1016/j.atmosres.2020.105308.
Notti, D., Giordan, D., Caló, F., Pepe, A., Zucca, F., & Galve, J. P. (2018). Potential and Limitations of Open Satellite Data for Flood Mapping. *Remote Sensing*, *10*(11). https://doi.org/10.3390/rs10111673.
Numata, I., Roberts, D.A., Chadwick, O.A., Schimel, J., Sampaio, F.R., Leonidas, F.C., & Soares, J.V. (2007). Characterization of pasture biophysical properties and the impact of grazing intensity using remotely sensed data. *Remote Sensing of Environment*, 109(3). https://doi.org/10.1016/j.rse.2007.01.013.
Nyborg, J., Pelletier, C., & Assent, I. (2022). Generalized Classification of Satellite Image Time Series with Thermal Positional Encoding. *IEEE/CVF Conference on Computer Vision and Pattern Recognition Workshops (CVPRW)*, New Orleans, LA, USA, 2022, pp. 1391-1401. https://doi.org/10.1109/CVPRW56347.2022.00145.
OPEKEPE - Payment and Control Agency for Guidance and Guarantee Community Aid (2020). UC 1a: Earth Observation Monitoring & Traffic Lights. Available online: https://www.niva4cap.eu/uploads/downloads/webinar_UC1a_PRESENTATION_2020_5_20_v3.pdf (accessed on 14.09.2021).
Ozdogan, M., Yang, Y., Allez, G., & Cervantes, C. (2010). Remote Sensing of Irrigated Agriculture: Opportunities and Challenges. *Remote Sensing*, *2*(9). https://doi.org/10.3390/rs2092274.
Paasche, H., Paasche, K., & Dietrich, P. (2020). Uncertainty as a Driving Force for Geoscientific Development. *Nature and Culture*, 15(1). https://doi.org/10.3167/nc.2020.150101.
Pause, M., Raasch, F., Marrs, C., & Csaplovics, E. (2019). Monitoring Glyphosate-Based Herbicide Treatment Using Sentinel-2 Time Series - A Proof-of-Principle. *Remote Sensing*, *11*(21). https://doi.org/10.3390/rs11212541.
Phan, T.N., Kuch, V., & Lehnert, L.W. (2020). Land Cover Classification using Google Earth Engine and Random Forest Classifier – The Role of Image Composition. *Remote Sens*. 12. https://doi.org/10.3390/rs12152411.
Povey, A.C., & Grainger, R.G.: (2015). Known and unknown unknowns: uncertainty estimation in satellite remote sensing, *Atmos. Meas. Tech.*, 8. https://doi.org/10.5194/amt-8-4699-2015.
Probst, E., Klug, P., Mauser, W., Dogaru, D., & Hank, T. (2018). Water use efficiency of selected crops in the romanian plain – model studies using Sentinel-2 satellite images. *Scientific Papers. Series E. Land Reclamation, Earth Observation & Surveying, Environmental Engineering*, 7.
Qi, J., Chehbouni, A., Huete, A.R., Kerr, Y.H., & Sorooshian, S. (1994). A modified soil adjusted vegetation index. *Remote Sensing of Environment*, 48(2). https://doi.org/10.1016/0034-4257(94)90134-1.
Ray, N., & Burgman, M.A. (2006). Subjective uncertainties in habitat suitability maps, *Ecological Modelling*, 195(3-4). https://doi.org/10.1016/j.ecolmodel.2005.11.039.
Reitz, O. (2024). Erfassung von Ernteerträgen mit Satellitenbildern und Maschinellem Lernen - das Projekt FernEE 2.0 (Recording crop yields with satellite images and machine learning - the FernEE 2.0 project). *WISTA - Wirtschaft und Statistik*, 4/2024.
Richardson, A.J. & Wiegand, C.L. (1977). Distinguishing Vegetation from Soil Background Information. *Photogrammetric Engineering and Remote Sensing*, 43.
Rinke, K., Globevnik, L., Šubelj, G., & Snoj, L., (2022). Satellite-based monitoring of cyanobacteria in bathing waters. *ETC/ICM Technical Report 07/2022: European Topic Centre on Inland, Coastal and Marine Waters*, 35.
Rivera-Marin, D., Dash, J., & Ogutu, B. (2022). The use of remote sensing for desertification studies: A review, *Journal of Arid Environments*, 206, https://doi.org/10.1016/j.jaridenv.2022.104829.
Ronay, I., Kizel, F., & Lati, R. (2022). The effect of spectral mixtures on weed species classification. *ISPRS Ann. Photogramm. Remote Sens. Spatial Inf. Sci.*, https://doi.org/10.5194/isprs-annals-V-3-2022-477-2022.
Roteta, E., Bastarrika, A., Ibisate, A., & Chuvieco, E. (2021). A Preliminary Global Automatic Burned-Area Algorithm at Medium Resolution in Google Earth Engine. *Remote Sensing*, *13*(21), 4298. https://doi.org/10.3390/rs13214298.
Rustamov, R.B., & Hasanova, S.N. (2014). Exceptional importance of the test site/in-situ data integrated into satellite information in earth observation. *International Journal of Physical Sciences*, 2(3).
SMEKUL - Saxon State Ministry for Energy, Climate Protection, Environment and Agriculture (2017). AL 7 - Überwinternde Stoppeln (AL 7 – Overwintering Stubbles). Available online: https://www.smul.sachsen.de/foerderung/download/AL_7.pdf (accessed on 30.09.2021).
SMUL - Saxon State Ministry for the Environment and Agriculture (2024). Sachsen überweist Direkt- und Ausgleichszahlungen an Landwirtschaftsbetriebe (Saxony transfers direct and compensatory payments to

farms). Available online: https://www.medienservice.sachsen.de/medien/news/1082608 (accessed on 17.03.2025).
Sarvia, F., De Petris, S., & Borgogno-Mondino, E. (2022). Mapping Ecological Focus Areas within the EU CAP Controls Framework by Copernicus Sentinel-2 Data. *Agronomy*, *12*(2). https://doi.org/10.3390/agronomy12020406.
Samarinas, N., Spiliotopoulos, M., Tziolas, N., & Loukas, A. (2023). Synergistic Use of Earth Observation Driven Techniques to Support the Implementation of Water Framework Directive in Europe: A Review. *Remote Sensing*, 15(8). https://doi.org/10.3390/rs1508198.
Schmid, A. & Maidl, F. X. (2005). Einflussfaktoren auf spektraloptische Reflexionssignaturen zur Bonitur der Biomasse und des Stickstoffstatus von Winterweizen (Factors influencing spectral optical reflectance signatures for scoring the biomass and nitrogen status of winter wheat). *Informatik. Informatik Live! Band 1*. Bonn: Gesellschaft für Informatik e.V., pp. 350-354. Regular Research Papers. Bonn (Germany). 19.-22. September 2005.
Schmidt, S.I., Schröder, T., Kutzner, R.D., Laue, P., Bernert, H., Stelzer, K., Friese, K., & Rinke, K. (2024). Evaluating Satellite-Based Water Quality Sensing of Inland Waters on Basis of 100+ German Water Bodies Using 2 Different Processing Chains. *Remote Sens*, 16. https://doi.org/10.3390/rs16183416.
Schröder, T., Schmidt, S.I., Kutzner, R.D., Bernert, H., Stelzer, K., Friese, K., Rinke, K. (2024). Exploring Spatial Aggregations and Temporal Windows for Water Quality Match-Up Analysis Using Sentinel-2 MSI and Sentinel-3 OLCI Data. *Remote Sens*., 16. https://doi.org/10.3390/rs16152798.
Scholand, D., & Schmalz, B. (2024). Automated quantification of contouring as support practice for improved soil erosion estimation considering ridges. *International Soil and Water Conservation Research*, 12(4). https://doi.org/10.1016/j.iswcr.2024.07.001.
Schulz, C., Holtgrave, A.-K., & Kleinschmitt, B. (2021). Large-scale winter catch crop monitoring with Sentinel-2 time series and machine learning - An alternative to on-site controls? *Computers and Electronics in Agriculture* 186. https://doi.org/10.1016/j.compag.2021.106173.
Schwieder, M., Wesemeyer, M., Frantz, D., Pfoch, K., Erasmi, S., Pickert, J., Nendel, C., & Hostert, P. (2022). Mapping grassland mowing events across Germany based on combined Sentinel-2 and Landsat 8 time series. *Remote Sensing of Environment*, 269. https://doi.org/10.1016/j.rse.2021.112795.
Serra, P., & Pons, X. (2015). Uncertainty visualization of remote sensing crop maps enriched at parcel scale: a contribution for a more conscious GIS dataset usage. *Journal of maps*, 12(5). http://dx.doi.org/10.1080/17445647.2015.1113390.
Sicre C.M., Baup F., & Fieuzal R. (2014). Determination of the crop row orientations from Formosat-2 multi-temporal and panchromatic images, *ISPRS Journal of Photogrammetry and Remote Sensing*, 94. https://doi.org/10.1016/j.isprsjprs.2014.04.021.
Singh, S. K., Saxena, R., Porwal, A., Ray, N., & Ray, S.S. (2017). Assessment of hailstorm damage in wheat crop using remote sensing. *Current Science*, *112*(10). http://www.jstor.org/stable/26163949
SLfL - Saxon State Office Agriculture (1999). Die Landwirtschaftlichen Vergleichsgebiete im Freistaat Sachsen (The Agricultural Comparable Region in the State of Saxony). Available from: https://publikationen.sachsen.de/bdb/artikel/13524 (accessed 29 January 2024).
Smets, B., Cai, Z., Eklundh, L., Tian, F., Bonte, K., Van Hoost, R., De Roo, B., Jacobs, T., Camacho, F., Sánchez-Zapero, J., Martinez-Sánchez, E., Swinnen, E., Scheifinger, H., Hufkens, K., & Jönsson, P. (2021). Copernicus Land Monitoring Service. High Resolution Vegetation Phenology and Productivity (HR-VPP). Seasonal Trajectories and VPP parameters.
Safonova, A., Ghazaryan, G., Stiller, S., Main-Knorn, M., Nendel, C., & Ryo, M., (2023). Ten deep learning techniques to address small data problems with remote sensing. *International Journal of Applied Earth Observation and Geoinformation*, 125. https://doi.org/10.1016/j.jag.2023.103569.
Sonntag, W.-I., Wienrich, N., Severin, M., Schulze Schwering, D. (2022). Precision Farming – Nullnummer oder Nutzbringer? Eine empirische Studie unter Landwirten (Precision farming - a no-go or a boon? An empirical study among farmers). *Berichte über Landwirtschaft. Zeitschrift für Agrarpolitik und Landwirtschaft*, 100(2). https://doi.org/10.12767/buel.v100i2.411.
StaLa - Statistical Office of the Free State of Saxony (2018). *Statistisches Jahrbuch Sachsen 2018 (Statistical Yearbook Saxony 2018*). Available online: https://www.statistischebibliothek.de/mir/receive/SNHeft_mods_00022230 (accessed on 29.01.2024).
Storey, J., Roy, D.P., Masek, J., Gascon, F., Dwyer, J., & Choate, M.J.R.S.O.E. (2016). A note on the temporary misregistration of Landsat-8 Operational Land Imager (OLI) and Sentinel-2 Multi Spectral Instrument (MSI) imagery. *Remote Sens. Environ.*, *186*. https://doi.org/10.1016/j.rse.2016.08.025.
Stumpe, C., Leukel, J. & Zimpel, T. (2024). Prediction of pasture yield using machine learning-based optical sensing: a systematic review. *Precision Agric 25*, 430–459. https://doi.org/10.1007/s11119-023-10079-9.
Sudmanns, M., Tiede, D., Augustin, H., & Lang, S. (2020). Assessing global Sentinel-2 coverage dynamics and data availability for operational Earth observation (EO) applications using the EO-Compass. *International Journal of Digital Earth* 13(7). https://doi.org/10.1080/17538947.2019.1572799.
Tassi, A., & Vizzari, M. (2020). Object-Oriented LULC Classification in Google Earth Engine Combining SNIC, GLCM, and Machine Learning Algorithms. *Remote Sens*. 12. https://doi.org/10.3390/rs12223776.
Thomson, J., Hetzler, E., MacEachren, A., Gahegan M., & Pavel, M. (2005). A typology for visualizing uncertainty. *Conference proceeding in Visualization and Data Analysis 2005, 146–157*.
Tian, J., Zhu, X., Shen, Z., Wu, J., Xu, S., Liang, Z., & Wang, J. (2020). Investigating the urban-induced microclimate effects on winter wheat spring phenology using Sentinel-2 time series. *Agricultural and Forest Meteorology*, 294. https://doi.org/10.1016/j.agrformet.2020.108153.

Teucher, M., Thürkow, D., Alb, P., & Conrad, C. (2022). Digital In Situ Data Collection in Earth Observation, Monitoring and Agriculture - Progress towards Digital Agriculture. *Remote Sensing*, 14(2). https://doi.org/10.3390/rs14020393.

Tollerud, H. J., Brown, J. F., & Loveland, T. R. (2020). Investigating the Effects of Land Use and Land Cover on the Relationship between Moisture and Reflectance Using Landsat Time Series. *Remote Sensing*, *12*(12), 1919. https://doi.org/10.3390/rs12121919.

Triebnig, G., Csonka, B., Kolitzus, D., Grobler, D., Achtsnit, S., Brand, S., Pari, S., Wanko, E., & Jankovic, N. (2024). Agri-Dashboard to Support CAP Monitoring Based on the experiences of the 1st operational year of CAP Area Monitoring System. https://doi.org/10.13140/RG.2.2.14868.51841.

Velden v.d., D., Klerkx, L., Dessein, J., & Debruyne, L. (2025). Governance by satellite: Remote sensing, bureaucrats and agency in the Common Agricultural Policy of the European Union. *Journal of Rural Studies*, 114. https://doi.org/10.1016/j.jrurstud.2024.103558.

Venter, Z.S., Barton, D.N., Chakraborty, T., Simensen, T., & Singh, G. (2022). Global 10 m Land Use Land Cover Datasets: A Comparison of Dynamic World, World Cover and Esri Land Cover. *Remote Sens*., 14. https://doi.org/10.3390/rs14164101.

Villanueva, A.J., Granado-Díaz, R. & Colombo, S. (2024) Comparing practice- and results-based agri-environmental schemes controlled by remote sensing: An application to olive groves in Spain. *Journal of Agricultural Economics*, 75. https://doi.org/10.1111/1477-9552.12573.

Wang, Z., Deng, Y., & Fan, Y. (2018). Validation plays the role of a "bridge" in connecting remote sensing research and applications, *Advances in Space Research*, 62(1). https://doi.org/10.1016/j.asr.2018.04.018.

Wang, J., Zhen, J., Hu, W., Chen, S., Lizaga, I., Zeraatpisheh, M., & Yang, X. (2023). Remote sensing of soil degradation: Progress and perspective. *International Soil and Water Conservation Research*, 11(3). https://doi.org/10.1016/j.iswcr.2023.03.002.

Werther, M., & Burggraaff, O. (2023). Dive into the unknown: embracing uncertainty to advance aquatic remote sensing. *Journal of Remote Sensing*, 3. https://doi.org/10.34133/remotesensing.0070.

Wu, B., Zhang, M., Zweng, H., Tian, F., Potgieter, A.B., Qin, X., Yan, N., Chang, S., Zhao, Y., Dong, Q., Boken, V., Plotnikov, D., Gou, H., Wu, F., Zhao, H., Deronde, B., Tits, L., & Loupiann, E. (2023). Challenges and opportunities in remote sensing-based crop monitoring: a review. *National Science Review*, 10(4). https://doi.org/10.1093/nsr/nwac290.

Xue, J., & Su, B. (2017). Significant Remote Sensing Vegetation Indices: A Review of Developments and Applications, *Journal of Sensors*. https://doi.org/10.1155/2017/1353691.

Yulianto, F., Nugroho, G., Chulafak, A.G., Suwarsono, S. (2021). Improvement in the Accuracy of the Postclassification of Land Use and Land Cover Using Landsat 8 Data Based on the Majority of Segment-Based Filtering Approach. *The Scientific World Journal*. https://doi.org/10.1155/2021/6658818.

Zeng, L., Wardlow, B.D., Xiang, D., Hu, S., & Li, D. (2020). A review of vegetation phenological metrics extraction using time-series, multispectral satellite data. *Remote Sensing of Environment*, 237. https://doi.org/10.1016/j.rse.2019.111511.

Zhang, Y., & Mishra, R.K. (2012). A review and comparison of commercially available pan -sharpening techniques for high resolution satellite image fusion. *IEEE International Geoscience and Remote Sensing Symposium*, Munich, Germany, 2012. https://doi.org/10.1109/IGARSS.2012.6351607.

Zhao, Y., Potgieter, A.B., Zhang, M., Wu, B., & Hammer, G.L. (2020). Predicting wheat yield at the field scale by combining high-resolution Sentinel-2 satellite imagery and crop modelling. *Remote Sensing*, 12. https://doi.org/10.3390/rs12061024.

Zyl, J.J. van, Chapman, B.D., Dubois, P., & Shi, J. (1993). The effect of topography on SAR calibration. *IEEE Transactions on Geoscience and Remote Sensing*, 31(5). https://doi.org/10.1109/36.263774.

Acknowledgements

First, I would like to thank Prof. Dr. Peter Dietrich for giving me the opportunity to write my dissertation. Without this voluntary support, I would not have been able to complete this thesis, which I greatly appreciate. I would also like to thank the Environmental Research Center (UFZ) Leipzig and the UFZ Department of Monitoring and Exploration Technologies (MET) for providing resources without which I would not have been able to carry out the necessary publications.

I am grateful to Prof. Dr. Peter Dietrich and Prof. Dr. Volker Hochschild for the supervision and evaluation of this thesis, and to Prof. Dr. Thomas Scholten, and Dr. Harald Neidhardt for being referees in the thesis defense.

I would also like to thank the Saxon State Office for Environment, Agriculture and Geology (LfULG) and especially Mr. Klaus Wallrabe for the opportunity to investigate and publish governmental scientific issues of remote sensing in this level of detail.

Appendix

Manuscript 1

Mapping overwintering grain stubbles using machine-learning methods and image compositions for CAP-control and Water Framework Directive connected activities

Journal of Applied Remote Sensing, 014515-1, Jan–Mar 2023, Vol. 17(1)

Sebastian Goihl[1]*

[1]Saxon State Office for Environment, Agriculture and Geology, Box 100510, 01076 Dresden, Germany

*Correspondence: Sebastian.Goihl@smekul.sachsen.de

Received: 03 August 2022; Accepted: 25 January 2023; Published: 20 February 2023

Reference: https://doi.org/10.1117/1.JRS.17.014515

Abstract

By leaving grain stubble on the field over the winter, farmers can actively contribute to nature conservation. Animals receive food and living space on these areas, endangered herbs too, while at the same time it is reducing the input of substances into water and function as covered ground to protect the fertile soil from erosion. Remote Sensing can deliver information on this type of land cover, which is also important for the agricultural administration. The farmer can be compensated by government to let stubbles on the fields. The results of this study shows, that there is a high potential to detect overwintering stubbles fields area for Common Agriculture Policy (CAP)-control to verify agricultural funding with SVM (96.5%) by combining remote sensing classification methods with geodata analysis techniques using geoinfomation systems (GIS), negative buffering (-20 m) and using threshold settings for correct classified pixel per field. These results give occasion for optimism for the further processing of this land cover by using as an application for the government to support CAP- and Water Framework Directive-activities.

Keywords: Overwintering Stubbles; Machine Learning; Sentinel-2 (S-2); Google Earth Engine (GEE); agricultural monitoring, CAP-control, Water Framework Directive, interannual land cover

1 Introduction

Knowledge of the current land cover, the historical land cover, the hotspots and the intensity of land cover change are an important data source for scientist, politicians and other decision makers. The human influence on ecosystems, the water balance, biodiversity, urban development and climate and climate change often play a decisive role in studies about land use/land cover (LULC) (Koschke et al. 2012, Kabisch et al. 2019, Vizzari & Sigura 2015, Tan et al. 2020, Linh et al. 2012). Remote sensing systems are significant to provide area-wide and recurring information about LULC (Gutman et al. 2005). This development is particularly evident in the field of monitoring agricultural areas (Khabbazan et al. 2019, Seo et al. 2019, Reinermann et al. 2020, Khan et al. 2010). In the case of agriculture, there are two perspectives. First, the perspective of the official administration. Authorities must check, for example, whether subsidies are being paid out correctly because the cultivation declarations of the farmers are correct. To support this in an area-wide manner, the European Commission (EC) has decided that the use of remote sensing should increasingly

replace on-site inspections of declared fruit types (Neriaux et al. 2021, Sen4CAP Consortium 2021) in the Common Agriculture Policy (CAP).

Secondly, that of the farmer who is concerned about the condition of his/her fields and does precision farming (Segarra et al. 2020, Vizarri et al. 2019). In addition to the management of land in the vegetation period, the question of what happens between the cultivation periods is currently becoming increasingly important. Such land cover also includes *overwintering stubble* (OS) (SMEKUL 2017) in the Federal State of Saxony, Germany, which plays an important role in water, nature and soil conservation (Vickery et al. 2019). Farmers are financially compensated by the state if these OS are left on the field.

This study aims three main targets. First, to search for a good image composition over European autumn and winter for monitoring *overwintering stubble* land cover. Here it was comparatively examined whether the determination of a final image composition is decisive for the further course of the processing. Secondly, a method was searched to minimize the need for elaborate, costly and time-consuming on-site inspections in the field using these area-wide remote sensing image compositions. In the end, at least 90% of the investigation area should be confirmed by remote sensing. Thirdly, it is to be investigated how probable and trustworthy classifications of the object of investigation outside the declared areas are, because a farmer can voluntarily leave them on the field without claiming compensation from the state. This information is very important, as only with this knowledge, the overall picture of winter land cover can be estimated.

The monitoring of overwintering stubble continues to offer great potential for the development of a service on the implementation status and control of this land cover in the case of CAP as a part of the cross-compliance EU standards on good agricultural and environmental condition of land. There are plenty of studies on the crop residues, which are thematically close to the stubble fields (Dvorakova et al. 2020, Hively et al. 2018, Quemada & Daughtry 2016, Daughtry et al. 1996, Hiloidhari & Baruah 2011, Cai et al. 2019). Particularly for the measurement of harvest residues on the surface to determine carbon balances (soil organic carbon (SOC)), soil fertility and biomass potentials, knowledge of harvest residues has been investigated (Dvorakova et al. 2020, Hively et al. 2018, Quemada & Daughtry 2016, Daughtry et al. 1996, Hiloidhari & Baruah 2011). The unique spectral absorption properties (Quemada & Daughtry 2016) have already been sufficiently researched and even considered within a

separate index (cellulose absorption index (CAI)) to discriminate crop residues from soil (Daughtry et al. 1996). Monitoring of crop residues must not be underestimated, as these are important for farmland ecosystems and provide protection against water erosion (Cai et al. 2019). Information about covered soils over the winter is also very valuable for advising farmers on water-conserving land management and soil protection in case of the requirements of the Water Framework Directive (WFD) (Techen et al. 2015).

For instance, there are studies on monitoring (annual) catch crops (Denize et al. 2019, Schulz et al. 2019) or own web-based applications for detecting catch crops as an alternative to on site controls (Schulz et al. 2021). The winter land use types studied by Denize et al. (2019) are winter crops, grasslands, catch crops, crop residues and bare soil. Here, stubble fields are missing because “crop residues” used as a broader term. In general, little evidence can found in studies of the methods by which *wintering stubble* can be mapped using remote sensing.

2 Material and Methods

2.1 Study Area

The study area was located in the south of federal state of Saxony (Figure 1) which is inside the mid and south part of Sentinel-2 tile grid 33UUS (ESA 2021). The training region of interest was selected based on the available ground-thruth-data, as these indicate the regions in which the target object can be found on a comparatively large number of areas. A particularly large number of *wintering stubble* were in the selected region for the end of 2019. By selecting the Eastern Ore Mountains, it was ensured that the results of a classification could be checked and evaluated on a representative number of fields.

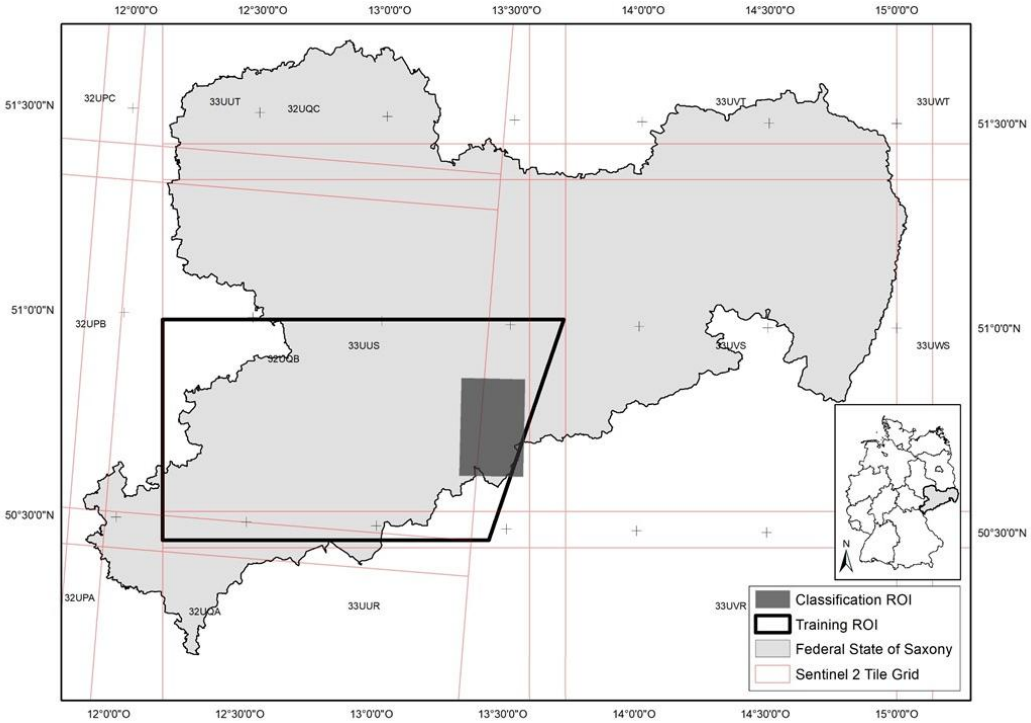

Figure 1: Study area location in Saxony (Germany) and extent of region of interest polygons (classification and training areas).

2.2 Overwintering stubble fields as study object

Overwintering stubble means that stubble and crop residues of grain, grain legumes, oilseeds or root crops left on the field after the harvest (Figure 2). The used in-situ data was taken from the agri-environmental measure (SMEKUL 2017) and has specific cultivation requirements to define our target object: This measure excludes maize and millet. Mechanical tillage may not be carried out until February 15 of the following year at the earliest. Also, no fertilizers or pesticides may be applied to such a field, unless they are approved for organic farming. Bird and small mammal species should be provided with food and resting places (Vickery et al. 2019), which extends through the developing vegetation through autumn and into winter. In addition, endangered field herbs are given the opportunity to complete their development cycle (SMEKUL 2017).

(**a**) (**b**)

Figure 2: Two examples (a) and (b) for crop residues like a "stubble field" in the winter. Above all, the rooted lower stalk parts of the plants form a comprehensive land cover, which is later supplemented by burgeoning vegetation (loose grain, wild herbs). Photos taken by the author on the 03/15/2020.

The investigation period for overwintering stubble is between two phases of agricultural cultivation of land in western- and mid-Europe. Stubble only remained in the fields after the harvest, which is why the earliest start of the investigation has been in late summer (European temperate climate zone). Lou et al. argue that using time series improve the image classification results significantly (Lou et al. 2021). Therefore, in this study time series was used for better classification results and to take into account the developments on the stubble field over the course of the winter. Care was taken to let the time periods become not shorter than two months for each period, because the influence of cloud cover in winter and autumn over Central Europe should not be underestimated (Sudmanns et al. 2020). This minimum length is intended to ensure that sufficient cloud-free images are available to create the composite.

Crop calendar data shows, that the end of the season (EOS) for grain like winter wheat in mid-Europe is in July and August (Franch et al. 2022, FAO 2025). So, the first investigation period will start connected with the end of season in July (Date: 01.07.2019) (Section 2.4.1; Table 2, Column: Period of time). With the start of sowing new crops on the overwintering stubble fields in March, tilling, and freezing of the herbs in January and February the observation period for stubble ended (SMEKUL 2017) (Date: 31.03.2020) (Section 2.4.1; Table 2, Column: Period of time). Increasing Normalized Difference Vegetation Index (NDVI) (Lunetta et al. 2006, Singh et al. 2016) on stubble fields near Großhartmannsdorfer large pond (Großhartmannsdorfer Großteich) (Figure 6) in autumn investigated with the EO-Browser (https://apps.sentinel-hub.com/eo-browser/) shows a significant growth to the time period after harvest and before frost in 2019. The above-mentioned vegetation is developing, so the autumn forms the second period in order to map this particular parameter in the best possible way (01.10.2019 to 31.12.2019). With the end of the

second period, the third period begins in January at 01.01.2020. There are many possibilities for the temporal creation of the image compositions, which is why alternative periods and their effect on the classification also tested (Figure 3, Table 3).

2.3 Data preparation

Images from Sentinel-2 (Phiri et al. 2020) satellites were used for classification. Using this freely available data, recordings with a high temporary density and high spatial resolution are guaranteed (ESA 2021). The Sentinel-2 bands deals with different spatial resolution (10 m, 20 m and 60 m) and were all resampled in this work to 10 m pixel size.

There are two sources of ground truth data in this study. First, the newest Corine Land Cover (CLC) vector data (year 2018) from the Copernicus Land Monitoring Service at pan-European scale that is freely available at https://land.copernicus.eu/pan-european/corine-land-cover (CLC 2021). CLC maps up to 44 land use and land cover classes. The dataset is available from 1990 onwards, and at 6-year intervals from 2000 onwards. The minimum mapping unit (MMU) is 25 ha, with updates to with an MMU of 5 ha (CLC 2021). Secondly, there are the agricultural promotion declaring vector-data of all agricultural parcels in 2019 and 2020, which carry the information as to whether the wintering stubble measure has been applied for in 2019. As part of the agricultural subsidy, this data is collected annually by farmers declaring their fields on digital platforms of the agricultural administration, determining the type of crop cultivated and applying for further subsidies. Due to CAP regulations, the geodata of the fields must be highly accurate (exact area data up to the fourth decimal place). Due to data protection, this datasets are not freely accessible. By selecting only the wintering stubble marked fields from 2019 and updating these features at the CLC features, the final ground truth dataset has been build.

For machine learning all over the Saxony part underlying the training area (size circa 5050 km², Figure 1), 5.000 training points and 500 validation points created randomly. The CLC attribute table has been generalized to nomenclature level 2 (CLMS 2021). With the implanted class of wintering stubble, there are eleven classes in the training point data set (Table 1). As seen in Table 1, the implemented wintering stubble class had only a small proportion in the study area. Since this has been the main object to be examined, manual intervention was conducted in the random distribution of training and validation points. Points were taken from other classes and placed on the surfaces of the target object, so that significantly, more points were assigned for training and

validating the wintering stubbles than this class would be entitled to base on the surface area. The classification area (size circa 460 km²) was a smaller subpart of the training area, because in Google Earth Engine (GEE), as processing environment, there were pixel limitations (Gorelick et al. 2017).

Table 1: Area of interest statistics (Training ROI) in CLC Level 2 nomenclature. Distribution of training and validation points per class. The class 99 represents the implanted overwintering stubbles. Classes 22 and 33 not trained due to their small size.

CLC Land Cover (Level 2 class)	Training CLC km²; (%)	Training Points; (%)	Validation Points; (%)
11 Urban Fabric	549.98; (10.88)	532; (10.64)	51; (10.20)
12 Industrial, commercial transport	142.02; (2.81)	125; (2.50)	15; (3.00)
13 Mine, dump and construction	18.69; (0.37)	11; (0.22)	1; (0.20)
14 Artificial vegetated areas	70.38; (1.39)	66; (1.32)	9; (1.80)
21 Arable land	1825.15; (36.11)	1762; (35.24)	171; (34.20)
22 Permanent crops	*0.48; (0.01)*	*0; (0.00)*	*0; (0.00)*
23 Pastures	936.63; (18.53)	900; (18.00)	78; (15.60)
31 Forests	1425.04; (28.19)	1391; (27.82)	114; (22.80)
32 Scrub/herbaceous vegetation	45.89; (0.91)	44; (0.88)	3; (0.60)
33 Open spaces/no vegetation	*0.24; (0.00)*	*0; (0.00)*	*0; (0.00)*
41 Inland wetlands	1.03; (0.02)	2; (0.04)	0; (0.00)
51 Inland waters	24.63; (0.49)	25; (0.50)	5; (1.00)
99 Wintering Stubbles*	**14.19; (0.28)**	**142; (2.84)**	**53; (10.60)**
Total	5054.34; (100)	5000; (100)	500; (100)

* implanted land cover class.

2.4 Methodology

There are three different steps of data analysis in this study to achieve the three goals mentioned above (Chapter 1). The first step is divided into two parts to find a good band and time period combination for classification. The second step proofs known overwintering stubble fields on chosen classification results (useful vs less useful). The third analysis step elicits the possibilities to identify unknown wintering stubble fields based on the optimal case classification result.

2.4.1 Image Composition and Classification

To find the best dataset for classification several image compositions were constructed and feature importance proofed. In addition to the satellite bands some popular auxiliary datasets were calculated to enhance the accuracy of the classification by providing a greater information basis (Segarra et al. 2020, Dvorakova et al. 2020, Quemada & Daughtry 2016, Lou et al. 2021, Lunetta et al. 2006, Mzid et al. 2021, Gao 1996, Najafi et al. 2019, Phan et al. 2020, Tassi & Vizzari 2020). For this purpose were selected NDVI (Lunetta et al. 2006, Singh et al. 2016), the Bare Soil Index (BSI) (Mzid

et al. 2021), the Normalized Difference Moisture Index (NDMI) (Gao 1996) and the Sentinel Normalized Difference Tillage Index (SNDTI) (Najafi et al. 2019).

From a filtered and cloud-masked Sentinel-2 image-collection the above-mentioned indices (NDVI, NDMI, BSI and SNDTI) were calculated (Figure 1). Using the main statistics of the indices (mean, maximum and standard deviation) data augmentation was implemented. The gaps in cloudy images were filled with the use of median metrics (temporal aggregation method) (Phan et al. 2020). By calculating the median pixel values for each band, a final image composite (Tassi & Vizzari 2020) was generated. This method causes in a significant reduction of data too (Carrasco et al. 2019). For the time series analysis, the same number of bands and indices was calculated for each period and then stacked (Phan et al. 2020).

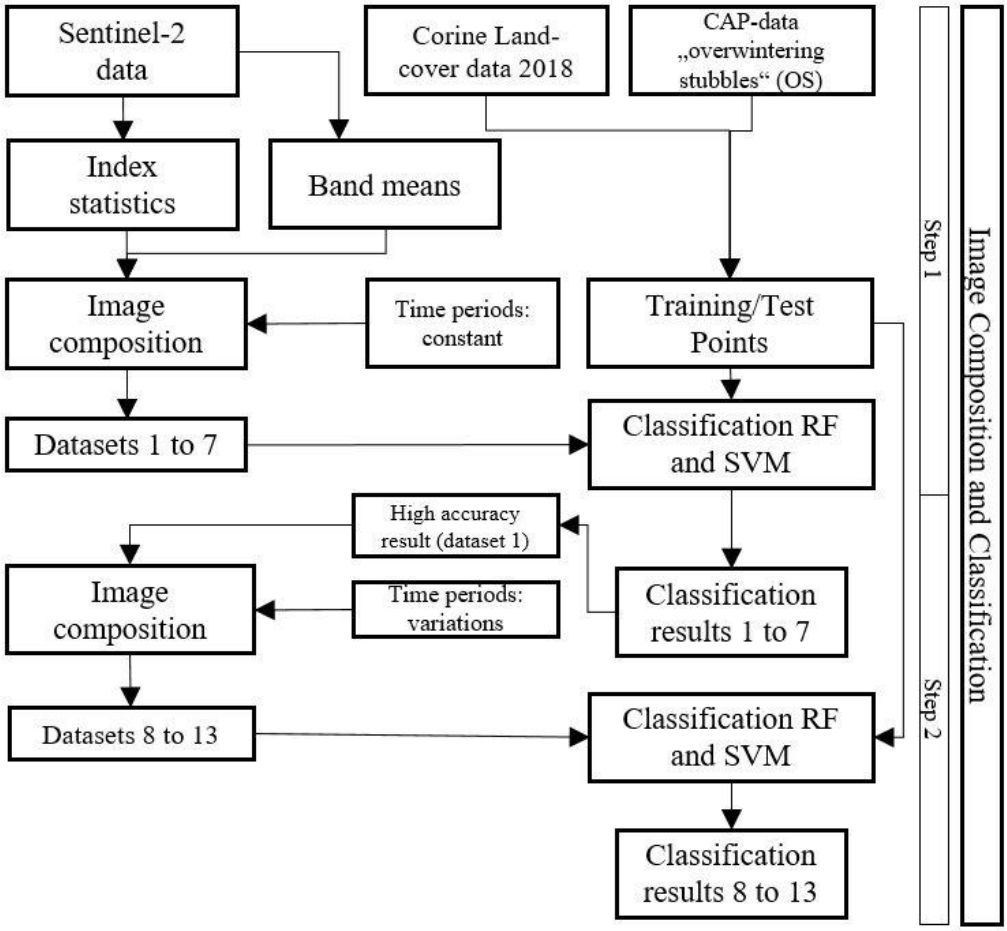

Figure 3: Processing scheme of the image composition and classification step.

As can be seen in Figure 3, in the first step, the time periods are constant for the creation of the image compositions in view of the development of the field after the harvest as explained in Section 2.2. Now the image compositions were ready for classification. Here the main work focused on the investigation of the best band and index composition and does not change the time periods. Machine Learning (ML)

methods of data land cover classification has been used (Phan et al. 2020, Tassi & Vizzari 2020, Mira et al. 2019) for classification, which have already been successfully used in remote sensing and image composition (Phan et al. 2020). RF and SVM provide extremely accurate LULC classifications, are highly efficient, well performing without any assumptions about the data distribution (Tassi & Vizzari 2020) and are widely applied (Phan et al. 2020). The classification created the datasets 1 to 7 (Table 2).

Table 2: Details of studied dataset compositions 1 to 7 used for classification. Understrike 2 "_2" means second period (2019-10-01 to 2019-12-31). Understrike 3 "_3" means third period (2020-01-01 to 2020-03-31).

Dataset	Description	No. of Bands and Indices	Period of time
Dataset 1	Band means of the Sentinel-2 bands (B2, B3, B4, B6, B8, B8A, B11, B12) and statistic parameters (std, max, mean) from spectral indices NDVI, BSI, NDMI and SNDTI.	60	
Dataset 2	Band means of the Sentinel-2 bands (B2, B3, B4, B6, B8, B8A, B11) and statistic parameters (std, max, mean) from spectral indices NDVI, BSI and NDMI.	48	
Dataset 3	Band means of the Sentinel-2 bands (B2, B3, B4, B6, B8, B8A, B11) and statistic parameters (std, max, mean) from spectral indices NDVI and BSI.	39	
Dataset 4	Band means of the Sentinel-2 bands (B2, B3, B4, B6, B8, B8A, B11) and statistic parameters (std, max, mean) from spectral index NDVI.	30	
Dataset 5	Only the bands and indices, which shows the highest variable importance in the classification of datasets 1 to 4 (B4, B6, B8A, B11, B12, sndtimax, sndtimean, sndtistd, ndmimax, ndmimean, ndmistd, bsimax, bsimean, B6_2, B8A_2, B11_2, B12_2, sndtimax_2, sndtimean_2, sndtistd_2, ndmimax_2, ndmistd_2, bsistd_2, B2_3, B6_3, B8A_3, B11_3, B12_3, ndvimean_3, ndvistd_3, sndtimax_3, sndtimean_3, sndtistd_3, ndmimax_3, ndmimean_3, ndmistd_3, bsistd_3)	39	1: 2019-07-01, 2019-09-30 2: 2019-10-01, 2019-12-31 3: 2020-01-01, 2020-03-31
Dataset 6	Only the bands and indices, which may be high, correlated to the land cover of overwintering stubbles (ndvimax, ndvistd, sndtistd, ndmimax, ndmimean, bsistd, B2_2, ndvimax_2, ndvimean_2, bsimax_2, bsimean_2, sndtistd_2, ndvimax_3, ndvimean_3, sndtistd_3, bsimax_3, bsimean_3).	17	
Dataset 7	Only spectral indices NDVI, BSI, NDMI and SNDTI. Each with three parameters (std, max, mean).	36	

After completing the classification of datasets 1 to 7 and calculating the OA (Chapter 3, Table 4), these results are immediately used in the development of the temporally variable image composites. Dataset 1, a datasets with the predominant highest

accuracies, serves as the basis and used for the classification of datasets 8 to 13 (Table 3). This datasets examine the influence of changing time periods. However, there are thousands of bands, index and time composition combination possibilities which cannot be investigated.

Table 3: Details of studied dataset compositions 8 to 13 used for classification.

Dataset	Description	No. of Bands and Indices	Periods of time
Dataset 8	Dataset 1 (highest accuracy dataset from datasets 1 to 7, see Table 2)	60	1: 2019-06-01, 2019-08-31 2: 2019-09-01, 2019-12-31 3: 2020-01-01, 2020-04-30
Dataset 9		60	1: 2019-06-01, 2019-09-30 2: 2019-10-01, 2020-02-28 3: 2020-03-01, 2020-05-31
Dataset 10		60	1: 2019-07-01, 2019-10-30 2: 2019-11-01, 2020-02-28 3: 2020-03-01, 2020-04-30
Dataset 11		40	1: 2019-07-01, 2019-09-30 2: 2019-10-01, 2019-12-31
Dataset 12		40	1: 2019-10-01, 2019-12-31 2: 2020-01-01, 2020-03-31
Dataset 13		80	1: 2019-07-01, 2019-08-31 2: 2019-09-01, 2019-12-31 3: 2020-01-01, 2020-02-28 4: 2020-03-01, 2020-05-31

2.4.2 Test known „Overwintering Stubble" fields and improve accuracy

A well-known problem in remote sensing are misclassifications at the edges of the field. This is because the pixel size of satellite data do not fit exactly with the detailed information about location, form and extent of the real land cover like agricultural field boundaries. These pixels also mix the information of neighboring areas and lead to incorrect classifications. For this reason, the unaffected core pixels were the focus of the investigation (Table 6).

By using the GIS-tool negative buffer in Sentinel-2 pixel size (-10 m or -20 m), the mixed pixels and edge effects were minimized in order to investigate only the core field pixels (Figure 4). The influence of the edge pixels on the classification result now became verifiable.

In a subsequent step (Figure 4), limit values are used for the area of the respective field. When the area of the field reaches a set threshold value (limit value 50%, 65%, 75%) classified as overwintering stubbles, all the field area will be marked as classified correctly in this proposal of an area control methodology. Setting a threshold is important because we know that usually never all pixels of a field classified correctly.

The limit value also represents the confidence in the method and the proportion of misclassifications that can be ignored for the evaluation per field.

The setting of the threshold value only depends on the strict requirements that must be applied in order to view land cover a correctly classified and is the responsibility of the authorities who have to carry out the funding.

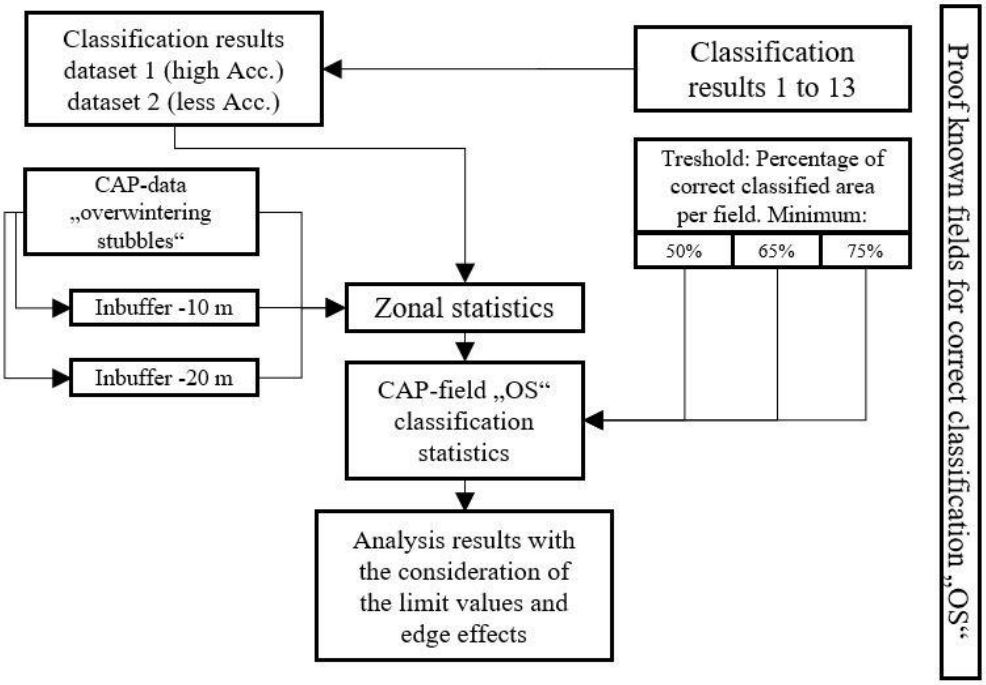

Figure 4: Processing scheme of proofing of known fields for correct classification.

2.4.3 Search method for voluntary left and not reported but classified "Overwintering Stubbles"

Only the view on the fields for the agricultural subsidy has been applied for now (Chapter 2.4.2). It is necessary to check whether these stubbles could have been left voluntarily and not reported, or whether it is a classification error as main target number three of this study, too. Knowledge of the location and area of such voluntary activities is important to obtain a complete overall picture of this land cover and to translate this information into active management of WFD content. There are no in-situ-information about this voluntarily fields. For this purpose, all areas were first removed from the classified raster data set where it is known that the land cover *overwintering stubble* was registered. All remaining classified stubble areas, which are located on agricultural land, were then examined via a logical tabular comparison by pre- and post-crop information (Figure 5).

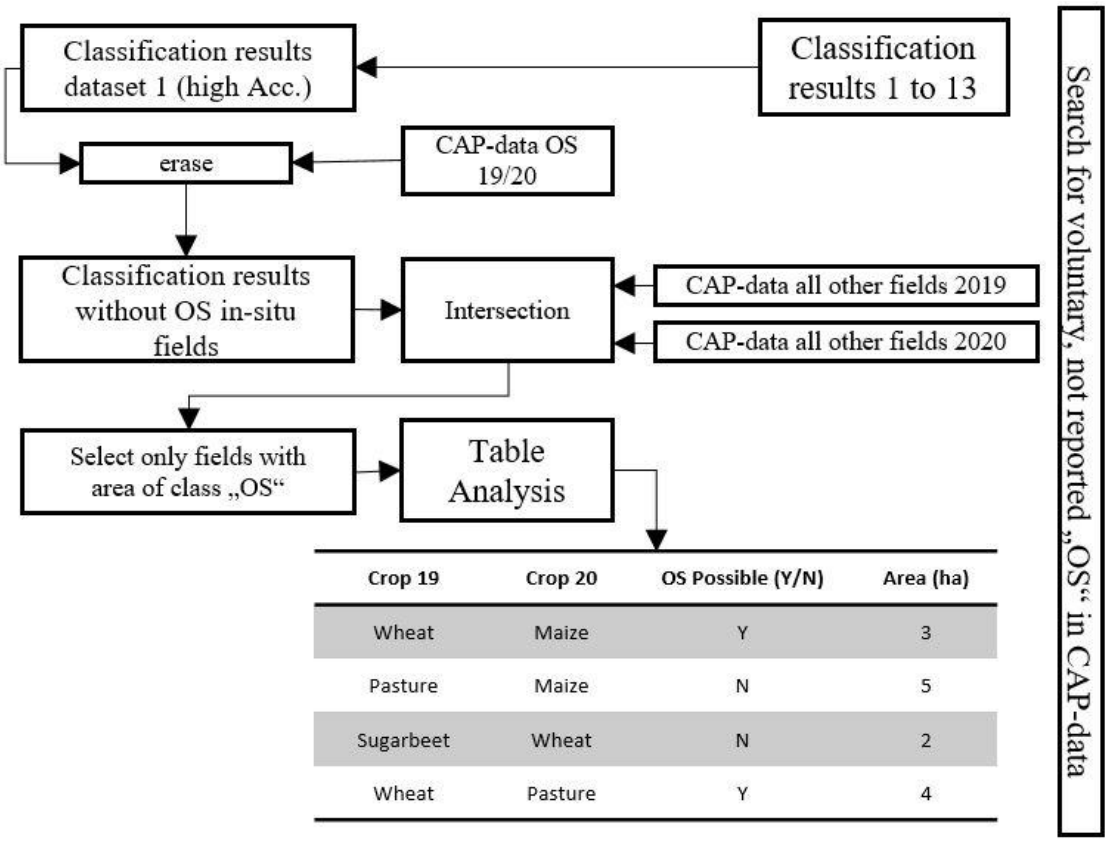

Crop 19	Crop 20	OS Possible (Y/N)	Area (ha)
Wheat	Maize	Y	3
Pasture	Maize	N	5
Sugarbeet	Wheat	N	2
Wheat	Pasture	Y	4

Figure 5: Processing scheme of the search for voluntary, not reported overwintering stubble fields

Taking into account the crop rotation in the year of the classified stubble and in the following year, it is at least possible to say whether it would be likely that stubble was left on an area or not. For example: If *overwintering stubble* were classified on a wheat field at the end of the year and maize follows the next year, then the farmer may well have left the stubble standing. In contrast, stubble can also be classified on grassland, but this is then neither logical nor probable (Figure 5). Finally, the areas of the supposed fields were added up and compared between “stubble probably possible” and “stubble not possible”. Desirable were especially many "possibly correct classifications" compared to few "not possible classifications".

3 Results

3.1 Dataset classification results and selection

Dataset 1 achieved the best results in overall accuracy (RF with 80.3% and SVM with 82.1%) for the periods used in datasets 1 through 7 and the highest producer and user accuracies for the class “Overwintering Stubble” in detail. These accuracies were also exactly in the range other classifications (Tassi & Vizzari 2020) achieved. Over all

measured accuracy parameters, the RF was consistently weaker in the OA than the SVM (Table 4).

The use of the bands from dataset 1 on other time periods produced comparable but no better results (datasets 8 to 13). According to Table 4 and to outline the range of classification results, an above all metrics particularly good dataset (1) was compared with an above all metrics less good dataset (2) in the following. This selection guarantees good comparability, since datasets 1 and 2 refer to the same time periods.

Table 4: Dataset 1 to 13 classification accuracies for RF and SVM and class "Overwintering Stubble" producer accuracy (PA) and user accuracy (UA).

	Overall Acc. RF	Overall Acc. SVM	Kappa's Coeff. RF	Kappa's Coeff. SVM	Stubble PA RF	Stubble UA RF	Stubble PA SVM	Stubble UA SVM
Dataset 1	**0.803**	**0.821**	**0.773**	**0.774**	**0.926**	**0.951**	**1.00**	**0.964**
Dataset 2	**0.741**	**0.768**	**0.695**	**0.695**	**0.740**	**0.920**	**0.963**	**0.897**
Dataset 3	0.741	0.804	0.628	0.752	0.704	0.947	0.926	0.926
Dataset 4	0.741	0.777	0.695	0.717	0.740	0.909	0.851	0.885
Dataset 5	0.786	0.804	0.762	0.751	0.926	0.961	0.963	0.963
Dataset 6	0.759	0.777	0.716	0.692	0.852	0.956	0.852	0.920
Dataset 7	0.777	0.821	0.704	0.774	0.888	0.960	0.963	0.963
Dataset 8	0.795	0.821	0.751	0.774	0.815	0.960	1.000	0.900
Dataset 9	0.777	0.804	0.716	0.751	0.740	0.952	0.963	0.929
Dataset 10	0.786	0.804	0.737	0.751	0.815	0.957	0.923	0.961
Dataset 11	0.732	0.821	0.699	0.775	0.777	0.955	0.963	0.929
Dataset 12	0.714	0.759	0.637	0.694	0.555	0.882	0.666	0.947
Dataset 13	0.795	0.821	0.703	0.772	0.852	0.954	0.963	0.963

3.2 Wintering stubbles classification results

For both datasets (1 and 2), RF was more weaker than the SVM. From a purely visual point, these differences do not stand out with such clarity (Figure 6, highlighted by pink rectangles).

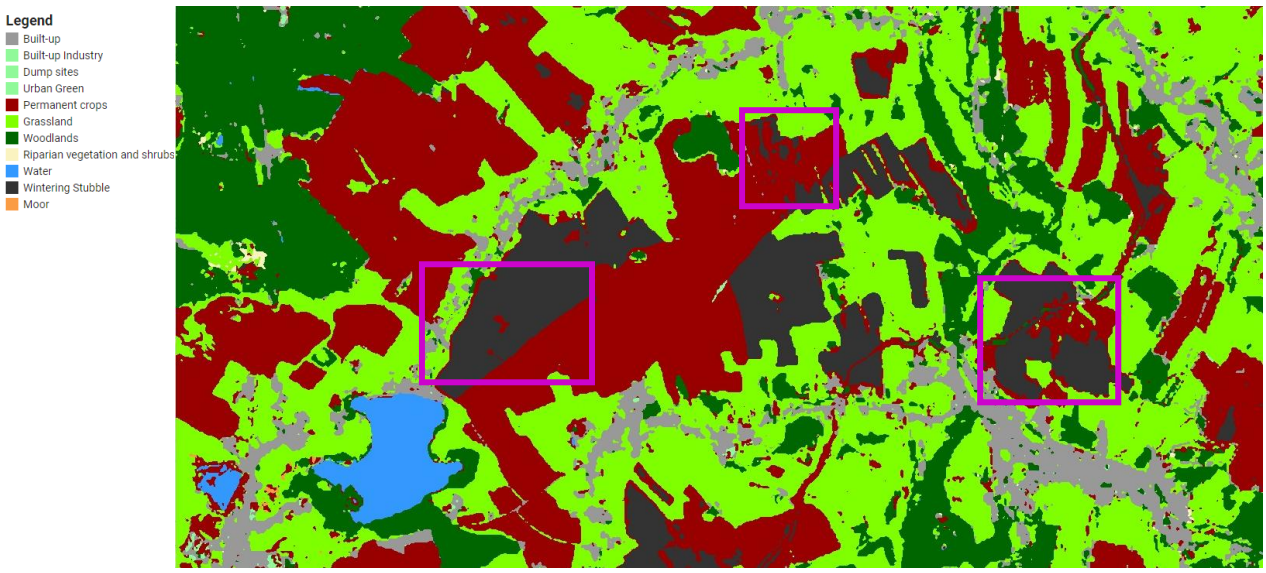

(**a**)

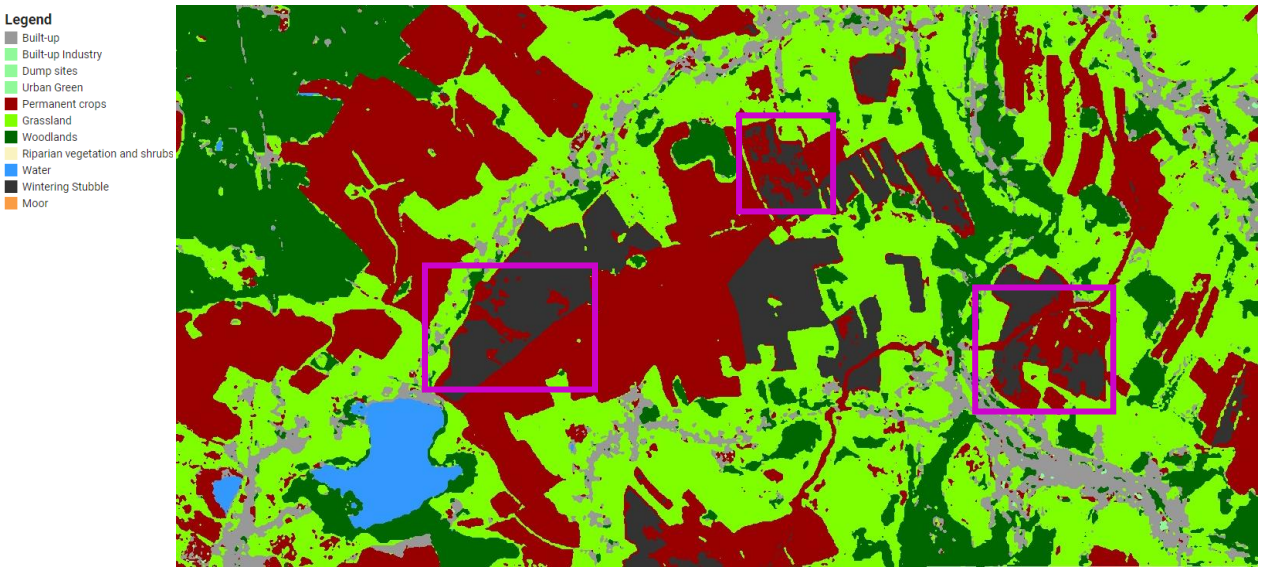

(**b**)

Figure 6: Classification results example in the region west of the dam "Großhartmannsdorfer large pond" ("Großhartmannsdorfer Großteich") south of the city Freiberg, Saxony: (a) Result of dataset 1 classification using SVM (best scenario at comparable periods). Dark grey represents the stubble classification class. (b) Result of dataset 2 classification using RF (worst scenario at comparable periods). Dark grey represents the stubble classification class. Pink rectangles areas of big difference on real stubble fields in winter 2019/2020 and shows the misclassification class "permanent crops".

The SVM classification was a few percentage points better than the OA for both datasets. In addition, the correct stubble classification using SVM was between 8 and 10 percent points better than with the RF (Table 5). The result of the classified stubble areas with the SVM also in dataset 2 (less good accuracies) with 83.8% corresponded almost exactly to the result of dataset 1 (high accuracies) with 84.2%. Only in the setting of limit values could further improvements be worked out, which when using the SVM then achieves a result of 92.6% area found of all fields to be checked for dataset 1 compared to the still very good 87.8% in the dataset 2. Using the same-thresholds for each field, as the 65%-threshold to ensure that most of the pixel in the area of interest were correct classified, the SVM improved the total classification results by almost 8.4% compared to the RF. The application of the SVM was much more robust than the RF.

Table 5: Result range of best and worst OA datasets with the same investigation periods.

Parameter	Dataset 1 RF (best OA)	Dataset 2 RF (worst OA)	Dataset 1 SVM (best OA)	Dataset 2 SVM (worst OA)
Stubble area found in ha	517.34	498,33	572.75	569,71
Stubble area not found in ha	162.51	181,52	107.10	110,14
Correct stubble classification	0.761	0.733	**0.842**	0.838
Share of number of fields with >65% correct classified stubble	0.577	0.549	0.746	0.746
Share of field area with >65% correct classified stubble	0.768	0.707	**0.926**	0.878

As Table 6 shows, the introduction of the negative buffer to consider edge effects removed almost a seventh of fields of the target object, but this only leads to a very

small loss of area (0.16% or 0.4%). These fields would need to be checked on site in a further step if this method will be used for control activities.

Table 6: Classification improvements using a negative buffer in the target fields at the best scenario (Dataset 1 SVM). Comparison between different ranges of negative buffer.

Dataset 1 SVM	Method: Buffer -10 m	Method: Buffer -20 m
Correct stubble classification	**0.894**	**0.912**
Share of fields with >65 % correct classified stubble	0.871	0.867
Share of field area with >65 % correct classified stubble	**0.961**	**0.965**
No. of fields excluded from evaluation by buffering	9	11
No. of fields remaining	62	60
Stubble area total with excluded fields	679.85 ha	679.85 ha
Stubble area of excluded fields	1.21 ha	2.96 ha
Area share of excluded stubble fields	0.0016	0.004

Table 7 shows that the larger the selected buffer, the smaller the actual examination area, since the field edges move inwards. The best classification of 98.4% results in a low limit value (>50%) in combination with a large buffer (-20 m). As the limit value decreases, the results were better, since other classes were increasingly tolerated to the same extent. The sense of this buffer-approach was also reflected directly in the results (Table 7) by improving the classification result by more than 5% (buffer -10 m) from 84.2% to 89.4% and up to almost 7% (buffer -20 m) from 84.2% to 91.2%. Also the sum of field area with >65% correct classified stubble improved close to 4% from 92.6% to 96.1% and 96.5%. It was not surprising that this increase was lower, because here, based on limit values, entire areas were switched to correctly classified after core field analysis. Because the result of these inner areas was then used to consider the entire field. Nevertheless, big area stubble fields were only under a minor influence of the edge effects and rather switched to the correct classified label than small fields. If only the investigation of small fields was improved by the negative buffering, then these can only added small areas to increase the total area sum on the threshold-based accuracy on field scale.

Table 7: Classification improvements using a negative buffer in the target fields. Detailed analysis of dataset 1 and SVM (best case) and the influence of threshold on classification results.

Parameter	Dataset 1 SVM		
Buffer in m	0	-10	-20
Number of fields	71	62	60
Total stubble field area in ha	679.85	581.82*	491.66*
Stubble field area found in classification (ha)	572.72	519.99	449.99
Share of correct found area	0.842	0.894	**0.915**
Improve results by	0	0.052	**0.073**
Share of stubble field area at threshold 0.5	0.956	0.962	**0.984**
Share of stubble field area at threshold 0.65	0.926	0.961	**0.965**
Share of stubble field area at threshold 0.75	0.785	0.800	**0.880**

* Total area decreases because the buffer affects all fields. To see the influence of the buffering on the results see Table 6.

Table 8 is directly connected to reach target 8 of this study. The classification of dataset 1 showed 75 fields with as stubble-classified pixels using SVM and 61 using RF, which were not requested for agricultural funding. Table 8 shows, that in the best scenario (dataset 1), both classifiers showed only very tiny proportions of the area as stubble compared to total field area (maximum 2.6%). By examining the crop rotation of 2019 to 2020, it showed that only half of these classifications could also be right outside the target object (RF 53%, SVM 51%). Large differences existed in the additional classified area size between RF and SVM. The SVM mapped five times more stubble outside known fields than the RF (about 150 ha compared to about 30 ha). This extra classification of area had not added any value to stubble areas that may had been presented, but actually lowered the probability of areas that may have been correctly classified. Classifications of overwintering stubble only had a small share of total field area by 0.8% (RF) and 2.6% (SVM).

Table 8: As stubble classification area outside the target object but inside agricultural area boundaries. Possibility of correct classification using pre- and post-investigation crop data.

Parameter	Dataset 1 RF	Dataset 1 SVM
Fields affected, total area in ha	8118.03	12401.17
Stubble classification area sum at affected fields in ha	69.39	323.64
Share of stubble pixels (%) at affected fields	0.008	0.026
Outside target fields possible correct classification in ha	37.07	165.13
Outside stubble area found not correct in ha	32.32	150.50
Share of possible correct areas (%)	0.53	0.51

4 Discussion

It could be shown that the selection of a suitable method (Maxwell et al. 2018) (RF vs SVM) had a great influence on the classification (Table 5). It could also be shown that the selection of a data set with highest accuracies, created by image composition and the same method (SVM), no longer had a major influence on the classification of overwintering stubble (Table 5). Steps in the further processing of the data, such as minimizing the edge effects (Table 6) or setting self-selected thresholds (Table 7), can significantly improve the result. In this study, a complete stubble detection method was developed and discussed. Minimizing edge and mixed pixel effects (Kolecka et al. 2018) is for wide target objects like farmland a useful method. It becomes very powerful using thresholds for a two-color field based traffic lights system (OPEKEPE 2020, Devos et al. 2017), which can established in a further step as operative application.

In this research, the SVM was more powerful than the RF because this study worked with high resolution Sentinel-2 data (Sheykhmousa et al. 2020). The RF was stronger

as the SVM in case of low spatial resolution images. There were many similar OA results between the different datasets and machine learning methods. This suggests that the classification was running on a stable system.

The good results also show that the approach to using time-series image compositions was selected correctly according to the investigation object. The study clearly shows four important findings:

1. With Corine Land Cover as a kind of training data proxy, the actual target object can be planted in a complete classification scheme. A comprehensive mapping of all land coverages in the investigation area is not necessary. The need for sufficient amount of data only remains for training the investigation object, which makes it very cost efficient (Demir et al. 2013). Although the Corine Land Cover data have great spatial resolution inaccuracies regarding the actual land cover (Minimum Mapping Unit = 25 ha) and the study period for land cover classifications was chosen very unfavorably (late summer, autumn and winter), an OA-classification results comparable to other studies could still be achieved (Tassi & Vizzari 2020).
2. The pixel-based approach connected with GIS-analysis and threshold-based statistics shows very good results. Without the erroneous influence of the edge pixels, however, it remains to decide how many of the inner pixels had to be correctly classified before the entire area is recognized as correctly classified. The setting of this limit value was very important. In this study, the threshold was mainly set at 65%. This was an arbitrary value combined with the intention that one would like to make sure that in any case a secured majority of the pixels had been classified with the desired class. There were already approaches that reduced this value to such an extent that fields were categorized as the class whose class has only the highest relative proportion within the area (Devos et al. 2020). The results further indicate that, purely pixel-based, there were still many uncertainties when it came to identifying the stubble. At this point, the main question is why some fields were not recognized.
3. By sacrificing fields of small size or unfavorable shape, influenced by edge and mixed pixels, the remaining areas achieve very good classification results in the case of agricultural promotion and CAP-control. For the necessary future on-site inspection, results of well over 90% by this remote sensing approach, like

in this study and defined in Chapter 1, mean a significant minimization of the workload to be performed.

4. The results also show that the approach presented here was not recommended for use in the area of the Water Framework Directive (WFD). This was because the hoped-for additional information to the known information was fraught with too many uncertainties. Probable classifications and improbable classifications were close to each other in their proportions (about 50 to 50). In addition to the classification, data on the crop rotation will be necessary at this time in order to adjust classified areas according to this question. At this point, the proposed methodology still offers much potential for development. Stubble classification depends heavily on in-situ data, which are subject to strict funder specifications in this measure. Additional in-situ information on stubble voluntarily left standing over the winter is needed.

Sentinel-1 and Sentinel-2 were together very effective in identifying land use during winter on agricultural fields (Denize et al. 2019). So data fusion, like the combination of radar and multispectral data should be a next step of image composition (Luo et al. 2021, Orynbaikyzy 2020). Here, too, additional bands and indices can be derived, i.e. the Radar Vegetation Index (RVI) (Kim et al. 2012). Carrasco et al. (2019) says, that combined datasets have outperformed single-sensor datasets.

The enhancement of the classification to include additional classes of annually land cover or search for other winter land covers (Denize et al. 2019). In relation to the agricultural context, the additional class of catch crops would be included at this point (Denize et al. 2019, Schulz et al. 2019, Schulz et al. 2021). For this land cover on arable land, the covered investigation period would not have to be extended.

Due to the high accuracy detecting wintering stubble fields by combining ML and GIS, the in this research presented method can be put directly in an application for wintering stubble detection (e.g. as an applied remote sensing tool for the government).

5 Conclusion

This study tested different image composition methods (bands, indices, time series and different seasonal composition strategies) to generate spectral input data for a specific annually target object (wintering stubbles) classification using different machine learning methods (RF and SVM).

This study has succeeded in showing a rapidly implementable approach to how regulatory monitoring of agricultural lands can be implemented under CAP. The high accuracies achieved will ensure a cost-efficient use of remote sensing as a service in the agricultural administration, since many follow-up checks like on-site inspections will be no longer needed.

This study makes an important contribution to application-oriented remote sensing, since the agricultural administration is rarely addressed here as a target audience, although there is a high financial and social relevance behind these activities. The fact that the administration is already aware of the reported fields with "overwintering stubble" generally facilitates the implementation of the presented method, since the potential user only has to check by remote sensing whether the information is correct. However, the obstacles associated with identifying voluntarily stubble fields left, without funding, quickly became apparent. At this point, the in-situ data (fields with OS, but whose farmers are not bound by the terms of the measure and are therefore allowed to farm these fields differently than in the current in situ data) were missing and the information on the previously cultivated crop in the field was not sufficient to create convincing results for an application. Also, this study makes an important contribution in showing how to create a low-cost training dataset for machine learning and also addresses the rarely studied land cover of "overwintering stubble" in unprecedented detail.

Disclosures

There are no relevant financial interests in the manuscript and no other potential conflicts of interest.

Acknowledgments

I am grateful that the Google Earth Engine provides computational capacities and Sentinel data free of charge. This research received no external funding.

Code, Data, and Materials Availability

The GEE codes processing Sentinel 2 data in this study are freely available online. GEE code for S2-dataset creation at https://code.earthengine.google.com/c74024361c9b1b87f40c02bc196e46d0 and the GEE code for the S2-dataset-classifaction https://code.earthengine.google.com/842613f876d490524e57ad4dbcaf1e39. Since a large number of datasets calculated in this study, there is a link to the creation of Dataset 1 and the classification of this dataset at this point to maintain clarity.

References

Beriaux, E., Jago, A., Lucau-Danila, C., Planchon, V., & Defourny, P. (2021). Sentinel-1 Time Series for Crop Identification in the Framework of the Future CAP Monitoring. *Remote Sens.* 13, 2785. https://doi.org/10.3390/rs13142785.

Cai, W., Zhao, S., Wang, Y., Peng, F., Heo, J., & Duan, Z. (2019). Estimation of Winter Wheat Residue Coverage Using Optical and SAR Remote Sensing Images. *Remote Sens*. 11, 1163. https://doi.org/10.3390/rs11101163.

Carrasco, L. O'Neil, A.W., Morton, R.D., & Rowland, C.S. (2019). Evaluating Combinations of Temporally Aggregated Sentinel-1, Sentinel-2 and Landsat 8 for Land Cover Mapping with Google Earth Engine. *Remote Sens.* 11, 288. https://doi.org/10.3390/rs11030288.

CLC - CORINE Land Cover (2021). Available online: https://land.copernicus.eu/pan-european/corine-land-cover (accessed on 09.08.2021).

CLMS - Copernicus Land Monitoring Service (2021). CORINE Land Cover nomenclature conversion to Land Cover Classification system. Available on https://land.copernicus.eu/eagle/files/eagle-related-projects/pt_clc-conversion-to-fao-lccs3_dec2010 (accessed on 15.10.2021).

ESA - European Space Agency (2021). Data products. Available online: https://sentinels.copernicus.eu/web/sentinel/missions/sentinel-2/data-products (accessed on 18.10.2021).

Daughtry C.S.T., McMurtry III, J.E., Chapelle, E.W., hunter, W.J., & Steiner, J.L. (1996). Measuring crop residue cover using remote sensing *techniques*. *Theor Appl Climatol*. 54, 17–26. https://doi.org/10.1007/BF00863555.

Demir, B., Minello, L., & Bruzzone, L. (2013). Definition of Effective Training Sets for Supervised Classification of Remote Sensing Images by a Novel Cost-Sensitive Active Learning Method. *IEEE Transactions on Geoscience and Remote Sensing* 52 (2), 1272-1284. https://doi.org/10.1109/TGRS.2013.2249522.

Denize, J., Hubert-Moy, L., Betbeder, J., Corgne, S., Baudry, J., & Pottier, E. (2019). Evaluation of Using Sentinel-1 and -2 Time-Series to Identify Winter Land Use in Agricultural Landscapes. *Remote Sens*. 11, 37. https://doi.org/10.3390/rs11010037.

Devos, W., Fasbender, D., Lemoine, G., Loudjani, P., Milenov, P., & Wirnhardt, C. (2017). Discussion document on the introduction of monitoring to substitute OTSC. *JRC Technical Reports*. https://doi.org/10.2760/258531.

Devos, W., Luketic, N., Milenov, P., & Borio, D. (2020). Checks by Monitoring quality inspection: EU requirements and methodology. *JRC Technical Reports* (2020). Available online: https://wikis.ec.europa.eu/display/GUIDANCEANDTOOLSFORCAP/Checks+by+monitoring?preview=/86968800/86968899/CbMQA_DD_1_1.pdf.

Dvorakova, K., Shi, P., Limbourg, Q., & van Wesemael, B. (2020). Soil Organic Carbon Mapping from Remote Sensing: The Effect of Crop Residues. *Remote Sens*. 12, 1913. https://doi.org/10.3390/rs12121913.

Franch, B., Cintas, J., Becker-Reshef, I., Sanchez-Torrez, M.J., Roger, J., Skakun, S., Sobrino, J.A., van Tricht, K., Degerickx, J., Gilliams, S., Koetz, B., Szantoi, Z., & Whitcraft, A. (2022). Global crop calendars of maize and wheat in the framework of the WorldCereal project. *GIScience & Remote Sensing*, 59:1, 885-913. https://doi.org/10.1080/15481603.2022.2079273.

FAO - Foreign Agricultural Service (2025). Crop Calendars for Europe. Available online: https://ipad.fas.usda.gov/rssiws/al/crop_calendar/europe.aspx (accessed on 28.07.2022).

Gao, B.C. (1996). NDWI - a normalized difference water index for remote sensing of vegetation liquid water from space. *Rem. Sens. Environ*. 58, 257–266 (1996). https://doi.org/10.1016/S0034-4257(96)00067-3.

Gorelick, N., Hancher, M., Dixon, M., Ilyushchenko, S., Thau, D., & Moore, R. (2017). Google Earth Engine: Planetary-scale geospatial analysis for everyone. *Remote Sensing of Environment,* 202, 18-27 (2017). https://doi.org/10.1016/j.rse.2017.06.031.

Gutman, G., Byrnes, R.A., Masek, J., Covington, S., Justice, C., Franks, S., & Headley, R. (2005). Towards monitoring land-cover and land-use changes at a global *scale*: the global land survey 2005. *Photogrammetric Engineering and Remote Sensing* 74(1), 6-10.

Hiloidhari, M., & Baruah, D.C. (2011). Crop residue biomass for decentralized electrical power generation in rural areas (part 1): Investigation of spatial availability. *Renewable and Sustainable Energy Reviews* 15, 1885-1892. https://doi.org/10.1016/j.rser.2010.12.010.

Hively, W.D., Lamb, B.T., Daughtry, C.S.T., Shermeyer, J., McCarty, G.W., & Quemada, M. (2018). Mapping Crop Residue and Tillage Intensity Using WorldView-3 Satellite Shortwave Infrared Residue Indices. *Remote Sens*. 10, 1657. https://doi.org/10.3390/rs10101657.

Kabisch, N., Selsam, P., Kirsten, T., Lausch, A., & Blumberger, J. (2019). A multi-sensor and multi-temporal remote sensing approach to detect land cover change dynamics in herogeneous urban landscapes. *Ecol. Indic*. 99, 273–282. https://doi.org/10.1016/j.ecolind.2018.12.033.

Khabbazan, S., Vermunt, P., Steele-Dunne, S., Ratering Arntz, L., Marinetti, C., van der Valk, D., Iannini, l., Molijn, R., Westerdijk, K., & van der Sande, C. (2019). Crop Monitoring Using Sentinel-1 Data: A Case Study from The Netherlands. *Remote Sens*. 11, 1887. https://doi.org/10.3390/rs11161887.

Khan, M.R., de Bie, C.A.J.M., van Keulen, H., Smaling, E.M.A., & Real, R. (2010). Disaggregating and mapping crop statistics using hypertemporal remote sensing. *International Journal of Applied Earth Observation and Geoinformation*, 12(1), 36-46. https://doi.org/10.1016/j.jag.2009.09.010.

Kim, Y., Jackson, T., Bindlish, R., Lee, H., & Hong, S. (2012). Radar vegetation index for estimating the vegetation water content of rice and soybean. *IEEE Geosci. Remote Sens. Lett*. 9, 564–568 (2012).

Kolecka, N., Ginzler, C., Pazur, R., Price, B., & Verburg, P.H. (2018). Regional Scale Mapping of Grassland Mowing Frequency with Sentinel-2 Time Series. *Remote Sens*. 10, 122. https://doi.org/10.3390/rs10081221.

Koschke, L., Fürst, C., Frank, S., & Makeschin, F. (2012). A multi-criteria approach for an integrated land-cover-based assessment of ecosystem services provision to support landscape planning. *Ecol. Indic*. 21, 54–66. https://doi.org/10.1016/j.ecolind.2011.12.010.

Linh, N.H.K., Erasmi, S., & Kappas, M. (2012). Quantifying land use/land cover change and landscape fragmentation in Danang City, Vietnam: 1979-2009. *International Archives of the Photogrammetry, Remote Sensing and Spatial Information Sciences*, Volume XXXIX-B8.

Lunetta, R.S., Knight, J.F., Ediriwickrema, J., Lyon, J.G., & Worthy, L.D. (2006). Land-cover change detection using multi-temporal MODIS NDVI data. *Remote Sens. Environ*. 105, (2006) https://doi.org/10.1016/j.rse.2006.06.018.

Luo, C., Liu, H.-J., Lu, L.-P., Liu, Z.-R., Kong, F.C., & Zhang, X.-L. (2021). Monthly composites from Sentinel-1 and Sentinel-2 images for regional major crop mapping with Google Earth Engine. *Journal of Integrative Agriculture* 20(7), 1944-1957. https://doi.org/10.1016/S2095-3119(20)63329-9.

Maxwell, A.E., Warner, T.A., & Fang, F. (2018). Implementation of machine-learning classification in remote sensing: an applied review. *International Journal of Remote Sensing* 9, 2784-2817. https://doi.org/10.1080/01431161.2018.1433343.

Mira, N.C., Catalo, J., & Nico, G. (2019). Multi-temporal crop classification with machine learning techniques. *Proc. SPIE, Remote Sensing for Agriculture, Ecosystems, and Hydrology* XXI. https://doi.org/10.1117/12.2532132.

Mzid, N., Pignatti, S., Huang, W., & Casa, R. (2021). An Analysis of Bare Soil Occurrence in Arable Croplands for Remote Sensing Topsoil Applications. *Remote Sens*. 13, 474. https://doi.org/10.3390/rs13030474.

Najafi, P., Navid, H., Feizizadeh, B., Eskandari, I., & Blaschke, T. (2019). Fuzzy Object-Based Image Analysis Methods Using Sentinel-2A and Landsat-8 Data to Map and Characterize Soil Surface Residue. *Remote Sens.* 11, 2583. https://doi.org/10.3390/rs11212583.

Orynbaikyzy, A. (2020). Crop Type Classification Using Fusion of Sentinel-1 and Sentinel-2 Data: Assessing the Impact of Feature Selection, Optical Data Availability, and Parcel Sizes on the Accuracies. *Remote Sens*. 12, 2779. https://doi.org/10.3390/rs12172779.

Phan, T.N., Kuch, V., & Lehnert, L.W. (2020). Land Cover Classification using Google Earth Engine and Random Forest Classifier – The Role of Image Composition. *Remote Sens*. 12, 2411. https://doi.org/10.3390/rs12152411.

Phiri, D. Simwanda, M., Salekin, S., Nyirenda, V., Murayama, Y., & Ranagalage, M. (2020). Sentinel-2 Data for Land Cover/Use Mapping: A Review. *Remote Sens.* 12, 2291. https://doi.org/10.3390/rs12142291.

Quemada, M., & Daughtry, C.S.T (2016). Spectral Indices to Improve Crop Residue Cover Estimation under Varying Moisture Conditions. *Remote Sens*. 8, 660. https://doi.org/10.3390/rs8080660.

Reinermann, S., Asam, S., & Kuenzer, C. (2020). Remote Sensing of Grassland Production and Management - A Review. *Remote Sens*. 12, 1949. https://doi.org/10.3390/rs12121949.

SMEKUL - Saxon State Ministry for Energy, Climate Protection, Environment and Agriculture (2017). AL 7 - Überwinternde Stoppeln. (AL 7 – Overwintering Stubbles). Available online: https://www.smul.sachsen.de/foerderung/download/AL_7.pdf (accessed on 30.09.2021).

Schulz, C., Keck, N., Kleinschmitt, B. (2019). Reduction of On-side Controls of Catch Crop Fields with Sentinel-2 and Sentinel-1 Phenological Reference Profiles. *2019 10th International Workshop on the Analysis of Multitemporal Remote Sensing Images (MultiTemp)*, 1-3. https://doi.org/10.1109/Multi-Temp.2019.8866901.

Schulz, C., Holtgrave, A.-K., & Kleinschmitt, B. (2021). Large-scale winter catch crop monitoring with Sentinel-2 time series and machine learning - An alternative to on-site controls? *Computers and Electronics in Agriculture* 186. https://doi.org/10.1016/j.compag.2021.106173.

Segarra, J., Buchaillot, M.L., Araus, J.L., & Kefauver, S.C. (2020). Remote Sensing for Precision Agriculture: Sentinel-2 Improved Features and Applications. *Agronomy* 10, 641. https://doi.org/10.3390/agronomy10050641.

Sen4CAP Consortium (2021). Sentinels for Common Agriculture Policy. Available online: http://esa-sen4cap.org/ (accessed on 30.09.2021).

Seo, B., Lee, J., Lee, K.-D., Hong, S., & Kang, S. (2019). Improving remotely-sensed crop monitoring by NDVI-based crop phenology estimators for corn and soybeans in Iowa and Illinois, USA," *Field Crops Research.* 238, 113-128. https://doi.org/10.1016/j.fcr.2019.03.015.

Sheykhmousa, M., Mahdianpari, M., Ghanbari, H., Mohammadumanesh, F., Ghamisis, P., & Homayouni, S. (2020). Support Vector Machine Versus Random Forest for Remote Sensing Image Classification: A Meta-Analysis and Systematic Review. *IEEE Journal of Selected Topics in Applied Earth Observations and Remote Sensing* 13, 6308-6325. https://doi.org/10.1109/JSTARS.2020.3026724.

Singh, R.P., Singh, N., Singh, S., & Mukherjee, S. (2016). Normalized Difference Vegetation Index (NDVI) Based Classification to Assess the Change in Land Use/Land Cover (LULC) in Lower Assam, India. *Int. J. Adv. Remote Sens. GIS* 5. https://doi.org/10.23953/cloud.ijarsg.74.

Sudmanns, M., Tiede, D., Augustin, H., & Lang, S. (2020). Assessing global Sentinel-2 coverage dynamics and data availability for operational Earth observation (EO) applications using the EO-Compass. *International Journal of Digital Earth* 13(7), 768-784. https://doi.org/10.1080/17538947.2019.1572799.

Tan, J., Yu, D., Li, Q., Tan, X., & Zhou, W. (2020). Spatial relationship between land-use/land-cover change and land surface temperature in the Dongting Lake area, China. *Sci Rep* 10, 9245. https://doi.org/10.1038/s41598-020-66168-6.

Tassi, A., & Vizzari, M. (2020). Object-Oriented LULC Classification in Google Earth Engine Combining SNIC, GLCM, and Machine Learning Algorithms. *Remote Sens*. 12, 3776. https://doi.org/10.3390/rs12223776.

Techen, A.-K., Ries, E., & Steinführer, A. (2015). Evaluierung der Gewässerschutzberatung in Hessen im Kontext der EU-Wasserrahmenrichtlinie: Auswirkungen auf Wissen und Handeln von Landwirten. *Thünen Report* 33. https://doi.org/10.3220/REP1446716352000.

OPEKEPE - Payment and Control Agency for Guidance and Guarantee Community Aid. (2020). UC 1a: Earth Observation Monitoring & Traffic Lights. Available online: https://www.niva4cap.eu/uploads/downloads/webinar_UC1a_PRESENTATION_2020_5_20_v3.pdf (accessed on 14.09.2021).

Vickery J.A., Feber, R.E., & Fuller, R.J. (2019). Arable field margins managed for biodiversity conservation: A review of food resource provision for farmland birds. *Agriculture, Ecosystems & Environment*, 133(1-2), 1-13. https://doi.org/10.1016/j.agee.2009.05.012.

Vizzari, M., Santaga, F., & Benincasa, P. (2019). Sentinel 2-Based Nitrogen VRT Fertilization in Wheat: Comparison between Traditional and Simple Precision Practices. *Agronomy* 9, 278. https://doi.org/10.3390/agronomy9060278.

Vizzari, M. & Sigura, M. (2015). Landscape sequences along the urban–rural–natural gradient: A novel geospatial approach for identification and analysis. *Landsc. Urban Plan*. 140, 42–55. https://doi.org/10.1016/j.landurbplan.2015.04.001.

Manuscript 2

Determining the Usefulness of the Copernicus High Resolution Vegetation Phenology and Productivity Product (HR-VPP) with Official Agricultural Data on Cropland in Case of the 2018 Drought in the Federal State of Saxony, Germany

Journal of Water and Climate Change, 2023, Vol. 14 (11)

Sebastian Goihl[1]*

[1]Saxon State Office for Environment, Agriculture and Geology, Box 100510, 01076 Dresden, Germany

*Correspondence: Sebastian.Goihl@smekul.sachsen.de

Received: 12 December 2022; Accepted: 22 October 2023; Published: 06 November 2023

Reference: https://doi.org/10.2166/wcc.2023.501

Abstract

Remote sensing-based data on vegetation condition provide important information for agriculture. In this study, the potential uses of the freely available High Resolution Vegetation Phenology and Productivity Product (HR-VPP) are tested. This test examines the 2018 drought year in the state of Saxony, Germany, and the capabilities and limitations of the HR-VPP product in use with Integrated Administration and Control System (IACS) data. The results show that field and crop type specific spatial (re)analyses of a drought are possible and that there is still great potential in this data analysis. Using the data in a new proposed VPP-based Farm-Level Temporal Comparison Indicator (VPP-FLTCI), it was not possible to tease out patterns in why farms applied for state drought aid in 2018 compared to other farms. In the future, even better and more detailed analyses based on the HR-VPP can be expected, as the data series with now a total of five years is still very short to generate sufficient references especially in Central European agriculture, which is characterized by crop rotation.

Keywords: Agriculture, Drought, Remote Sensing, Sentinel-2, HR-VPP, Productivity, Copernicus, FLTCI

Highlights:

- Unique analysis brought official IACS-data together with open CLMS HR-VPP-product
- Detailed 2018 drought reanalysis was possible on crop type scale
- Detailed 2018 drought reanalysis was possible on regional and spatial type scale
- VPP data could not explain farms drought aid applications alone

1 Introduction

A large number of Earth observation satellites collect today information on vegetation. This information supports decision-making processes in agriculture (Segarra et al. 2020), forestry (Lastovicka et al. 2020, Philipp et al. 2021), nature conservation (Lastoviacka et al. 2020, Smith 2021), climate impact (Gouveia et al. 2017) and climate change monitoring studies (Chen et al. 2019). Satellite measured vegetation information is often calculated and presented with vegetation indices (Xue & Su 2017). Climate change is making monitoring fire (Brigitte et al. 2012) and drought events (Gouveia et al. 2017) increasingly important globally and regionally. Agricultural production in Europe repeatedly suffers losses (Beillouin et al. 2020, Reinermann et al. 2019) due to such drought events, which are as high as in 2018 that government aid for farmers was made possible (D'Agostino 2018). In Germany alone, 292 million

Euro was paid out to farmers as part of drought aid (Handelsblatt 2022). The Federal State of Saxony accounted for around 33 million Euro of this (10.3%) (Media Service Saxony 2022). However, the monitoring of agricultural drought is important not only on regional scale, because on global scale there are high financial losses on agriculture due drought events and affected millions of people (Hazaymeh & Hassan 2016, Sutanto et al. 2019).

To measure agricultural drought (as a differentiation from hydrological drought, meteorological drought and socio-economic drought (Hazaymeh & Hassan 2016), knowledge of soil water deficit respectively in particular plant available water, which in turn leads to the loss of agricultural yields (Liliane & Charles 2020), is particularly necessary. The opposite approach is taken by remote sensing data on vegetation, since the condition of this can be used to indirectly infer the supply of soil water. Existing products to estimate soil moisture in the area of interest are for example the "Soil Moisture Traffic Light" (https://life.hydro.tu-dresden.de/BoFeAm/dist/index.html (Kronenberg et al. 2022)) which used the water budget model LWF-Brook90R (Schmidt-Walter et al. 2020). Six classes of soil drought intensity are offered each by the "UFZ Drought Monitor" (https://www.ufz.de/index.php?de=37937) and the "BKG Drought Atlas" (https://atlas.bkg.bund.de/webapps/duerreatlas/), as both are based on the hydrologic mesoscale hydrologic model (mHM) (Samaniego et al. 2010, Kumar et al. 2013). In the neighboring Czech Republic, there was the Czech Drought Monitor System, which not only depicts current and modeled conditions, but also weekly reports on vegetation condition based on satellite images (Trnka et al. 2020). Here, drought forecast (+9 days and +2 months) calculated by numerical weather prediction models were implanted too. Global or continental drought monitoring systems (for example the European Drought Observatory) also exist, but will not be mentioned further here.

Using in-situ drought indicators like Standardized Precipitation Index (SPI) (McKee et al. 1993), Standardized Soil Moisture Index (SSI) (Hao & AghaKouchak 2013), and Multivariate Standardized Drought Index (MSDI) (Hao & AghaKouchak 2014) were also common. They could connected in models like the Global Integrated Drought Monitoring and Prediction System (GIDMaPS) (Hao et al. 2014), too.

Remote sensing data provided a large number of agricultural drought monitoring indices, similar to in situ indices, for this purpose (Hazaymeh & Hassan 2016). In contrast to commonly used in-situ based indices like SPI, the remote sensing indices

were calculated mainly by band recombination. Satellites from which spectral bands are used for this purpose are currently often Sentinel-2, Landsat 8 or Moderate Resolution Imaging Spectroradiometer (MODIS). Remote sensing indices can be used, for example to measure vegetation health (Trnka et al. 2020) like the Normalized Difference Vegetation Index (NDVI) or to calculate drought conditions with the Perpendicular Drought Index (PDI) (Ghulam et al. 2008). Also a monitoring of the vegetation water content with the Simple Ration Water Index (SRWI) (Zarco-Tejeda et al. 2003) or Normalized Different Water Index (NDWI) (Gao 1996), was possible. Kloos et al. (2021) figured out with correlation analysis over growing season from 2001 to 2020 in Bavaria (Germany), that Temperature Condition Index (TCI) and Vegetation Health Index (VHI) correlate strongly with soil moisture agricultural yield anomalies. They derived from this that these indices had the potential to detect agricultural drought in there study area. A soil moisture deficit in the growing season was the basis of agricultural drought, so soil moisture based indices described agricultural drought better than meteorological and hybrid drought indices (Chatterjee et al. 2022). There were also various satellite image-based products and services for soil moisture as an indicator of drought. For Europe, these would include for example the following products: Copernicus Global Land Service - Soil Surface Moisture (CGLS-SSM) (Bauer-Marschallinger & Massart 2022), Soil Moisture and Ocean Salinity (SMOS), ASCAT or Soil Moisture Active Passive (SMAP) (El Hajj et al. 2018, Portal et al. 2020). However, the spatial resolution of these products of at least 1 km is not sufficient for many applications, such as field-based evaluations. Remote sensing can also contribute to the understanding and measurement of drought events using indirect methods by looking at the dynamics of dams and lakes and their water surface extent (Büttig et al. 2022, Wieland & Martinis 2020, Dehkordi et al. 2022). There are also indirect in situ indicators, such as low water levels at river gauges.

Multi-criteria approaches (MCA), such as by Ihinegbu & Ogonwumi (2021) combined in situ observations (precipitation) with satellite imagery (land surface temperature, NDVI). Using this MCA they classified the neighboring federal state to the north of Saxony into three zones of drought prevalence with focus on agricultural fields and found that more than 77% of the fields were in the high drought zone in 2018. Philipp et al. (2021) said by using harmonic modelling method of NDVI, that in August 2018 the models indicate in Germany severe drought conditions across all forest. A strong correlation between in-situ and remote sensing data were observed for soil moisture

and the self-calibrated Palmer Drought Severity Index (Philipp et al. 2021). As will be shown in the next section, the HR-VPP is an aggregation of indices to a new product, too.

Not only is the current monitoring of a drought important, but also the forecasting of such events is essential. Bouras et al. (2021) analyzed, that models using multiple data sources outperformed models based on a single dataset in cereal yield forecasting. Two months before harvest, for yield prediction satellite drought indices (e.g. TCI) were a major source of information by contributing up to 73% to the prediction accuracy in Marocco. For forecasting, models like LISFLOOD using standardized meteorological drought indices (e.g. SPI or Standardized Precipitation Evaporation Index (SPEI)) were used with a higher skill prediction for longer drought events than for short ones (Sutanto 2019). By providing services, such as the Copernicus Land Monitoring Service (CLMS, https://land.copernicus.eu/ ready-made products are available to the data user. No in-house processing resources, ground truth surveys, and algorithms need to be applied to compute these products. There are problems associated with such simplification, since technical questions call for specific products that cannot answered satisfactorily with products "for the general public". In order to evaluate whether these products are usable at all, they have first be tested with regard to their limits and possibilities. Especially institutions from the areas of public authorities and administration can benefit from such ready products, since the participation in the use of Copernicus data is associated with expenses that this user group often cannot afford.

For monitoring and assessing drought, data on vegetation condition can be useful (Reinermann et al. 2019), as described above. Among the products offered is the High Resolution Vegetation Phenology and Product (HR-VPP) (Smets et al. 2021). However, whether these data are actually useful in case of agriculture, has yet to be evaluated. Therefore, this study aimed to resolve the following questions:

1. Is the annual HR-VPP product generally suitable to trace the impact of the 2018 drought in Saxony as a reanalysis?
2. Can regional differences of the drought effect be worked out (spatial level of municipalities/counties)?
3. Can crop-specific differences of the drought effect 2018 be worked out (spatial level of municipalities/counties)?
4. Can the available data be used to explain why which farms applied for drought relief and why which did not?

The results of this study can provide important information as to whether and under what circumstances users from the field of agriculture or agricultural administration can expect added value from these HR-VPP products.

A previous work with the HR-VPP product examines greenness in urban areas and concludes that the HR-VPP leads to large overestimates of urban greenness (Borgogno-Mondino & Fissore 2022). Bojanowski et al. (2022) concludes, that the parameters of vegetation phenology have a lower performance in crop recognition and recommend the use of temporal datasets, which are more powerful.

To date, there are not many studies on the evaluation of HR-VPP data in relation to field crops in case of drought and dry condition productivity. This is certainly related to the obstacle that Integrated Administration and Control System (IACS) data are not freely available. However, these official data allow insights into location and crop type that have previously been hidden from the public. In addition, the core question around the effect of the 2018 drought on agriculture in Saxony is a significant use case that is being addressed.

2 Study Area

The German federal state of Saxony (Fig. 1) is located in eastern Germany and shares the border with Poland to the east and the Czech Republic to the south. Agriculture is practiced on a good half of Saxony's 18.41 km² area.

Cereals were the most important field crop in Saxony. The area under cultivation fluctuated by several thousand hectares from year to year. Root crops initially lost importance in the period under consideration, but the area under cultivation were increasing again (SMEKUL 2022).

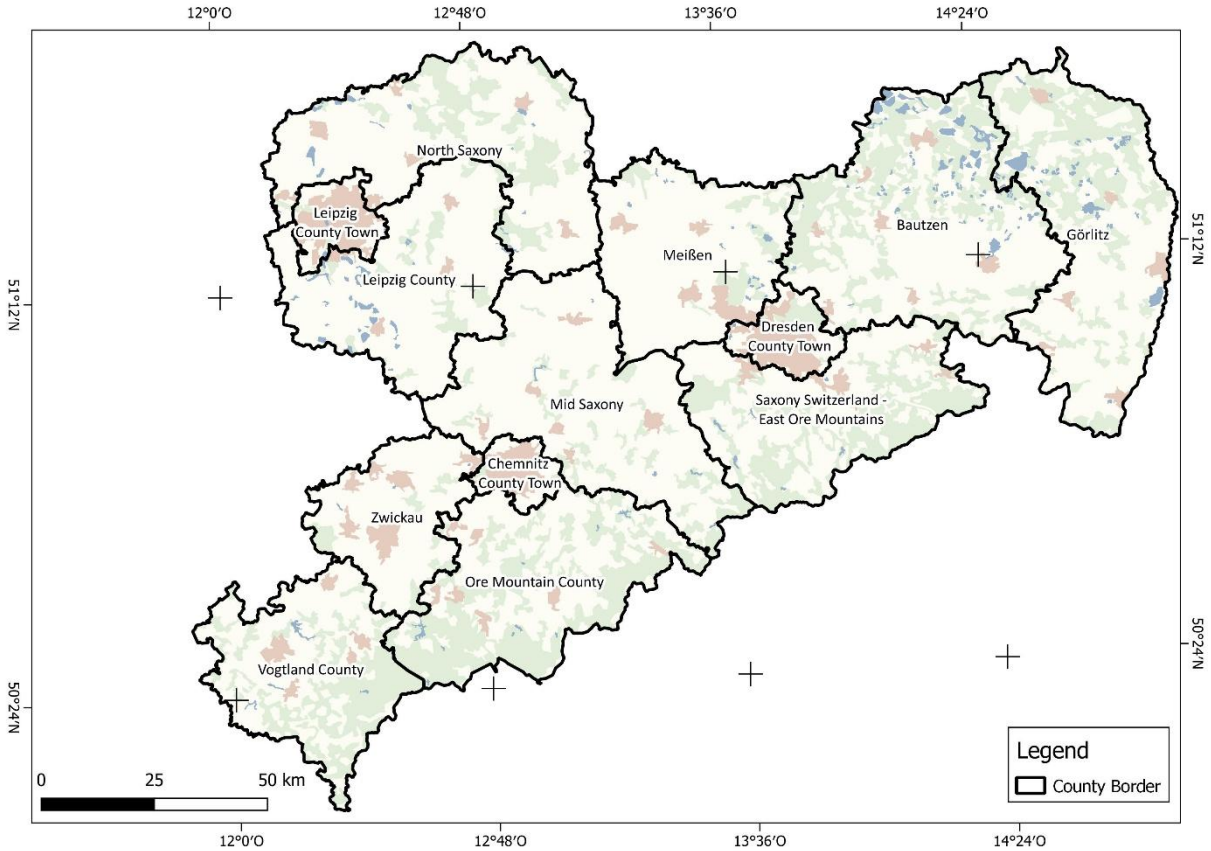

Figure 8: State of Saxony: location, land cover and counties. Reference System: WGS 84.

The drought year 2018 was particularly noteworthy: the average annual temperature in 2018 in Saxony was 10.3 °C. This is 2.2 Kelvin above the multi-year average (1961 to 1990), which is 8.1 °C. This makes it the warmest year since 1881. With almost 2,060 hours of sunshine (multi-year average 1961 to 1990: 1,549 hours). With about 475 l/m² of precipitation (multi-year average 1961 to 1990: 699 l/m²), 2018 was one of the years with the lowest precipitation since 1881 (SMEKUL 2019). As a result, the harvest volume, which varied from region to region, was significantly lower than usual, especially for winter cereals, but also for potatoes. Green corn and silage corn yielded only half the previous year's level. This and dried-up pastures caused fodder shortages on livestock farms (SMEKUL 2019).

The German State and the federal-state of Saxony drought aid program supported the most farmers and livestock keepers to maintain their liquidity despite the high losses and necessary and the need to make additional purchases. More than 30 million euros were available for this purpose in Saxony (Media Service Saxony 2022, SMEKUL 2019).

3 Datasets and pre-processing

In this study, four main data sources were used, for 2017, 2018, 2019 and 2020 respectively.

3.1 High Resolution Vegetation Phenology and Product (HR-VPP)

The first data source was the High Resolution Vegetation Phenology and Product (HR-VPP) (Smets et al. 2021), which can be obtained from the CLMS. This in turn links to the WEkEO portal to obtain data: https://www.wekeo.eu/ (login required). The HR-VPP was provided by tile, following the common provision of Sentinel-2 tiles (110 x 110 km with 10 km overlap at the edges). With 10 m x 10 m pixel resolution, there was no scale mismatch between the agricultural fields and the product used (Bouras et al. 2021). As a dimensionless value per pixel, the HR-VPP mapped a value that was, at its core, the length of the growing season and the amplitude (intensity) of it. Thirteen parameters are used to calculate this value (Table 1).

Table 1: VPP-Parameters after CLMS (2022, https://land.copernicus.eu/pan-european/biophysical-parameters/high-resolution-vegetation-phenology-and-productivity. PPI = Plant Phenology Index (Smets et al. 2021)).

Parameter	Parameter description	Unit
SOSD	Day of start-of-season	day-of-year
EOSD	Day of end-of-season	
MAXD	Day of maximum-of-season	
SOSV	Vegetation index value at SOSD	PPI
EOSV	Vegetation index value at EOSD	
MINV	Average vegetation index value of minima on left and right sides of each season	
MAXV	Vegetation index value at MAXD	
AMPL	Season amplitude (MAXV – MINV)	
LENGTH	Length of Season (number of days between start and end)	day
LSLOPE	Slope of the greening up period	PPI x day-1
RSLOPE	Slope of the senescent period	
SPROD	Seasonal productivity. The growing season integral computed as the sum of all daily values between SOSD and EOSD	PPI × day
TPROD	Total productivity. The growing season integral computed as sum of all daily values minus their base level value.	

Measurements are taken for these annual products from 01.01. to 31.12. of each calendar year. Currently, the product is provided for the years 2017 to 2021. The tiles used for this investigation in Saxony can be taken from the following table (Table 2).

Table 2: List of in this study used HR-VPP-Products. Data source: https://www.wekeo.eu.

Number	Product Name
1	VPP_2017_S2_T32UQA-010m_V101_s1_TPROD
2	VPP_2017_S2_T32UQB-010m_V101_ s1_TPROD
3	VPP_2017_S2_T33UUT-010m_V101_ s1_TPROD
4	VPP_2017_S2_T33UVT-010m_V101_ s1_TPROD
5	VPP_2017_S2_T33UUS-010m_V101_ s1_TPROD
6	VPP_2017_S2_T33UVS-010m_V101_ s1_TPROD
7	VPP_2018_S2_T32UQA-010m_V101_s1_TPROD
8	VPP_2018_S2_T32UQB-010m_V101_ s1_TPROD
9	VPP_2018_S2_T33UUT-010m_V101_ s1_TPROD
10	VPP_2018_S2_T33UVT-010m_V101_ s1_TPROD

11	VPP_2018_S2_T33UUS-010m_V101_ s1_TPROD
12	VPP_2018_S2_T33UVS-010m_V101_ s1_TPROD
13	VPP_2019_S2_T32UQA-010m_V101_s1_TPROD
14	VPP_2019_S2_T32UQB-010m_V101_ s1_TPROD
15	VPP_2019_S2_T33UUT-010m_V101_ s1_TPROD
16	VPP_2019_S2_T33UVT-010m_V101_ s1_TPROD
17	VPP_2019_S2_T33UUS-010m_V101_ s1_TPROD
18	VPP_2019_S2_T33UVS-010m_V101_ s1_TPROD
19	VPP_2020_S2_T32UQA-010m_V101_s1_TPROD
20	VPP_2020_S2_T32UQB-010m_V101_ s1_TPROD
21	VPP_2020_S2_T33UUT-010m_V101_ s1_TPROD
22	VPP_2020_S2_T33UVT-010m_V101_ s1_TPROD
23	VPP_2020_S2_T33UUS-010m_V101_ s1_TPROD
24	VPP_2020_S2_T33UVS-010m_V101_ s1_TPROD

The selected product differed in up to a maximum of two main growing seasons. The decision was made to use the first growing season ("s1" = Season 1) total productivity (“TPROD”), as this represented the main vegetation phase in Central Europe. In addition, this selection minimized effects of subsequent crops (winter crops seeding at autumn, catch crops), which are still cultivated and grown up in the same year of investigation but represented not the researched crop in this year.

3.2 Integrated Administration and Control System (IACS)

The second data source was non-freely available data from agricultural subsidies (Integrated Administration and Control System, IACS). These were collected as part of the farmers' application for agricultural subsidies and were also available in GIS-readable data for the years 2017 to 2020. For Saxony, these contain a total of around 165,000 to 170,000 digitized fields each year with information on up to 166 notifiable crop types. This were information on field areas around 900,000 ha depending on the year. Due to data protection regulations and the fact that these data were farm business secrets, they were not freely available. To fill the data gap for non-governmental researchers here, one could also alternatively use satellite-based crop type mapping (Bojanowski et al. 2022) instead of IACS data.

3.3 Application data of farmers for drought aid in Saxony 2018

Also, and for the same reasons, not freely available were the 2018 farm drought aid applications. These applications were documents and contain only economic information. However, the farm identifier number could be used to identify the farm and thus associated farmland in IACS. HR-VPP values for this farmland could now be compared between applicants and comparable land from farms that did not applied. Applications from around 310 farms with a farmland area of 150,000 ha in 2018 were available for this study. For comparison, a total of around 900,000 ha were registered in IACS in Saxony in the same year. Thus, the area of drought applications

corresponded to a share of circa 17%. This was a one-time government aid to date, so no other data was available for comparable years. The condition for a successful application is that farms submit this application for which the annual production from land production was at least 30 percent below the average of the previous three years and whose existence is threatened.

3.4 CORINE Land Cover-dataset 2018

To initially investigate whether the HR-VPP dataset was sensitive enough to different categories of land cover and land use to measure the 2018 drought, the 2018 CORINE Land Cover (CLC) dataset is used: https://land.copernicus.eu/pan-european/corine-land-cover. CLC divided the earth's surface into 44 classes as land cover/land use mapping (LULC), but not all classes were relevant for the study area Saxony. Of particular note was the minimum mapping unit of 25 ha per object. Subsequent alterations must have a minimum extent of 5 ha. CLC often had to work with generalizations in order to comply with the minimum mapping unit. These generalizations contradicted the high spatial resolution of the VPP product and associated land cover mapping capabilities (MMU = 100 m² VPP versus 250,000 m² CLC). For this reason, the linking of both products (VPP with CLC) could only serve to provide a first general overview of the possibilities and limitations of the VPP product.

4 Methods

The processing of the HR-VPP data was done in several steps (Fig. 2). For each year of the time series, a mosaic was created using the geographic information system. Before that, tiles existing in UTM 32N were transformed in the reference UTM 33N, then combined into a mosaic and clipped to the study area. For each CORINE Land Cover class zonal statistics were obtained and analyzed (section “Results 1”, Fig. 2). After determining whether a potential could generally be seen in the use of the data (section “Results 1”, Fig. 2), the detailed analysis was continued. For this purpose, the zonal statistics for the crops were calculated from the IACS data for each year. The sum of the VPP value per field was collected as the main statistical value. Since the area size of the field as well as the regional location were also known, a wide variety of crop-specific and spatial evaluations could now be performed. To obtain mean values per crop, VPP totals were summed by spatial study level (county, municipality, farm) and divided by the associated area. Predominantly mean values were calculated for the selected crop in the selected spatial unit (section “Results 2”, Fig. 2). The Welch

t-test was used to demonstrate whether VPP productivity significantly changes in 2018 compared to available years 2017, 2019, or 2020. The six most widely grown crops in Saxony were used for this purpose. In 2018, these were winter wheat (20.67%), winter rapeseed (13.85%), mowing pastures (12.73%), winter barley (9.9%), silage maize (7.3%) and meadows (6.6%). These crops together covered almost 72% of the total cultivated area in Saxony (about 650,000 ha) and thus could be seen as a representative analysis for the whole state area, but also for other crops.

Bringing in information on which farms have applied for drought aid allowed for further analysis in this direction on regional or local scale (section “Results 3”, Fig. 2).

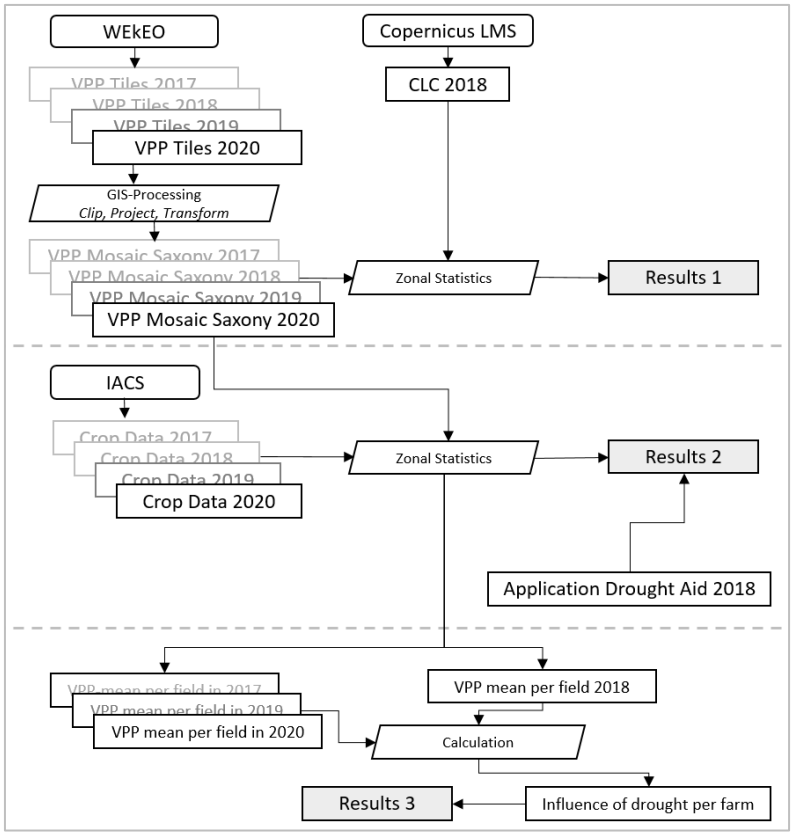

Figure 9: Main workflow of the HR-VPP data analysis.

In the last step, the farm-specific disadvantage in productivity triggered by the 2018 drought was calculated. The average values of the HR-VPP per field were used as the data basis for this and extrapolated to the farm. Due to the crop rotation in cultivation and the short time series of only 4 years of HR-VPP, only a few reference areas of the farm itself were available to validate the influence of the drought.

This lack of reference data in productivity was resolved by using the multi-year mean of the respective field crop in the spatial level of the municipalities. If a farm had areas in different communities, they were each compared to the mean typical for those

communities. The distribution of the farm's areas was intended to better resolve the different natural features of the state of Saxony. The very heterogeneous site conditions for agriculture in Saxony, ranging from river valleys to heath landscapes and from loess areas to the crest of the Ore Mountains, were thus minimized in their influence on the calculation of the value for the farms. The comparison of farms with land on good soils versus on poor soils was omitted. The influence of drought on vegetation productivity thus took into account individual farm site conditions.

The proposed VPP-"Farm-Level Temporal Comparison Indicator (VPP-FLTCI)" calculated here (Tab. 3) was a dimensionless value that allows comparison of the impact of drought on and between farms. Comparability was ensured because the comparison was always made within the cultivated crop types of a farm. This means that it was not an arable farm that was compared with a forage (grassland) farm, but the respective influences of the drought on the farm-specific crops.

Table 3: Calculation example for determining the farm-specific impact in VPP productivity loss in the 2018 drought.

A	B	C	D	E	F	G	H	I
			=20	20/D			F-G	H*E
Farm	**Crop**	**Municipal**	**Area in ha**	**Partial area**	**VPP mean for farm per crop and municipal in 2018**	**VPP mean at municipal in 2017, 2019, 2020**	**VPP difference**	**VPP difference partial at area**
Jon Doe	Corn	Warendorf	10	0.5	80	90	-10	-5
Jon Doe	Corn	Versmold	5	0.25	110	105	5	1.25
Jon Doe	Wheat	Versmold	5	0.25	70	100	-30	-7.5
VPP Farm-Level Temporal Comparison Indicator (FLTCI):								**-11.25**

Since the FLTCI was always determined by dividing with the area shares, the size of the farm and number or size of fields were not relevant in the collection of the final value. The consideration of the spatial cultivation conditions was an important contribution to this, since one could not compare arable farms with good conditions with arable farms with poor natural conditions. However, one could then very well compare, measured against the respective baseline, how strongly the drought affects productivity (section "Results 3", Fig. 2).

The same method was used to calculate "baseline" values for comparably normal years with less drought impact. This was the average per farm for the years 2017, 2019 and 2020 based on crops grown in that period and regionality based on the municipalities. For Table 3, this meant that column F no longer uses the VPP average for 2018, but instead uses the farm VPP average for the reference years 2017, 2019, and 2020. By using the reference, farm performance was captured. The underlying question here was whether farms from a lower VPP baseline were more likely to apply for drought assistance than farms with higher productivity in the reference years.

There were 419 municipalities as administrative units in Saxony in 2018. The use of a smaller spatial administrative area, like local districts, as a reference for averaging was not recommended. Many communal districts had not been able to collect reference data sets due to the short time series if this crop was not otherwise cultivated in this area and time period.

By using the FLTCI on a drought-year like 2018 compared to non-drought or less-drought-years as like the example in Table 3, it became a farm-level based drought indicator, too

5 Results

5.1 General suitability for 2018 drought reanalysis in Saxony

Preliminary investigation using the CLC dataset suggested the usability of the VPP product for more in-depth analyses. This was clearly illustrated in Figure 3 by the drops in the statewide VPP mean in 2018 for the CLC categories Arable Land (CLC code 211) and Pastures (CLC code 231). Control classes on which a reduction in vegetation productivity should have little effect, such as Urban Fabric (CLC code 111) and Waters (CLC code 511) showed constant values and no decrease in 2018.

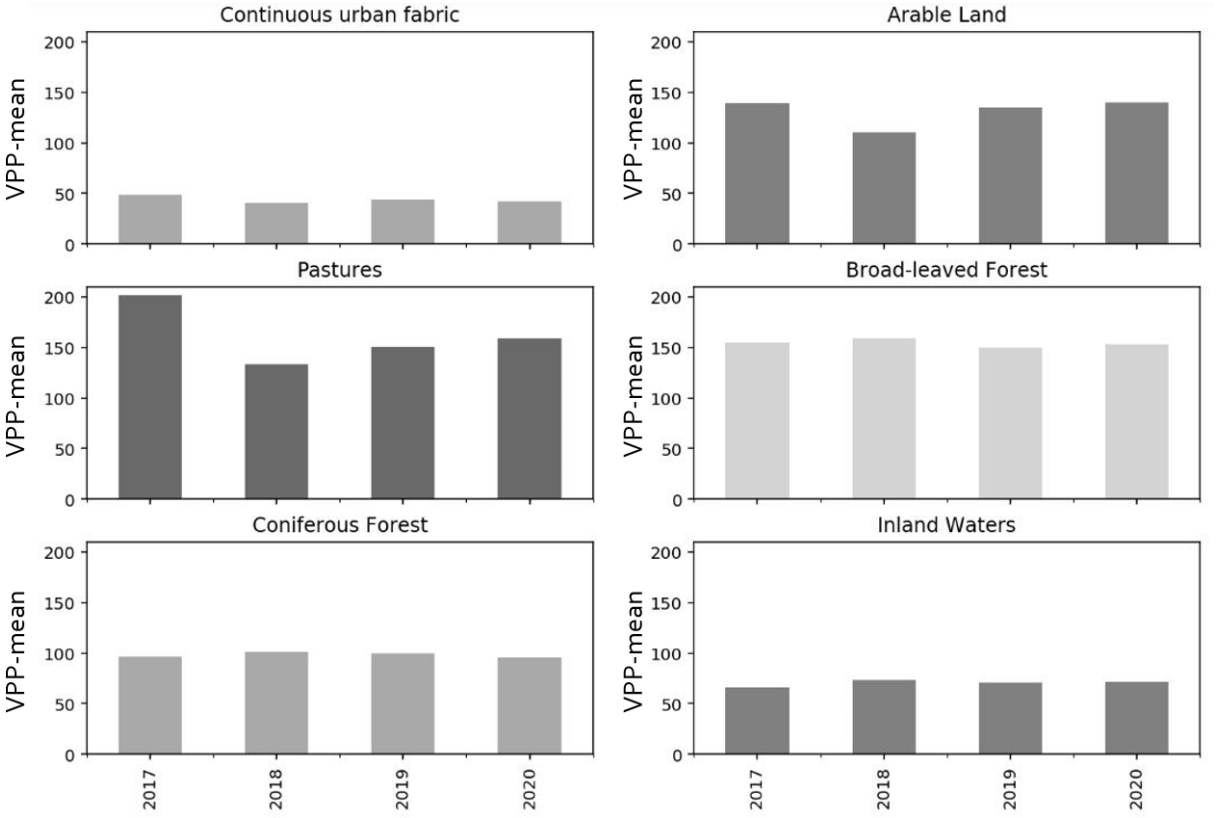

Figure 10: Development of average productivity for selected land cover categories according to Corine Land Cover for the years 2017 to 2020 in Saxony.

The results of the significance test showed (Table 4) that the VPP values of 2018 were mostly significantly different from those of other years (2017, 2019, or 2020) for the six crop types studied. No significant difference existed only for Winter Barley between 2017 and 2018, and Maize from 2018 to 2019 and 2020. However, the latter two years were also not notable for predominantly humid conditions during the growing season. Especially high water-consuming crops such as maize thus suffered from continued topsoil water depletion in subsequent years. This was also reflected in the drought-influenced productivity in 2018 and was continued in the following years, which was why the drought year can no longer be significantly separated from these within the VPP values. It could be seen that many crops also show significant differences between comparison years when compared to each other.

Table 4: Significance test p-values for different combinations of fruit types and years. The bold marked fields indicate testing of the same fruit types.

	p-Value	Winter Wheat			Winter Barley			Winter Rapeseed		
		2017	2019	2020	2017	2019	2020	2017	2019	2020
2018	Winter Wheat	**0.0**	**0.0**	**0.0**	**0.0**	**0.0**	**0.0**	**0.0**	**0.0**	**0.0**
	Winter Barley	0.4	1.7	**0.0**	1.3	**0.0**	**0.0**	**0.0**	**0.0**	**0.0**
	Winter Rapeseed	**0.0**	**0.0**	**0.0**	**0.0**	5.8	1.6	**0.0**	**0.0**	**0.0**
	Maize	**0.0**	**0.0**	**0.0**	**0.0**	**0.0**	**0.0**	**0.0**	**0.0**	**0.0**
	Mowing Pastures	**0.0**	**0.0**	**0.0**	**0.0**	1.2	2.0	**0.0**	**0.0**	**0.0**
	Pastures	**0.0**	**0.0**	**0.0**	**0.0**	7.6	8.3	**0.0**	**0.0**	**0.0**
	p-Value	Maize			Mowing Pastures			Pastures		
		2017	2019	2020	2017	2019	2020	2017	2019	2020
2018	Winter Wheat	**0.0**	7.2	2.6	**0.0**	**0.0**	**0.0**	**0.0**	**0.0**	**0.0**
	Winter Barley	5.8	4.8	9.7	**0.0**	**0.0**	**0.0**	**0.0**	**0.0**	**0.0**
	Winter Rapeseed	**0.0**	**0.0**	**0.0**	**0.0**	8.4	3.0	**0.0**	3.2	**0.0**
	Maize	**0.0**	1.8	3.1	**0.0**	**0.0**	**0.0**	**0.0**	**0.0**	**0.0**
	Mowing Pastures	**0.0**	**0.0**	**0.0**	**0.0**	**0.0**	**0.0**	**0.0**	**0.0**	**0.0**
	Pastures	**0.0**	**0.0**	**0.0**	**0.0**	**0.0**	**0.0**	**0.0**	**0.0**	**0.0**

5.2 Regional and crop-specific VPP-differences and drought effect

The VPP mean value for the years 2017, 2019 and 2020 was stable for the respective crop across all regions examined (Fig. 4). The spatial level of the counties thus masked the actual heterogeneity of the VPP values in the municipalities, which showed significantly greater differences from one another (Fig. 5).

Peas and spring cereals (oats and barley) showed predominantly low values (Fig. 4). Ponds used for pond farming had low values as expected, since this was actually not a comparable crop type in terms of land cover. High VPP values were reserved for grassland and arable feed crops (clover grass or field grass) as year-round land cover. Sugar beets also achieved high values. However, the highest productivity was in winter

rapeseed. Winter cereals and corn reached medium values in this consideration. A harvest date in early summer is certainly not insignificant for these values.

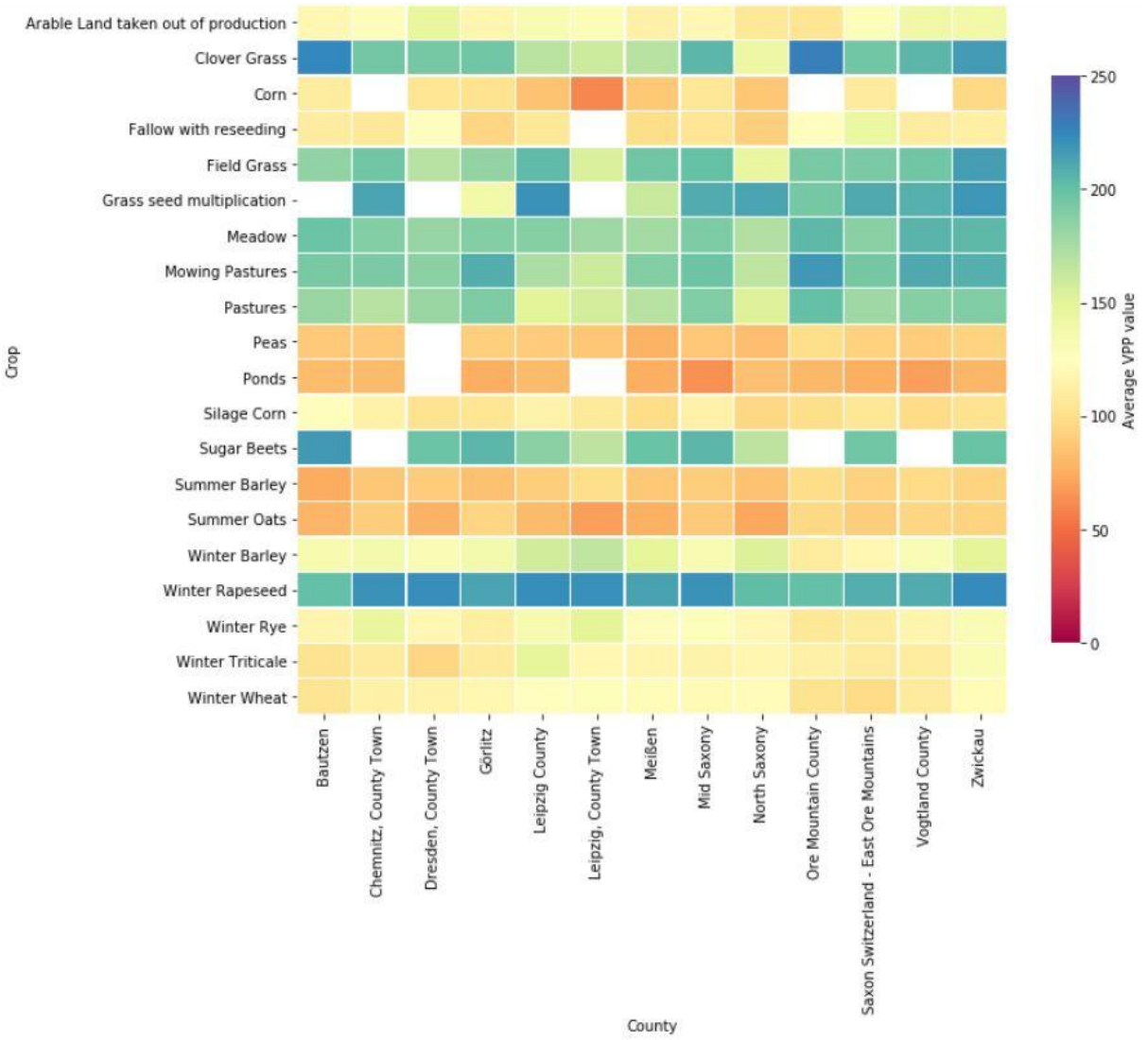

Figure 4: Average VPP values in 2017, 2019, and 2020 for the most widely grown crops in Saxony, broken down by county level.

These spatial differences could be shown in even greater detail for higher resolution spatial levels. For example, the VPP mean value per municipality for winter wheat in 2018 could serve as an example (Fig. 5). Clearly visible were the municipalities where winter wheat had high productivity. Municipalities with good production conditions were located directly next to municipalities with poor conditions, as could be clearly seen in the counties of North Saxony or Meißen.

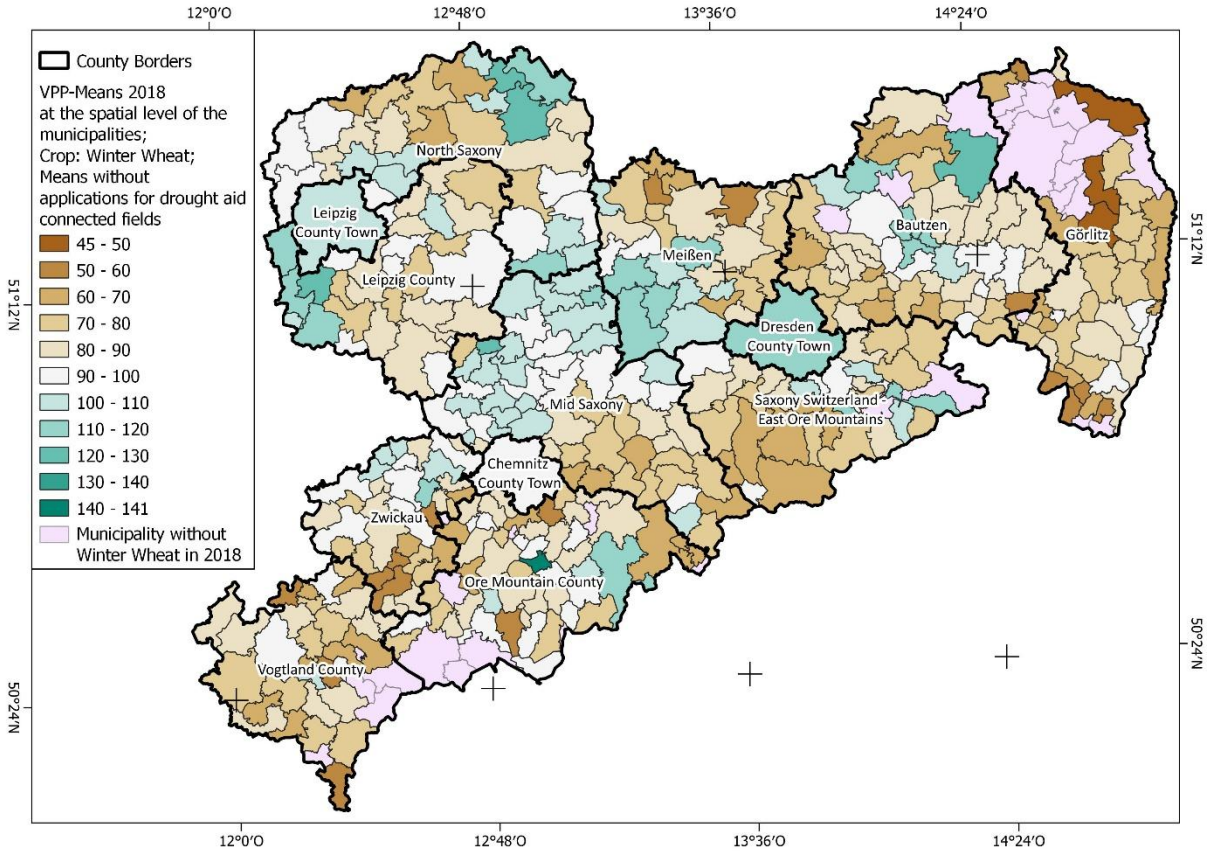

Figure 5: This map shows the VPP mean values for winter wheat in 2018 at the municipality level. There is a high variability between municipalities within the same county (see Meißen, Mid Saxony or North Saxony). Reference System: WGS 84.

In 2018, almost all crop types fell below the mean values of 2017, 2019 and 2020 in almost all counties (Fig. 6). In most cases, this was an undercut of 10 to 30%. It might be emphasized again at this point that here was only listed according to the farm data, which had not applied for drought aid. The district of Görlitz is particularly hard hit, while areas within urban areas were outliers, in this case Dresden, county town. Otherwise, it could be clearly seen that there was a lot of heterogeneity between the amount of losses, affectedness of the crop type and amount of loss rates between the counties. This allowed for a very detailed look at the 2018 drought pattern.

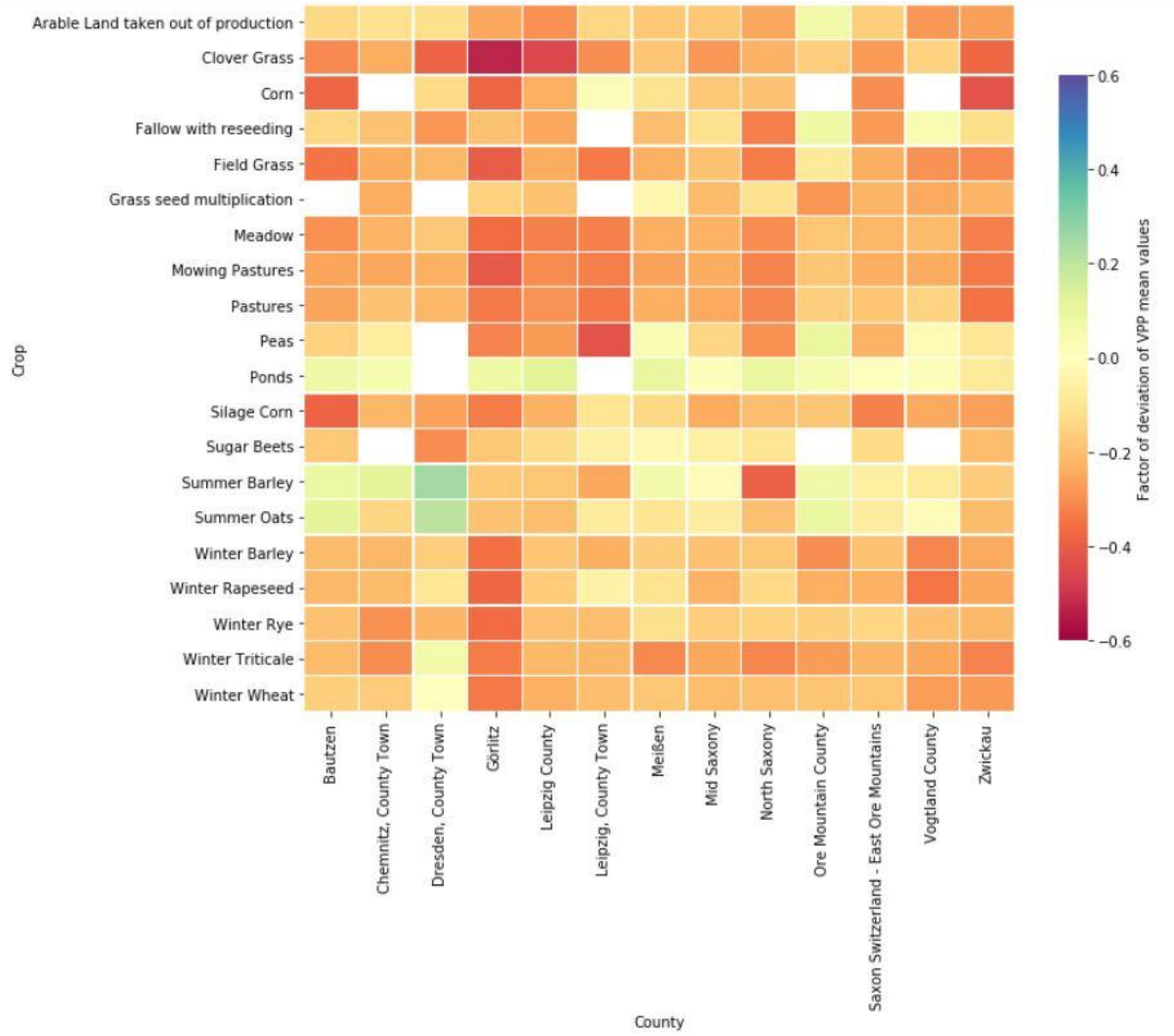

Figure 6: Percent deviation of VPP mean values per crop and county in Saxony in 2018 compared to reference years (mean from 2017, 2019 and 2020). Presented at this point: All farms without a drought relief application.

To map the effect of the 2018 drought, permanent grassland was best suited for the given time period. Changes in productivity, which the HR-VPP value for the areas between the years depicts, could then not be attributed to a change of crop types on the same field within the crop rotation. Figure 7 clearly showed that grassland in Saxony suffered losses in VPP at a wide variety of locations predestined for grassland, namely the floodplain of the river Elbe and the Ore Mountain ridge in the year before the drought (Fig. 7, 1a & 2a) and in the drought year 2018 for comparison (Fig. 7, 1b & 2b). This example could be applied to the entire state and symbolizes the possibilities of gaining knowledge from a crop-specific VPP evaluation.

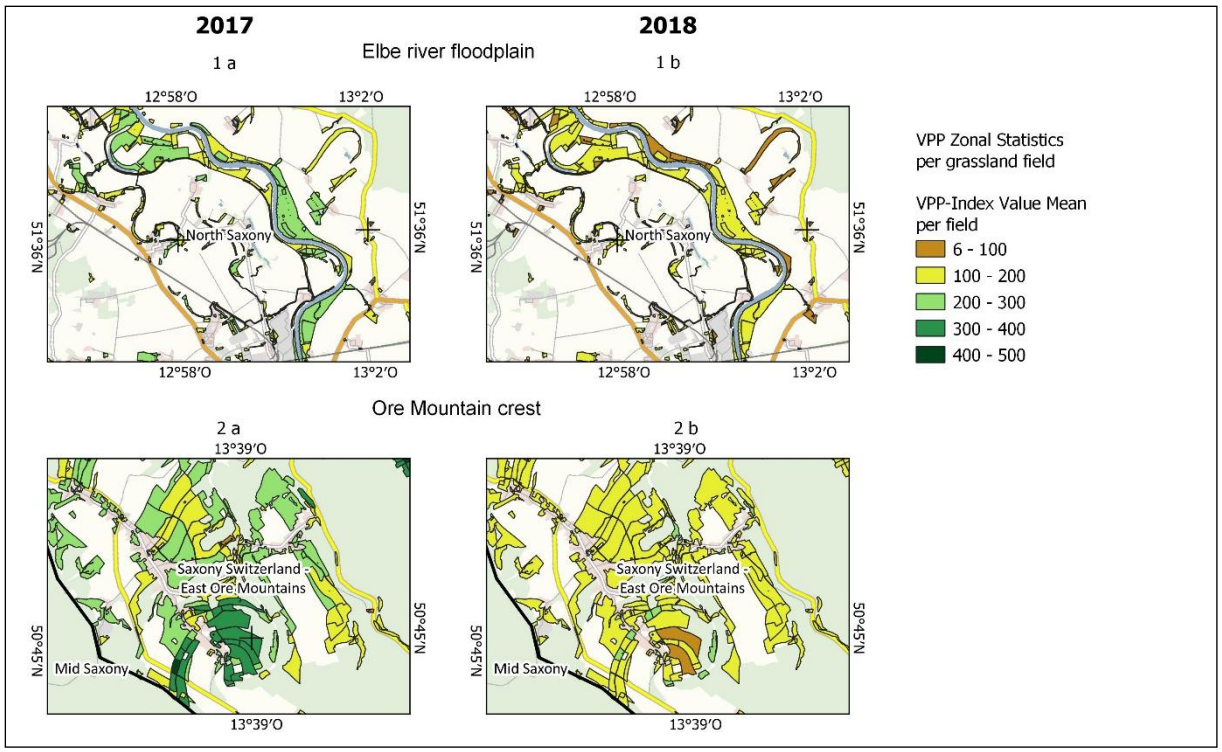

Figure 7: VPP-values per grassland fields on Elbe river floodplain and Ore Mountain Crest. The maps 1a and 2a demonstrate the values in 2017 before the drought year, the maps 1b and 2b in the drought year 2018. The productivity suffer heavy losses in 2018 compared to 2017. Although the locations are so different, neither is spared the effects of drought. Reference System: WGS 84.

Figure 8 was determined only on the basis of the fields belonging to farms that have applied for drought aid. There were immensely greater deviations from the mean value of the years 2017, 2019 and 2020 when the relative difference per county and top 20 crop type was drawn here in relation to the VPP values of the year 2018. This result suggested that farms that have applied for drought relief were indeed more affected by losses in productivity than farms that have not applied for drought aid.

These often deviated by another -10% to -20% and even more from the famers that did not submit an application. Outliers upwards could be found especially in the county towns, since only a small number of fields were included in the statistics. Overall, strong disparities could be seen between the individual counties and crop types, also in combination of both variables.

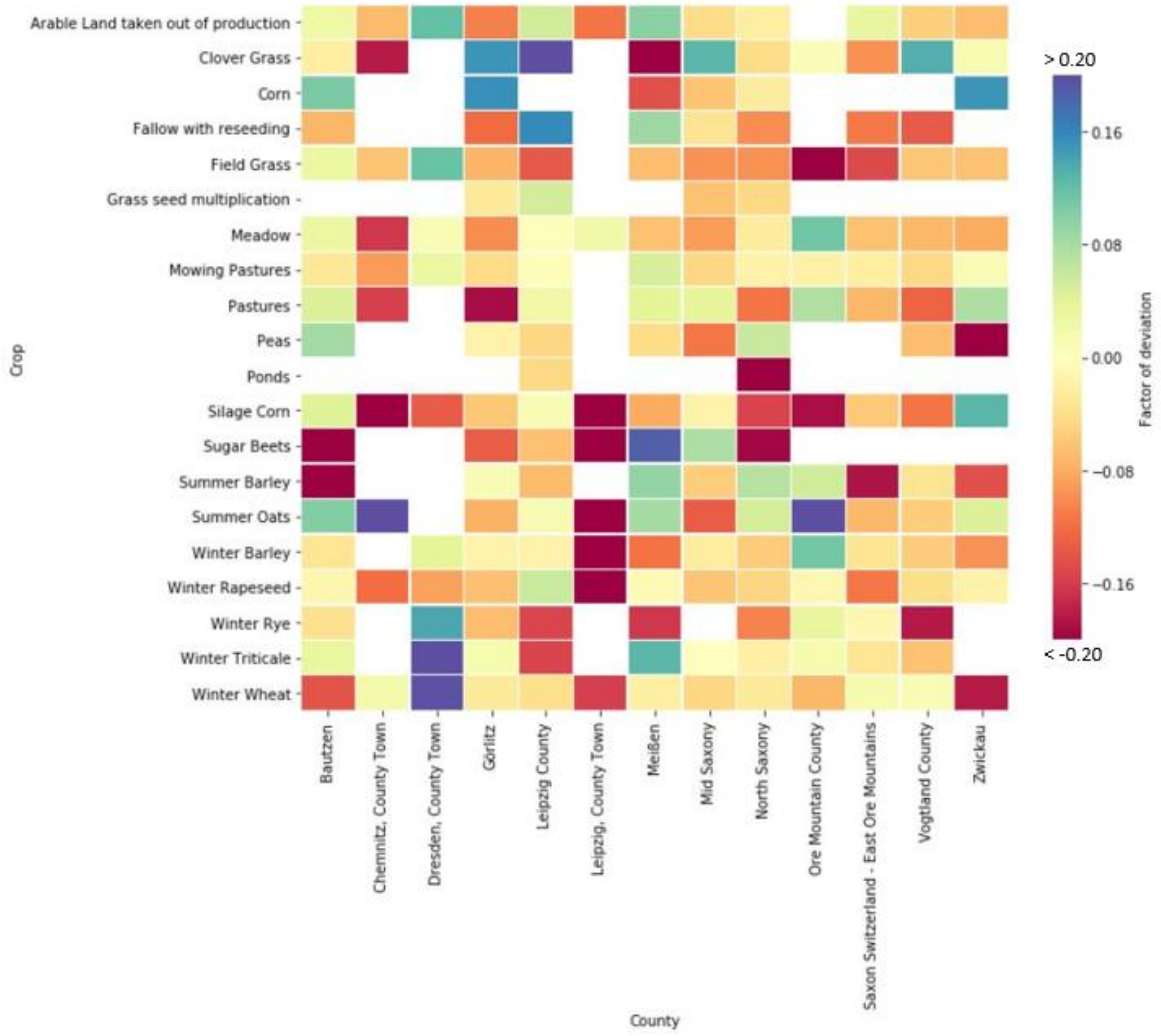

Figure 8: Factor of derivation of VPP means in 2018 of farms that applied for drought assistance from 2018 means of other farms that did not apply (Figure 6).

5.3 Explaining each farm application for financial support with VPP-data

Figure 9 showed that the calculated FLTCI value can hardly be used to distinguish between the groups of applicants for drought aid (yes or no) (see boxplot 1 with 3 or boxplot 2 with 4). Also, the importance of the reference period for averaging the comparative municipalities was shown here, which, without including the drought year, strongly increased the operational affectedness (see boxplot 2 and 4).

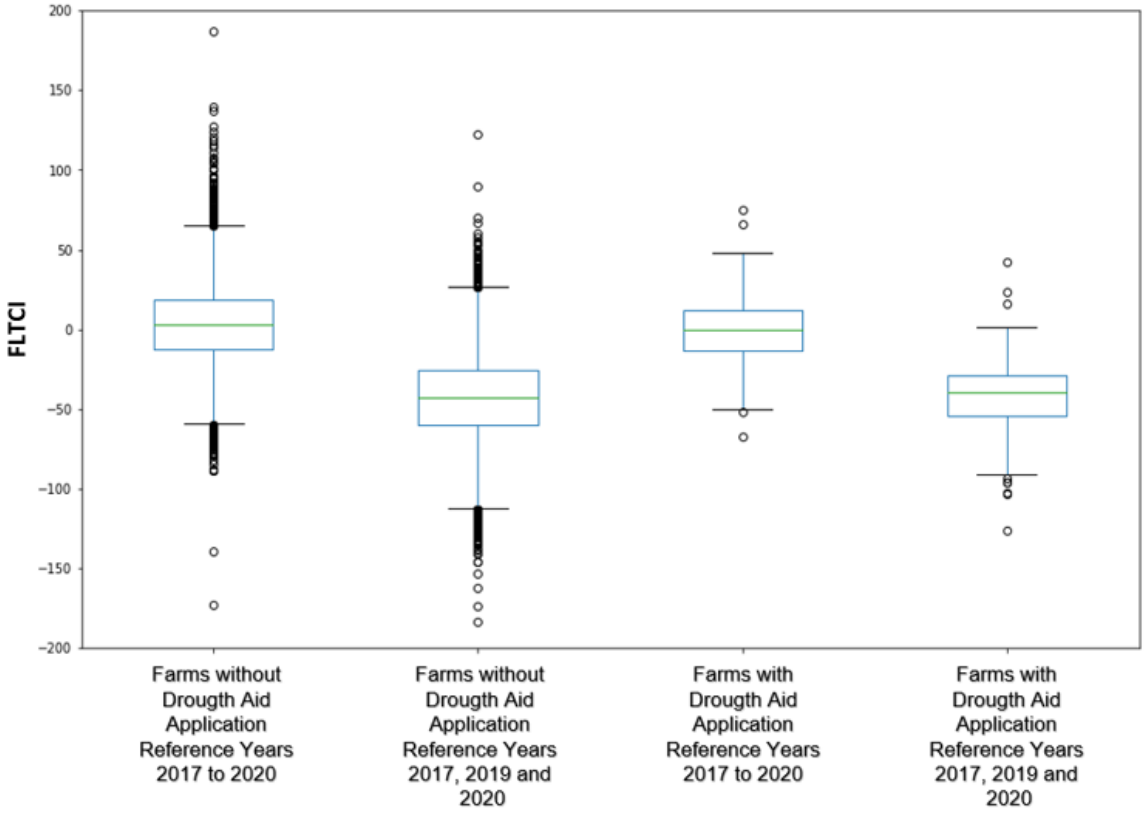

Figure 9: Comparison of FLTCI (y-axis) between applicants for drought aid (boxplots 3 and 4) and those who did not apply (boxplots 1 and 2). The influence of the selected reference period is particularly evident in boxplots 1 and 3, as these show the drought year 2018 as part of the reference year set (2017 to 2020). The median of boxplots 1 and 3 arrives zero. There is no clearly difference in the FLTCI statistics between farms without and with application for drought aid in 2018.

In a map (Fig. 10) for a region in northern Saxony, the relationship between low VPP values and applications for drought aid could be illustrated using winter wheat as an example. In this region, farms that did not applied tend to had areas with higher productivity in their fields than those that did.

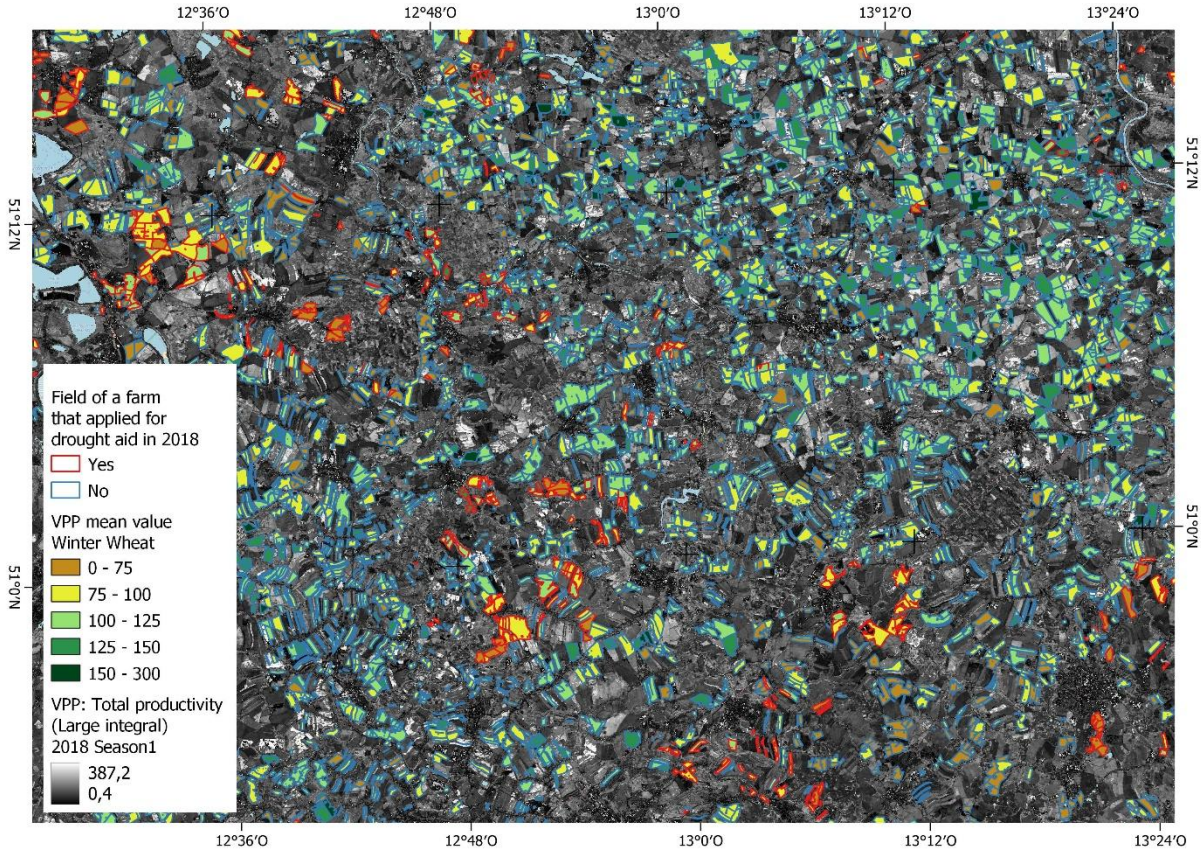

Figure 10: VPP-field mean for Winter Wheat in 2018. Field of farms which applicate for drought aid are marked with red borders, fields of farms without application for drought aid blue. What is astonishing is that the need for help on the farms seems to filter down to the field level, although the individual field cannot actually provide any information about the farm as a whole. Reference System: WGS 84.

Figure 11 was a graphical extension of Figure 9. The scatterplot below 0 represents on the y-axis the boxplots 2 (Fig. 11 a) and 4 (Fig. 11 b) in Figure 9, supplemented by the farm performance from the reference years. Both comparison groups showed a similar distribution in the scatterplot. The focal points overlaid between the farms without application (Fig. 11 a) and farms with application (Fig. 11 b) for drought aid. A majority of all farms slipped into a negative FLTCI in 2018.

No recognition of a particular pattern was possible at this point either. Farms that applied for drought aid were distributed to the same extent as those that did not. Farm performance in the reference years (x-axis) did not appeared to affect the distribution.

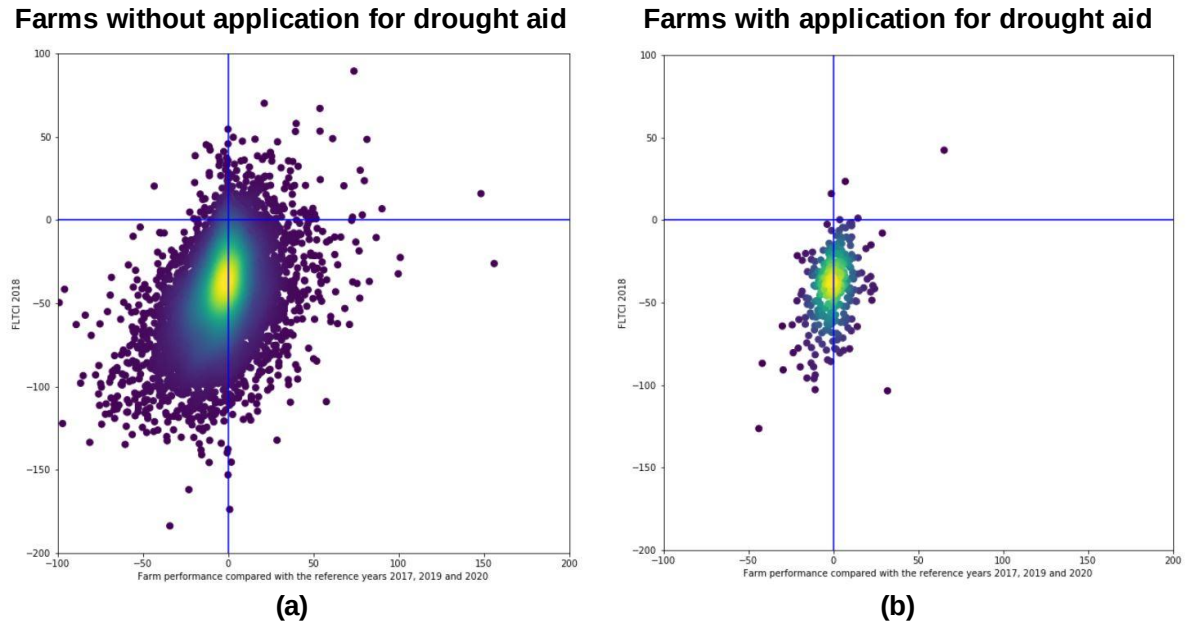

Figure 11: The zero lines divide the graphs a) and b) into four fields each. The square in the upper right-hand corner contains the farms that came through the 2018 drought year with higher productivity (y-axis) than in the comparison and that had higher VPP productivity than in the productivity of the reference years (x-axis). Accordingly: bottom right square: worse productivity in drought year 2018 + better than reference years; bottom left square: worse productivity in drought year 2018 + worse than reference years; top left square: better productivity in drought year 2018 + worse than reference years.

6 Discussion

For preliminary investigation of an unknown data set, the methodology of using Corine Land Cover data proved sufficient. Here, the analysis immediately yielded results that were within the expected range (Fig. 3). Since nationwide testing was performed, positive VPP trends could also have cancelled each other out with negative ones. This was a conceivable scenario for events that were not as extreme as 2018, since, for example, the growing season could be extended in the mountains (Trnka 2011), in Saxony the Ore Mountains, which is directly reflected in the VPP value. Why broad-leaved and coniferous forests (CLC codes 311 and 312) did not respond to the 2018 drought cannot be determined at this point.

These results were supported by the performed significance tests (Table 4), which highlight that the year 2018 turns out significantly different for a representative sample of crops.

This study also presented the first approaches of the evaluation possibilities of the VPP product. Crop species specifics and regional differences could be carried out in any combination, down to the farm and field level. In conjunction with IACS data, a wide variety of crop-specific and regional cartographic and statistical analyses could be performed (Fig. 4 to Fig. 8).

Figure 6 and 8 illustrate the drastic impact 2018 has had on VPP productivity. Figure 8, compared to Figure 6, showed the additional disadvantage of applicants compared to the non-applicant total of farms once again. Unfortunately, these results could not be validated because the dimensionless units of the VPP were difficult to communicate, for example in the field of agricultural management. When working with VPP data, it was important that this study were dealing with productivities derived from the satellite image alone. Thus, there was no yield model behind the output product as in other cases, such for field crops (Migdall et al. 2009) or for grassland (Reinermann et al. 2020). The HR-VPP remained in its own world as remote sensing product. Such remote sensing products must be translated and anchored for other disciplines, i.e. generally accepted, in order to develop their surplus value.

For agriculture, practitioners as well as decision makers in politics, values like VPP were not tangible. For them, the yield data or then yield losses caused by weather were the unit of communication to be chosen. When working with VPP data to provide information to stakeholders and decision makers, VPP will have a hard time being seen as a suitable parameter. Table 5 showed that comparisons between official harvest statistics (StaLa 2018) and losses in VPP productivity are difficult to nearly impossible. Reasons for this are that the periods of comparison are different and therefore do not replicate the same growing conditions. Only a small number of years was available for the VPP product, while the yield losses or the yield level were always compared with the yield data of the previous years (mostly 5 to 10 year average). Furthermore, the VPP measured the productivity of the whole plant, while for yield did this only for the usable part of a plant (e.g. rapeseed or wheat grains). When the grain matured quickly, as in 2018, the productivity losses then overestimated the actual yield losses by several percentage points (Table 5). For crops such as sugar beets or potatoes, the situation was aggravated by the fact that yield formation occurs below the earth's surface, and thus below the area that can be detected by the satellite alone (without connected growing model), which was why yield losses can be underestimated.

Table 5: Comparison between official statistical yield data (Reinermann et al. 2020) and VPP-data in calculating losses during the European summer drought 2018 for the Federal State of Saxony.

Crop	Harvest losses 2018 compared with ten-year average	Difference in VPP productivity 2018 to mean of 2017, 2019 and 2020	Difference harvest losses to losses in VPP productivity
Winter Rapeseed	-19%	-22%	-3
Winter Wheat	-13%	-22%	-9
Winter Barley	-12%	-23%	-11
Potatoes	-24%	-16%	+8
Sugar Beets	-24%	-12%	+12
Field Grass	-43%	-26%	+17
Pastures	-37%	-17%	+20
Silage Maize	-20 to -30%	-17%	min. +3

The VPP was also suitable as a time series to trace the impact of the 2018 drought. This was even possible precisely for fields or other land covers (Fig. 10), although such analyses were only appropriate if the land cover was constant, as was the case for grassland, for example. For cropland, such a comparison could not in good conscience be undertaken from the time series, since crop rotation ensured that one would be comparing different crop types. Overall, the VPP time series was still very short, now 5 years (2017 to 2021), so time series analyses reached their limits here. In this study, the problem was circumvented by using the VPP community statistics per crop as a local basis for comparison. Fig. 5 showed that this approach of using local growing conditions was justified.

The FTLCI per farm calculated via the methodology in Tab. 3 proved not to be useful for the application case of declaring applications for drought aid (Fig. 9 and Fig. 11). A threshold value in the FTLCI, below which the underperforming farms could be classified as most likely to apply, could not be derived.

A FTLCI indicator value remained that indicates whether the farm was more productive or not in 2018 compared to the local crop-specific mean than in the reference period (mean 2017, 2019, 2020) as seen in Figure 11. This value may have an important place in the descriptive statistics of such drought events in the future, but it remained unusable for now. This is partly due to the short HR-VPP time series, and partly due to the lack of data and methods of validation. A new drought event could help to check, validate and improve what has already been achieved in the form of the development of such an indicator FTLCI. However, this study was at the very beginning of this process and needs a longer VPP dataset and, unfortunately, more drought events to expand the knowledge in the use of the HR-VPP for this use case.

7 Conclusion

This work has shown that there was much potential in combining IACS data with CLMS HR-VPP data. It was possible to investigate targeted questions about crop productivity in detail on a species-specific and spatial level. Also, this potential was far from fully exploited in this study, as the VPP product could be considered for diverse use cases (nature conservation, forestry, urban green). Since the HR-VPP data were provided free of charge, this increased the potential for future applications, for example, the detailed analysis of extreme events, such as an agricultural drought in 2018, as demonstrated in this work. However, the long waiting time for a new HR-VPP year product proved to be an obstacle, for example, the year 2021 was not published on the WEkEO platform until November 2022.

While much potential could be seen in event reanalysis with VPP data, an even greater challenge was whether it will be possible to use this or similar remote sensing products to explain drought aid applications. In 2018, millions of euros were distributed as drought aid. Thousands of hectares of agricultural land have been associated with the applicants. If it is possible to figure out the patterns, including using remote sensing data, according to which probabilities of application per farm can potentially be predicted, one would create a valuable tool to assist policy makers. The target here was to be able to predict, as early as May and June, how many applicants and what application amount would be expected in the summer if a drought aid program were to be re-launched. The VPP data provided important starting points for this, but as an annual total product they will ultimately not be able to play a role in accompanying monitoring. A variety of reasons were possible why a farm ultimately made such an application for drought aid. Remote sensing data alone could not provide the sole parameters for explanation. From a large feature space of combinations, the pattern or patterns, if any, must first be found. Farm structure, number of livestock, location of land, soils, and local climate, in an infinite number of combinations, can help explain whether there were systematic bases for drought aid applications. Machine and deep learning technologies can help extract these patterns. Recognized patterns can then greatly improve the predictive accuracy of future models, so this is an important research need that can be derived from this study. It is also worth pointing out the possibility that no patterns can ever be found at all, and the rationale is different: Applying for drought aid involves bureaucracy. Farm data must be disclosed and the application submitted. The farm manager always decides individually whether this

makes sense for his farm or is feasible at all. Even the best model cannot adequately reflect such individual decisions. Despite high yield losses, there need not automatically be a threat to the farm's existence. Remote sensing can never provide this insight into the bookkeeping of a farm, which is why a farm-specific derivation of applications for drought aid will be extremely difficult. In the future, however, remote sensing can be used to identify regions at particular risk using HR-VPP. Combined with IACS data, this can be used to make statistical predictions of where high probabilities of future drought-related climate impacts will occur in agriculture.

Funding

This work received no funding.

References

Bauer-Marschallinger, B., & Massart, S. (2022). Quality Assessment Report. Update 2021. Surface Soil Moisture. Collection 1km. Version 1.0. https://land.copernicus.eu/global/sites/cgls.vito.be/files/products/CGLOPS1_QAR2021_SSM1km-V1_I1.00.pdf (accessed on 22.02.2023).

Beillouin, D., Schauberger. B., Bastos, A., Ciais, P., & Makowski, D. (2020). Impact of extreme weather conditions on European crop production in 2018. *Phil. Trans. R. Soc. B.*, *375*. https://doi.org/10.1098/rstb.2019.0510.

Bojanowski, J.S., Musial, J.P., & Sikora, S. (2022). Crop type classification using High-Resolution Vegetation Phenology and Productivity product. *2022 Living Planet Symposium*. https://doi.org/10.13140/RG.2.2.28205.15841.

Borgogno-Mondino, E., & Fissore, V. (2022). Reading Greenness in Urban Areas: Possible Roles of Phenological Metrics from the Copernicus HR-VPP Dataset. *Remote Sens.*, *14*, 4517. https://doi.org/10.3390/rs14184517.

Bouras, E.h., Jarlan, L., Er-Raki, S., Balaghi, R., Amazirh, A., Richard, B., & Khabba, S. (2021). Cereal Yield Forecasting with Satellite Drought-Based Indices, Weather Data and Regional Climate Indices Using Machine Learning in Morocco. *Remote Sens*. 13, 3101. https://doi.org/10.3390/rs13163101.

Brigitte, L., Laura Bourgeau-Chavez, L., & San-Miguel-Ayanz, J. (2012). Use of remote sensing in wildfire management. *Sustainable development-authoritative and leading edge content for environmental management*, pp, 55-82.

Büttig, S., Lins, M., & Goihl, S. (2022). WaterMaskAnalyzer (WMA) - A User-Friendly Tool to Analyze and Visualize Temporal Dynamics of Inland Water Body Extents. *Remote Sens*. 2022, 14, 4485. https://doi.org/10.3390/rs14184485.

Chatterjee, S., Desai, A.R., Zhu, J., Townsend, P.A., & Huang, J. (2022). Soil moisture as an essential component for delineating and forecasting agricultural rather than meteorological drought. *Remote Sensing of Environment* 269. https://doi.org/10.1016/j.rse.2021.112833.

Chen, Y., Guerschman, J.P., Cheng, Z., & Guo, L. (2019). Remote sensing for vegetation monitoring in carbon capture storage regions: A review, *Applied Energy*, *240*,. https://doi.org/10.1016/j.apenergy.2019.02.027.

Dehkordi, A.T.,Valadan Zoej, M.J., Ghasemi, H., Ghaderpour, E., & Hassan, Q.K. (2022). A New Clustering Method to Generate Training Samples for Supervised Monitoring of Long-Term Water Surface Dynamics Using Landsat Data through Google Earth Engine. *Sustainability* 2022, 14, 8046. https://doi.org/10.3390/su14138046

D'Agostino, V., Drought in Europe summer 2018: Crisis management in an orderly chaos. Available online: https://www.farm-europe.eu/blog-en/drought-in-europe-summer-2018-crisis-management-in-an-orderly-chaos/#:~:text=Almost%20187%20million%20euros%20were,declared%20the%20state%20of%20emergency. (accessed on 29.11.2022).

El Hajj, M., Baghdadi, N., Zribi, M., Rodríguez-Fernández, N., Wigneron, J.P., Al-Yaari, A., Al Bitar, A., Albergel, C., & Calvet, J.-C. (2018). Evaluation of SMOS, SMAP, ASCAT and Sentinel-1 Soil Moisture Products at Sites in Southwestern France. *Remote Sens*. 10, 569. https://doi.org/10.3390/rs10040569.

Gao, B. 1996 NDWI - A normalized difference water index for remote sensing of liquid water from space. *Remote Sens Environ,* 58, pp. 257-266.

Ghulam, A., Li, Z.-L., Qin, Q., Yimit, H., & Wang, J. (2008). Estimating crop water stress with ETM+ NIR and SWIR data. *Agricultural and Forest Meteorology* 148/11,. https://doi.org/10.1016/j.agrformet.2008.05.020.

Gouveia, C.M., Trigo, R.M., Beguería, S., & Vicente-Serrano, S.M. (2017). Drought impacts on vegetation activity in the Mediterranean region: An assessment using remote sensing data and multi-scale drought indicators, *Global and Planetary Change*, *151*, pp. 15-27. https://doi.org/10.1016/j.gloplacha.2016.06.011.

Ihinegbu, C., & Ogunwumi, T. (2021). Multi-criteria modelling of drought: a study of Brandenburg Federal State, Germany. *Modeling Earth Systems and Environment* 8, pp. 2035-2049. https://doi.org/10.1007/s40808-021-01197-2.

Handelsblatt (2022). Dürrehilfe: Knapp 292 Millionen Euro an Bauern ausgezahlt (Drought aid: Just 292 million euros paid out to farmers). Available online: https://www.handelsblatt.com/unternehmen/handel-konsumgueter/landwirtschaft-%09duerrehilfe-knapp-292-millionen-euro-an-bauern-ausgezahlt/25549686.html (accessed on 29.11.2022).

Hao, Z., & AghaKouchak, A. (2013). Multivariate standardized drought index: A parametric multi-index model. *Adv. Water Resour*. 57, pp. 12–18

Hao, Z., & AghaKouchak, A. (2014). A multivariate multi-index drought modeling framework. *J. Hydrometeor*. 15, pp. 89–101.

Hao, Z., AghaKouchak, A., Nakhjiri, N., & Farahmand, A. (2014). Global integrated drought monitoring and prediction system. *Sci Data* 1, 140001. https://doi.org/10.1038/sdata.2014.1.

Hazaymeh, K., & Hassan, Q.K. (2016). Remote sensing of agricultural drought monitoring: A state of art review, *AIMS Environmental Science* 3, pp. 604-630. https://doi.org/10.3934/environsci.2016.4.604.

Kloos S., Yuan Y., Castelli M., & Menzel A. (2021). Agricultural Drought Detection with MODIS Based Vegetation Health Indices in Southeast Germany. *Remote Sens*. 13(19):3907. https://doi.org/10.3390/rs13193907.

Kronenberg, R., Loung, T.T., Müller, M., Andreae, H., & Petzold, R. (2022). The Soil Moisture Traffic Light – A web-based information system for the daily assessment of water avail-ability. *Forest Ecology, Landscape Research and Nature Conservation,* 21, pp. 5-13

Kumar, R., Samaniego, L., & Attinger, S. (2013). Implications of distributed hydrologic model par-ameterization on waterfluxes at multiple scales and locations, *Water Resour.Res*., 49, https://doi.org/10.1029/2012WR012195.

Lastovicka, J., Svec, P., Paluba, D., Kobliuk, N., Svoboda, J., Hladky, R., & Stych, P. (2020). Sentinel-2 Data in an Evaluation of the Impact of the Disturbances on Forest Vegetation. *Remote Sens.*, *12*, 1914. https://doi.org/10.3390/rs12121914.

Liliane, T.N., & Charles, M.S. (2020). Factors Affecting Yield of Crops. In: *Agronomy: Climate Change & Food Security*. IntechOpen, London (UK).

McKee, T., Doesken, N., & Kleist, J. (1993). The relationship of drought frequency and duration to time scalces. *Proceedings of the 8th Conference of Applied Climatology*. American Meteorological Society, pp. 179–184

Media Service Saxony (2022). Dürrehilfen: Die meisten Anträge aus Nord- und Ostsachsen (Drought aid: Most applications from northern and eastern Saxony). Available online: https://www.medienservice.sachsen.de/medien/news/222617 (accessed on 29.11.2022).

Migdall, S., Bach, H., Bobert, J., Wehrhahn, M., Mauser, W. (2009). Inversion of a canopy reflectance model using hyperspectral imagery for monitoring wheat growth and estimating yield. *Precision Agric* 10, 508. https://doi.org/10.1007/s11119-009-9104-6.

Philipp, M., Wegmann, M., & Kübert-Flock, C. (2021). Quantifying the Response of German Forests to Drought Events via Satellite Imagery. *Remote Sens.,* 13(9):1845. https://doi.org/10.3390/rs13091845.

Portal, G., Jagdhuber, T., Vall-Llossera, M., Camps, A., Pablos, M., Entekhabi, D., & Piles, M. (2020). Assessment of Multi-Scale SMOS and SMAP Soil Moisture Products across the Iberian Peninsula. *Remote Sensing* 12, 3. https://doi.org/10.3390/rs12030570.

Reinermann, S., Gessner, U., Asam, S., Kuenzer, C., & Dech, S. (2019). The Effect of Droughts on Vegetation Condition in Germany: An Analysis Based on Two Decades of Satellite Earth Observation Time Series and Crop Yield Statistics. *Remote Sens.*, *11*, 1783. https://doi.org/10.3390/rs11151783.

Reinermann, S., Asam, S., & Kuenzer, C. (2020). Remote Sensing of Grassland Production and Management—A Review. *Remote Sens.*, *12*, 1949. https://doi.org/10.3390/rs12121949.

SMEKUL - Saxon State Ministry for Energy, Climate Protection, Environment and Agriculture (SMEKUL) (2022). *Agrarbericht in Zahlen 2022 (Agriculture report in numbers 2022)*. https://publikationen.sachsen.de/bdb/artikel/40693 (accessed on 29.11.2022).

SMEKUL - Saxon State Ministry for Energy, Climate Protection, Environment and Agriculture (SMEKUL) (2019). *Agrarbericht in Zahlen 2019 (Agriculture report in numbers 2019)*. https://publikationen.sachsen.de/bdb/artikel/33565 (accessed on 29.11.2022).

Samaniego, L., Kumar, R., & Attinger, S. (2010). Multiscale parameter regionalization of a grid-based hydrologicmodel at the mesoscale, *Water Resour. Res.,* 46, W05523, https://doi.org/10.1029/2008WR007327.

Schmidt-Walter, P., Trotsiuk, V., Meusberger, K., Zacios, M., & Meesenburg, H. (2020). Advancing simulations of water fluxes, soil moisture and drought stress using the LWF-Brook90 hydrological model*, R. Agric. For. Meteorol.*, 291. https://doi.org/10.1016/j.agrformet.2020.108023.

Segarra, J., Buchaillot, M.L., Araus, J.L., & Kefauver, S.C. (2020). Remote Sensing for Precision Agriculture: Sentinel-2 Improved Features and Applications. *Agronomy*, *10*, 641. https://doi.org/10.3390/agronomy10050641.

Smets, B., Cai, Z., Eklundh, L., Tian, F., Bonte, K., Van Hoost, R., De Roo, B., Jacobs, T., Camacho, F., Sánchez-Zapero, J., Martinez-Sánchez, E., Swinnen, E., Scheifinger, H., Hufkens, K., & Jönsson, P. (2021). Copernicus Land Monitoring Service. High Resolution Vegetation Phenology and Productivity (HR-VPP). Seasonal Trajectories and VPP parameters.

Smith, G., Kleeschulte, S., Soukup, T., Garcia, R., Banko, G., & Combal, B. (2021). An Operational Service for Monitoring Grassland Dominated Natura2000 Sites with Copernicus Data, *2021 IEEE International Geoscience and Remote Sensing Symposium IGARSS*. https://doi.org/10.1109/IGARSS47720.2021.9554934.

StaLa - Statistical Office of the State of Saxony (2018). *Statistisches Jahrbuch Sachsen 2018 (Statistical Yearbook Saxony 2018*). https://www.statistischebibliot-hek.de/mir/receive/SNHeft_mods_00022230.

Sutanto, S.J., van der Weert, M., Wanders, N., Blauhut, V., & Van Lanen, H.A.J. (2019). Moving from drought hazard to impact forecasts. *Nat. Commun*. 10, 4945. https://doi.org/10.1038/s41467-019-12840-z.

Trnka, M., Eitzinger, J., Semerádová, D., Hlavinka, R., Balek, J., Dubrovsky, M., Kubu, G., Stepanek, P., Thaler, S., Mozny, M., & Zalud, Z. (2011). Expected changes in agroclimatic conditions in Central Europe. *Climatic Change* 108, 261–289. https://doi.org/10.1007/s10584-011-0025-9.

Trnka M., Hlavinka P., Možný M., Semerádová, D., Štepánek, P., Balek, J., Bartošová, L., Zahradnícek, P., Bláhová, M., Skalàk, P., Farda, A., Hayes, M., Svoboda, M., Wagner, W., Eitzinger, J., Fischer, M., & Žalud, Z. (2020). Czech Drought Monitor System for monitoring and forecasting agricultural drought and drought impacts. *Int J Climatol*. 40:5941–5958. https://doi.org/10.1002/joc.65575958.

Wieland, M., & Martinis, S. (2020). Large-scale surface water change observed by Sentinel-2 during the 2018 drought in Germany. *International Journal of Remote Sensing* 41/12. https://doi.org/10.1080/01431161.2020.1723817.

Xue, J., Su, B. 2017 Significant Remote Sensing Vegetation Indices: A Review of Developments and Applications, *Journal of* Sensors. https://doi.org/10.1155/2017/1353691.

Zarco-Tejada P.J., Rueda, C.A., & Ustin, S.L. (2003). Water content estimation in vegetation with MODIS reflectance data and model inversion methods. *Remote Sens Environ,* 85.

Manuscript 3

Tillage direction analysis in agricultural fields from Digital Orthophotos and Sentinel-2 imagery

Remote Sensing Applications: Society and Environment, 2025, Vol. 37

Sebastian Goihl[1,2,3]*

[1]Helmholtz Centre for Environmental Research GmbH – UFZ, 04318 Leipzig, Germany
[2]Saxon State Office for Environment, Agriculture and Geology, 01326 Dresden, Germany
[3]Eberhard Karls University Tübingen, 72074 Tübingen, Germany

*Correspondence: Sebastian.Goihl@smekul.sachsen.de

Received: 14 November 2024; Accepted: 03 February 2025; Published: 04 February 2025

Reference: https://doi.org/10.1016/j.rsase.2025.101486

Abstract

For questions of soil and water protection, knowledge about agricultural management is relevant, especially in hilly and mountainous areas. In sloping areas, an area-wide knowledge of whether farming is done with or across the contour line would be very valuable for use in regional soil conservation management. In order to ascertain the prevalence of farming practices conducted with or against the slope in a given region, it is necessary to obtain data on the direction in which fields are cultivated. This information can be derived from remote sensing data through the application of geographic information system (GIS) methods. While previous studies have attempted to provide knowledge primarily through the use of small-scale but high-resolution Unmanned Aerial Vehicle (UAV) imagery, this study used medium-resolution imagery from satellite imagery (Sentinel-2 at 10 m x 10 m) and high resolution imagery (0.2 m x 0.2 m) Digital Orthophotos (DOP) from aircraft flights.

The use of medium-resolution satellite images (such as Sentinel-2) has yet to be explored in the context of addressing this research question, and this study represents their preliminary application in this domain. For this purpose, two GIS-based methods of analysis were proposed, which mainly made use of high-pass filtering, reclassification, vectorization, and compass orientation calculation. The results are promising, as in the best cases the correlation, between processing and ground truth orientation of the field tillage direction, for the DOP is R^2 of 0.867 for 170 fields and 2.687 ha. For the Sentinel-2 evaluation, an R^2 of 0.833 was obtained for 141 fields with 2.611 ha. Despite the different spatial resolution of both systems, the results are very comparable in terms of spatial coverage and accuracy of validation. However, for these two cases, this also meant that less than 50% of the total agricultural area and less than 20% of all fields in the study area could be covered. The data obtained from the DOP and Sentinel-2 sensors were collected at different times, resulting in the identification of distinct preferences for specific crop types. These preferences were observed to yield both accurate and less accurate evaluations, respectively. For instance, wheat exhibited favorable outcomes. Overall, the proposed approach demonstrated the capacity to derive area-wide information on farming direction with satisfactory results. Especially the temporarily high data availability of Sentinel-2 should be used to generate an overall picture using crop rotation and different phenological stages of arable crops in the long term.

Keywords: Remote Sensing; Tillage Direction; Sentinel-2; Digital Orthophotos; GIS-Analysis; Erosion

1 Introduction

Soil erosion is a significant global problem because the finite resource that is fertile soil is reduced by such events. Soil degradation usually takes place due to wind and/or water influence. However, the core cause here is often human activity through inappropriate land use, such as agricultural activity like overgrazing or deforestation. Overall, reduced agricultural land and declining soil fertility threaten the food security of the world's population (Wuepper et al. 2020). Soil protection and soil erosion are also important issues on a national and regional scale in Saxony, a state of the Federal Republic of Germany located in Central Europe (Plambeck 2020). Soil protection involves preventing erosion, degradation, and preserving soil health. For this reason, runoff pathways of water erosion on agricultural land were mapped area-wide in Saxony (Voß et al. 2010) and management solutions like greening this pathways (planting vegetation to enhance environmental sustainability) were proposed (Braeuning et al. 2015). In particular, multispectral remote sensing data can help to capture and assess erosion processes and thus contribute to targeted management, often at the local level, as a source of data (Sepuru & Dube 2018).

Adapted agricultural management can contribute to soil protection (Wuepper et al. 2020, Braeuning et al. 2015). In order to have a comprehensive database for the management of agricultural water protection, information on the types of crops cultivated, catch crops and soil-conserving management methods were important. A catch crop is planted to prevent soil erosion and nutrient loss. Another crucial parameter is the direction of cultivation, which is of particular importance in hilly and mountainous terrain. The direction of cultivation describes the main planting and farming orientation of the crop rows on a field.

Farming with a tillage direction oriented along the land slope can caused runoff paths and increased the water erosion in this area. Plowing or other tillage to constant elevations, called contour farming, may attenuate harmful impacts of tillage and is important for soil conservation (Lima et al. 2021). The runoff and sediment reduction benefited from contour tillage between a range of 30 and 50% (Jia et al. 2020). Nevertheless, it remains unclear whether contour farming is being employed and, if so, to what extent. Information on tillage direction can thus serve as a crucial indicator for the comprehensive assessment of erosion processes within a given landscape. There are also contrary assessments of the long-term impact and effectiveness of this tillage method (Maetens et al. 2012).

Along with tillage direction comes the concept of row planting as a very attractive approach for farmers. Plants are given an ideal orientation to light, and the row structure promotes air exchange on the land (Hassanein et al. 2019). A row structure is particularly conducive to modern agriculture, as it facilitates cultivation with large agricultural machinery. In UAV imagery or DOP imagery, depending on the spatial resolution, either the row plantings of arable crops or permanent crops can be used directly, or the tracks of agricultural machinery can be used to infer the main direction of cultivation (Figure 1).

a) DOP | b) Sentinel-2

Figure 1: The main tillage direction of a field can be clearly identified in the a) DOP by the tractor tracks, while in the b) Sentinel-2 image it can be identified by the line and row structures of the fields.

Current efforts come from the field of robotics and precision farming. Row detection via Unmanned Aerial Vehicles (UAV) aims to detect weeds outside the row and then target or remove them chemically or mechanically in real time, optimize plant health or irrigation systems (Lima et al. 2021, Hassanein et al. 2019, Fareed and Rehman 2020, Ronchetti et al. 2020, Pang et al. 2020, Bah et al. 2020, Rocha et al. 2022, Peña-Barragána et al. 2012). For this purpose, Hassanein et al. (2019) used RGB images encoded to the Hue Channel of the HSV color space and examined for homogeneity and then validated using Principle Component Analysis (PCA). Accuracy data for the method are based on purely visual interpretation, which was found to be good. Fareed and Rehman (2020), on the other hand, used Automated feature extraction from drone-based image point clouds (DIPC) and obtained F1 scores ranging from 0.85 to 0.94, depending on the method. These results were achieved via K-Means clustering, where important steps included vectorization of the UAV images, an elimination of non-row polygons using Area Treshold, Smooting, Polygon to Centerline, and Line-Gaps Fixing. Ronchetti et al. (2020) achieved an Overall Accuracy of more than 90% and a Producer Accuracy of more than 85% in the evaluation of UAV images using the tresholding

algorithms, classification algorithms and Bayesian segmentation for grapevine, pear and tomato. Using a neural network (RCNN), Pang (2020) achieved an estimated emergence rate of up to 95.8 % for maize. Bah et al. (2020) also used a CNN embedded in their method called CRowNet to obtain a crop row detection rate of 93.58 % with an IoU score per crop row above 70 %. Lima et al. (2021) developed an object-based image analysis (OBIA) for tillage method and were able to produce tillage maps with a very high accuracy of R^2 0.99 and R^2 0.93.

For high-resolution images and crops with large row spacing such as vineyard, sunflowers, cotton or young corn, the Hough transform method has proven to be very useful for row detection (Comba et al. 2015, Pérez-Ortiz et al. 2015, Bah et al. 2023). However, the good results of evaluating UAV images come at the expense of area performance, since UAVs can only view small survey areas efficiently and cost-effectively at a time. With a spatial resolution between common UAV and satellite systems, aerial photographs are viewed in remote sensing, also called Digital Orthophotos (DOP). If the vegetation is already closed to such an extent that the soil between the rows can no longer be detected with the existing ground resolution, the tractor tracks remain as a reference point, which can be detected as vegetation-free from the surrounding crops. This is possible because the tracks suitable (e.g. 0.60 to 0.80 m) to the sensor ground resolution. In an in parallel row planted agricultural field remained from the top view two object types, the crop as vegetation object and the soil as non-vegetation object (Hassanein et al. 2019). The crop row orientation or tillage direction at landscape scale resulting from the farmer's preferences in strong spatial heterogeneities influenced by field shape, size, slope, crop type, growth conditions and agricultural practices (Sicre et al. 2014). As lineaments defined, these orientations in form of lines or curves are in a satellite image the visual manifestation of crop rows and tillage management (tillage, seedlings, harvesting, irrigation etc.) (Sicre et al. 2014).

High-resolution satellite imagery has proven effective for row detection, achieving accuracies above 85% using machine and deep learning approaches (Santos et al. 2020). Campos et al. (2021) successfully identified grapevine rows using a binary mask of high-resolution NDVI data from Dove satellites (PlanetScope, 3 x 3 m). Due to the large spacing and wide plantation of vines, this permanent crop is well suited for high-resolution satellite (Sicre et al. 2014, Campos et al. 2021) mapping. Using Formosat-2 imagery (2 m and 8 m) (Sicre et al. 2014), applied directional spatial filters and

mathematical morphology algorithms to determine crop row orientation. For winter crops like wheat, barley, and rapeseed, optimal results were obtained immediately post-harvest or during deep tillage (R^2 from 0.27 to 0.99). For summer crops like sunflower, corn, and hemp, results varied significantly with crop type and image acquisition date (Sicre et al. 2014). The single-date approach was effective but limited by the timing of image capture. Not all crop types demonstrated equal row recognition, critical for accurate classification. In this study, with over 45,000 hectares analyzed, 90% of crop orientations were detected with an error margin below 40°.

In conclusion, the studies that utilized high-resolution data focused on the objective of identifying individual rows without addressing the issue of orientation. A correlation between row orientation and erosion processes was typically absent. In comparison to satellite data, UAV images are particularly costly and time-consuming to record per unit area, and were spatially limited. Consequently, they were generally only suitable for evaluating individual fields.

The utilization of medium spatial resolution remote sensing data, such as that provided by the Sentinel-2 satellite of the European Space Agency's Copernicus program, presents additional challenges. With at least 10 m ground resolution, the detection of individual lanes or tractor tracks is impossible. Even more widely separated row structures, as in the case of grapes as opposed to arable crops such as corn, canola, or cereals, are no longer identifiable. There was a lack of studies that therefore deal with satellite images of a medium resolution as no studies could be determined for this resolution range.

The aim of this study is to establish the methodological basis for the evaluation of remote sensing data in relation to the management direction of a field. Free data sources will be used, such as satellite images (Sentinel-2) or Digital Orthophotos (DOP). At the same time, the aim is to make area-wide statements about as many crops as possible, thus breaking away from the individual crop rows, the individual fields and the individual crop type and evaluating the crop type influence as a whole. At the end of this study, the methods for the different data sources and their results will be examined for their significance in order to derive recommendations for use.

The comprehensive information on this object of investigation was of significant value in connection with the height information. This allows for the estimation of the extent to which farmers cultivate land in proximity to slopes, and whether this practice increases the potential for soil erosion. Sentinel-2 imagery was deemed suitable for this purpose,

as it is available at no cost and covers a vast area. The extent to which the limitation of the spatial resolution negates the objective was investigated, with particular attention paid to the time of recording and the type of crop cultivated at that time.

For the analysis a purely GIS-based approach is chosen, which has the advantage is the transparent combination of a large variety of tools. Proven methods, e.g. filtering (Rocha et al. 2022, Sicre et al. 2014), binary classifications (Campos et al. 2021) or vectorization (Fareed & Rehman 2020) can be combined in a single workflow.

The distinctive feature of this study is the utilization of medium-resolution satellite images to ascertain the predominant management direction of agricultural fields. The deployment of DOP facilitates the categorization of the selected methodology in relation to existing higher-resolution data sets. The primary question at hand is whether these satellite images can be subjected to an analysis of comparable quality to that of high-resolution data such as DOPs.

2 Area of Investigation

The study area is located in the area of the city of Meerane in the west of the federal state of Saxony (Germany). The study area is heavily used for agriculture, with arable farming (approx. 85%) clearly taking precedence over grassland use. According to the landscape ecological characterization (LfULG 2023), the study area belongs to the East Thuringian loess hill country, which is characterized by flat to hilly plateaus with blankets of loess-like sediments. Yield capacity and yield security of the agricultural areas of the East Thuringian loess hill country are predominantly endangered to a high degree by water erosion. Slope and convergence areas show the highest degree of risk in the entire area (LfULG 2023).

The study area (Figure 2) has a W-E extension of 12 km and an N-S extension of 8 km. Agricultural use takes place on about 5.900 ha to 6.000 ha.

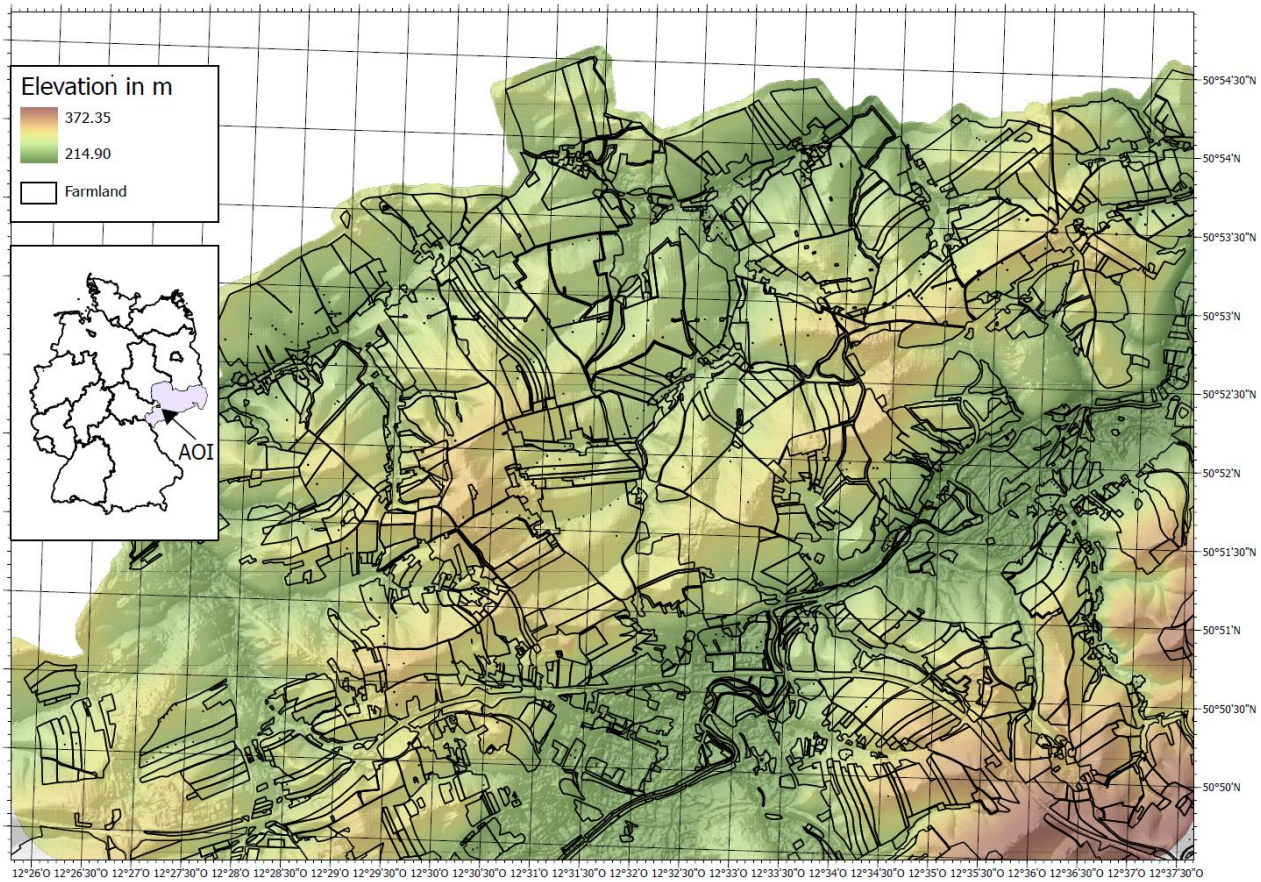

Figure 2: Area of Interest (AOI). City of Meerane in the western valley of the UG directly below the Germany overview map. Adjacent to the north is the state of Thuringia.

3 Materials and Methods

3.1 Data

In order to facilitate comprehension, all data were presented in Table 1 prior to the detailed explanations.

Table 1: Data and data sources used in this study.

Number	Dataset	Data source
1	Digital Orthophotos (DOP)	https://www.geodaten.sachsen.de/downloadbereich-dop-4826.html
2	Sentinel-2 Satellite Image	https://scihub.copernicus.eu/
3	Validation data	Digitization from geodata 1 or 2
4	Agricultural field data (IACS)	Ministry of Agriculture (Saxon State Ministry for Energy, Climate Protection, Environment and Agriculture)

3.1.1 Digital Orthophotos (DOP)

With a ground resolution of 20 cm per pixel, 3-channel RGB aerial photographs are provided free of charge by the Saxon State Survey (https://www.geodaten.sachsen.de/downloadbereich-dop-4826.html (accessed on 02.05.2023). Each downloadable tile has an edge length of 2 x 2 km. The images used

in this study (Table 2) date back to the spring survey of 2021 and represent the months of April and May (data state May 2023).

Table 2: DOPs used in this study from southwest to northeast.

Image Number (Acquisition date)	Image Number (Acquisition date)
33320_5634 (26.04.2021)	33326_5634 (26.04.2021)
33320_5636 (26.04.2021)	33326_5636 (26.04.2021)
33320_5638 (26.04.2021)	33326_5638 (26.04.2021)
33322_5634 (26.04.2021)	33326_5640 (26.04.2021)
33322_5636 (26.04.2021)	33328_5634 (26.04.2021 & 09.05.2021)
33322_5638 (26.04.2021)	33328_5636 (26.04.2021 & 09.05.2021)
33322_5640 (26.04.2021)	33328_5638 (26.04.2021 & 09.05.2021)
33324_5634 (26.04.2021)	33328_5640 (26.04.2021 & 09.05.2021)
33324_5636 (26.04.2021)	33330_5634 (09.05.2021)
33324_5638 (26.04.2021)	33330_5636 (09.05.2021)
33324_5640 (26.04.2021)	33330_5638 (09.05.2021)
	33330_5640 (09.05.2021)

3.1.2 Sentinel-2 Satellite Image

Multispectral images of the satellite Sentinel-2 (S-2) ESA Copernicus program were used as satellite image source. The maximum ground resolution is 10 x 10 m. A pre-processed image at level 2A (https://scihub.copernicus.eu/ (accessed on 26.04.2023) was obtained. The cloud-free Sentinel-2 image from 15.06.2022: S2B_MSIL2A_20220615T101559_N0400_R065_T33UUS_ 20220615T132635 was. For the development of the methodological procedure, the different recording times of DOP and Sentinel-2 are considered uncritical for the further procedure.

3.1.3 Validation data

Validation data were manually digitalized based on the DOP and Sentinel-2 image (Figure 3). To digitize the management direction of a field from the DOP, polylines were created along the lanes visible in the imagery. A total of 1.356 polylines were digitized for the DOPs. For the validation, data for 519 fields with a total of 5.374 ha were mapped in the study area, of which 390 ha were grassland. A similar procedure was used to generate the validation data for the S-2 surveys. However, no lanes could be digitized from S-2 images, as they are not recognizable due to the spatial resolution (Figure 1 (b), Figure 3 (b)). Instead, the row structures of the crops visible in the satellite image were post-digitized with lines. For the validation of the Sentinel-2 image, 712 lines were recorded. The validation lines correspond to 219 fields with an area of 4.008 ha, 18 ha of which were grassland. It should be noted that the turning areas of the

agricultural machines accompanying the edge of the field should be excluded for such an observation.

a) DOP b) Sentinel-2

Figure 3: Digitizing cultivation direction (shown as red lines) in (a) DOP along detectable lanes and in (b) Sentinel-2 image of line structures in fields.

3.1.4 Agricultural field data (IACS)

As part of the EU's Common Agricultural Policy, farmers who apply for agricultural subsidies report their areas as geodata to the relevant authorities, including information on the crops grown. These data are subject to strict data protection regulations and are not freely available, since the protection of trade secrets outweighs the public interest. However, the data are available for this study. The entity responsible for the management of the data in question is the Ministry of Agriculture (Saxon State Ministry for Energy, Climate Protection, Environment and Agriculture).

3.2 Method

The general procedure of the investigation can be seen in Figure 4. Analogously, a validation data collection was also carried out for both processing methods (DOP and S-2). The results were then compared with each other. For DOP, the tillage direction will be derived from the tractor tracks, since these are not spatially resolved to the extent that individual row structures on fields can be identified (Hassanein et al. 2019). For Sentinel-2 images, however, row structures are used that are already visually recognizable in the image and are based on the working width and driving direction of the machines used (Sicre et al. 2014).

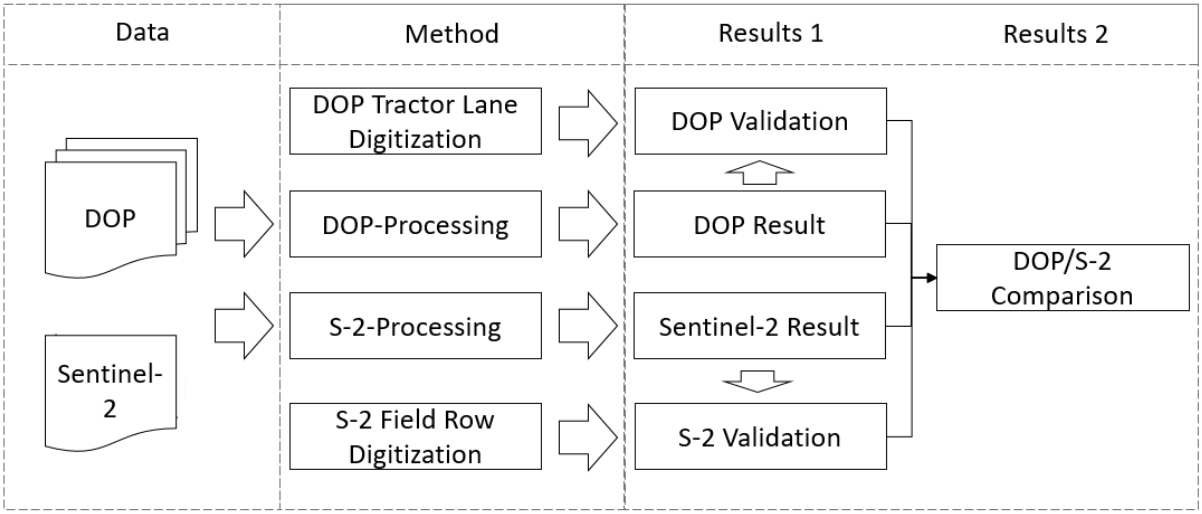

Figure 4: Main working flow of the study.

3.2.1 Digital Orthophotos processing method

The aim of the processing is to extract the tractor tracks from the raster DOPs in such a way that they are available as vector lines and can be used as input data for the ArcGIS Pro tool "Linear Directional Mean" (LDM). The processing took place with ArcGIS Pro as well as with QGIS. The entire process chain for the evaluation of the DOPs can be seen in Figure 5.

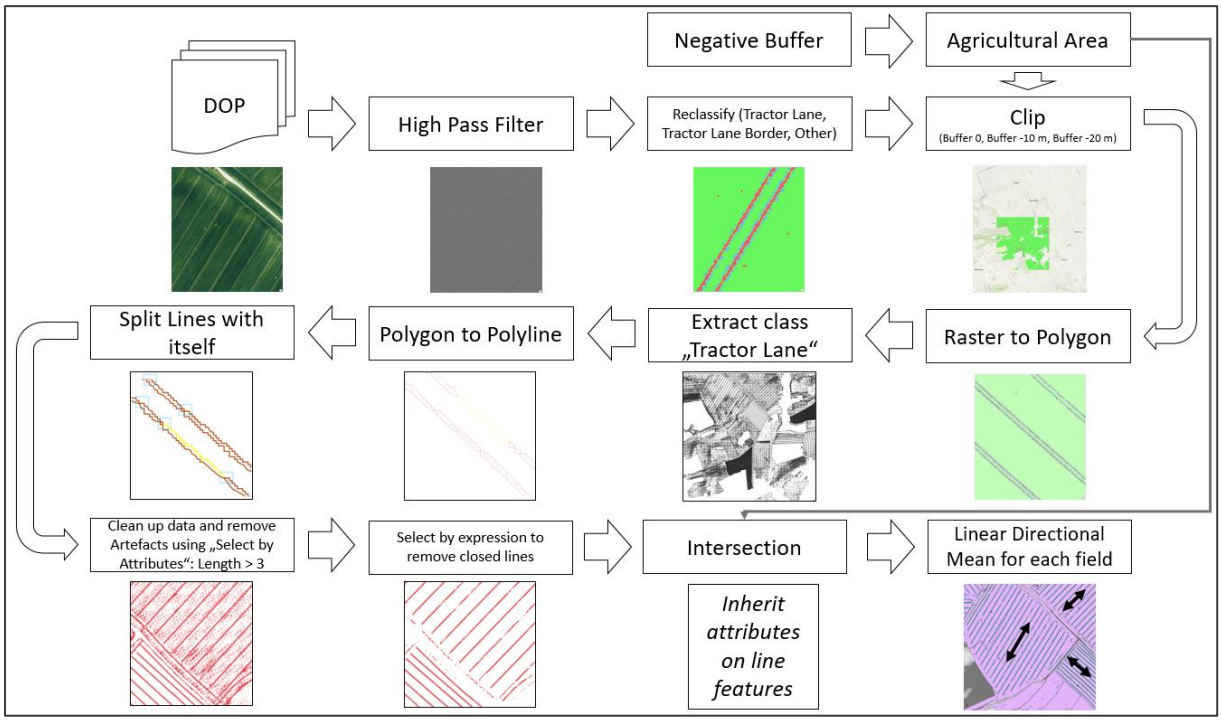

Figure 5: Procedure DOP analysis in GIS processing.

In batch processing, a 3x3 high-pass filter was applied to the 3-channel RGB DOP to highlight edges in a raster layer, emphasizing lane edges while maintaining homogeneous vegetation. The filtering created a transition area between tractor paths

and vegetation, resulting in quasi-unique raster cell values. To extract homogeneous lanes, values were reclassified into three areas: the lane (values up to >=60), the edge region (values <=80), and field vegetation (values -80 to +60). The filtered raster was trimmed to match impact data shapes, reducing data for raster-to-vector transformation. With only three classes, vectorizing became easier. The "lane" class vectors, larger than 0.1 m², were converted into closed polylines and split using QGIS's "Split Lines" tool. Lines not adjacent to others were removed using a QGIS query, and additional lines at DOP edges were also removed. Intersecting with field data, the remaining lines inherited crop attributes. Various negative buffer sizes (0, -10 m, -20 m) were tested at this point in order to determine the influence of the field boundary and turnaround zones. The Linear Directional Mean (LDM) tool calculated the compass orientation of lines within field boundaries, resulting in a compass angle for each field. This angle describes the cultivation direction, comparable to validation compass angles. The LDM-tool only uses the start and end points of a line for this.

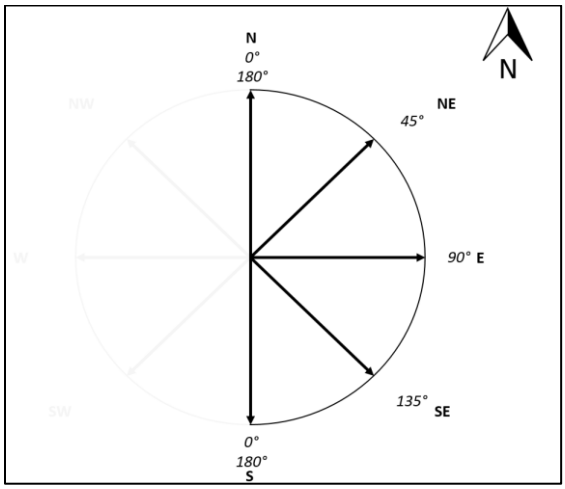

Figure 6: The result of the LDM consists in an indication of the angle of orientation of a line by means of a compass, e.g. a line oriented from NW to SE received the value 135.

3.2.2 Digital Orthophotos ground truth data creation

For the validation of the DOPs (Figure 7), polylines were manually digitized from orthophotos using a GIS system. Tractor tracks were clearly marked with start and end points, recording at least three lines per field. The distinctive characteristics of tractor tracks in agricultural fields allow for their reliable digitization. This comprehensive dataset provided a robust foundation for the "Linear Directional Mean (LDM)" calculation, thereby minimizing mapping errors. Polylines were digitized for all visible areas (both arable land and grassland), excluding turning zones to prevent skewed results. Prior to employing the LDM tool, DOP lines were intersected with 2021 field

data to accurately assign lines to their respective fields and crop types. The LDM tool then calculated the mean compass angle for each field.

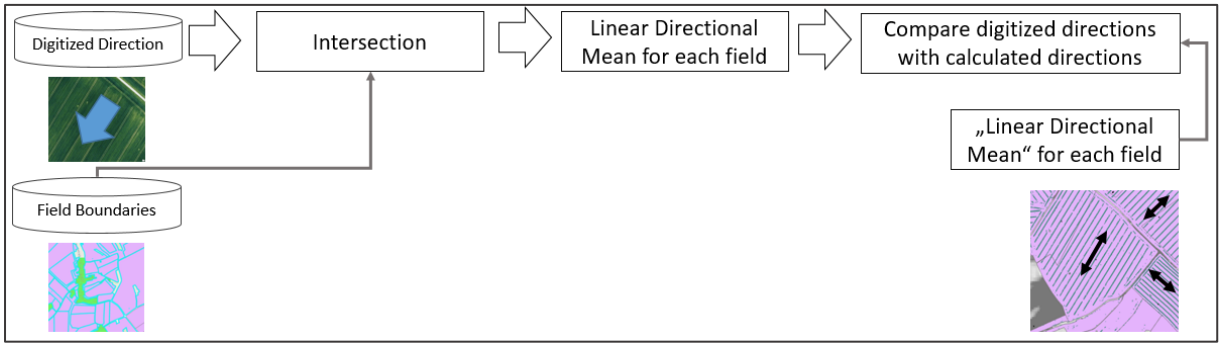

Figure 7: DOP and Sentinel-2-Validation data creation procedure.

3.2.3 Sentinel-2 processing method

The aim of the processing is to extract the row structures of the agricultural crops from the raster Sentinel-2 image in such a way that these were available as vector lines to be used as input data set for the ArcGIS Pro tool "Linear Directional Mean" (LDM). The processing took place with ArcGIS Pro as well as with QGIS. The entire process chain for the evaluation of the Sentinel-2 image can be seen in Figure 8.

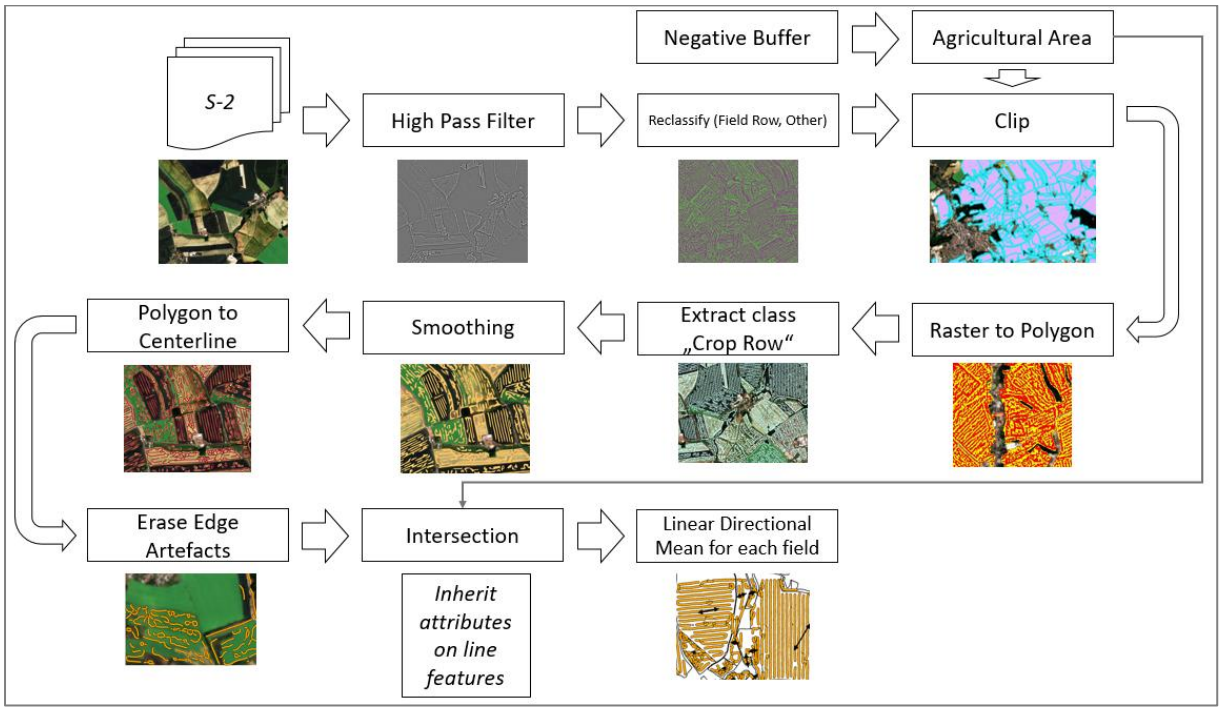

Figure 8: Sentinel-2 analysis in GIS processing workflow.

The initial steps are similar to the DOP evaluation, but with modified parameters. After applying a 3x3 high-pass filter, only two classes are formed. In this case, Sentinel-2 RGB images are used for filtering due to their clear line structure visibility. Other Sentinel-2 band combinations may be useful depending on vegetation conditions or soil moisture. However, images based on vegetation indices are not suitable, as the

vegetation signal in June is too saturated, obscuring line structures. Both filter classes effectively map the crop rows. Histogram analysis of the filtered image revealed that dividing the normal distribution at zero emphasizes the row structure, with class 1 > 0 and class 2 < 0 (Figure 9).

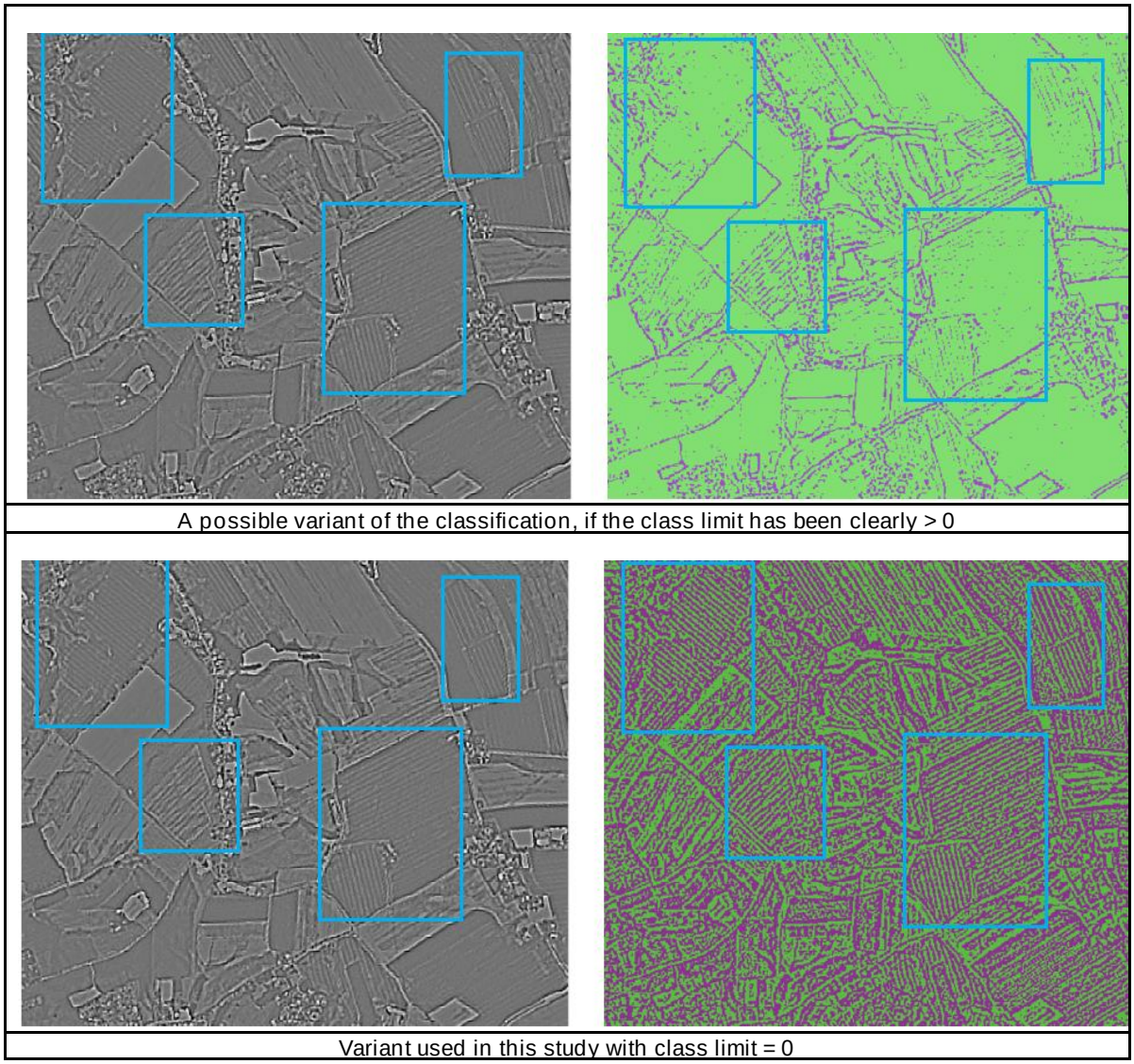

Figure 9: Detail on S-2-Reclassification process: The row structure still clearly visible in the high-pass filter image (the left image in each case) could be shown more or less clearly depending on the choice of class boundaries. In this study, the clearly visible variant was chosen, in which potentially both classes can be used to represent the management direction.

Due to the pixel size, large contiguous areas of the same classification were created and initially delimited by intersecting with field boundaries. Raster data was converted into vector polygons, and the class shown in green in Figure 9 (bottom right) was selected for its accurate line management in the inner field area. Polygons larger than 1,000 m² were chosen based on visual interpretation by the method developer. The polygons were then smoothed using the PAEK (Polynomial Approximation with Exponential Kernel) option with a 100 m smoothing tolerance. Using the "Polygon

Centerline" tool in ArcGIS Pro, the inner lines of the remaining polygons were determined. Edge lines of the Sentinel-2 image border were cut away by inward-buffered (-10 m) AOI boundaries. These inward lines were intersected with 2022 field data to transfer the attribute table to the lines. The Linear Directional Mean (LDM) tool calculated the mean compass angle for each field grouped by field ID.

3.2.4 Sentinel-2 ground truth data creation

To establish validation data, akin to the DOP procedure (Figure 7), Sentinel-2 imagery was used, with polylines digitized using QGIS. These polylines, marking visible row structures, provided a robust foundation for the Linear Directional Mean (LDM) process tool, reducing the need for single or paired line averages and mitigating mapping errors. Compared to DOP, fewer validation lines were recorded due to spatial resolution constraints, limiting mapping options (Figure 3). Only visible line structures were digitized, omitting turning zones as they do not contribute to main management direction determination and could skew results. Before LDM tool application, S-2 lines were intersected with 2022 field data to match lines accurately to field and crop type. Validation involved tabulating and comparing LDM compass directions with S-2 compass directions from the Method chapter. Deviations for individual crop types were systematically analyzed, guiding exclusion decisions for crops with challenging direction detection. The impact of excluding specific crop types on validation was recalculated.

The digitization of the validation data was over Sentinel-2 imagery is subject to more uncertainties, as spatial resolution has been the biggest obstacle here. A deviation of one or two pixels can mean between 5° and 7° degrees, so a higher tolerance level for deviations (e.g. 20°, Table 5) is advised when comparing validation and result. The discrepancies in the digitization process were attributable to two primary factors: the magnitude of the deviation from the actual direction of movement (pixel width) and the intensity of this deviation, which is influenced by the length of the digitized line. By extending the lines to their maximum length, it was possible to minimize the impact of this error.

3.2.5 Validation and statistical analysis

After the above processing steps, compass directions processed from the DOPs were available for each field (3.2.1), as well as the compass direction derived from the digitized ground truth data for each field (3.2.2). Validation was conducted by

comparing the LDM compass directions with those calculated in the previous methodology. The degree of deviation for each crop type was systematically examined, resulting in the exclusion of crop types where detecting the driving direction was particularly challenging. The effect of excluding these crops on the validation was then recalculated.

The same was done for the compass directions processed from the Sentinel-2 satellite image (3.2.3) in combination with the corresponding ground truth data from (3.2.4). The differences between the DOP and S-2 results were not calculated. Instead, similarities were searched for in the discussion (Section 5).

4 Results

4.1 DOP-processing results

Figure 10 clearly shows that the strength of the agreement between validation data and processing data was influenced by the exclusion of unfavorable criteria. Thus, the R^2 for all areas of arable land and grassland within the specified field boundaries reached only 0.379. If, however, the field edge is left out and the turning zone is also reduced, the R^2 increased to 0.526 with a buffer of the field edges of 10 m to the inside, and even to 0.633 with a buffer of -20 m to the inside.

Permanent grassland, on the other hand, is not known to arable land for the formation of tracks or crop rows and also has a protective effect against water erosion, is even essential for water protection in low mountain ranges (Plambeck 2020). Excluding grassland from validation from the outset, maintaining field geometries achieved an R^2 of 0.460. The effects of inward buffering increased this value again, this time to 0.622 at -10 m and 0.703 at -20 m.

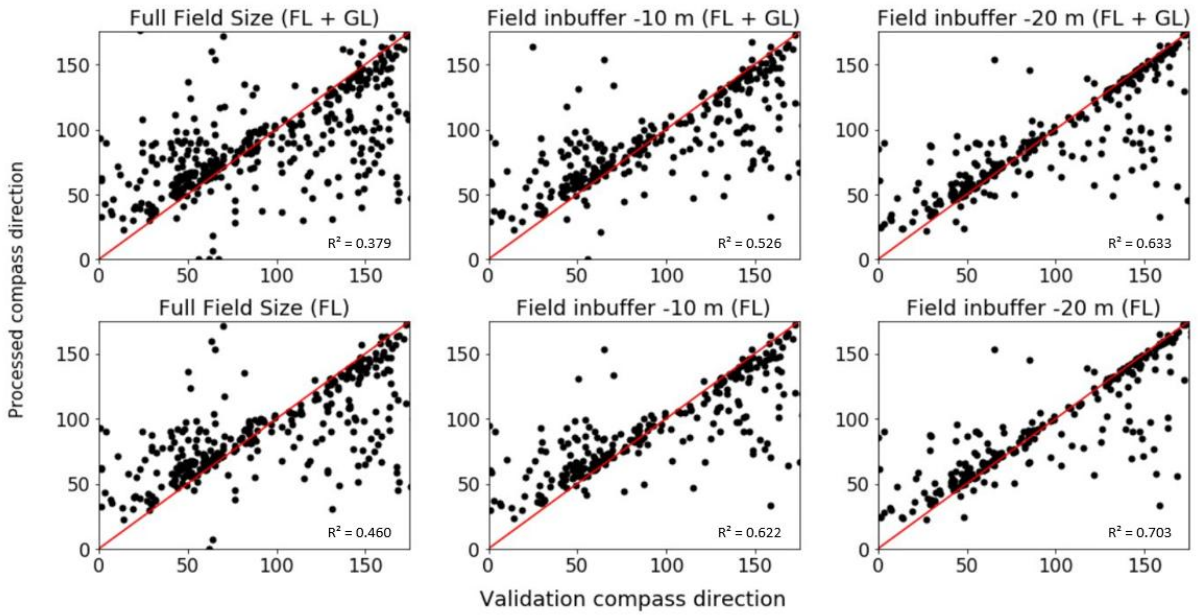

Figure 10: Scatterplots comparing the DOP-validation compass direction to the DOP-processed compass direction for each field which had validation data. Special consideration of edge effects (negative buffer in m) and differentiation between farmland (FL) and grassland (GL).

The diversity of crop types and the Central European cultivation conditions require a critical examination of the results obtained. Table 3 showed that especially for maize and rapeseed a large area sum remains in the range of large deviations between validation and result. The evaluation of the table refers to all areas in farmland and arable land which remained after the buffering of -20 m ($R^2 = 0.633$, Figure 10 top right and table 4 top right). Thus, after excluding the influence of the turning zone, the influence of crop types could be tested. With high percentages of area, permanent grassland (85.4%), maize (72.8%), field grass (66.3%) and winter rapeseed (44.7%) deviate from the validation data by more than 10 compass degrees.

Overall, with a buffer of -20 m, about 68 % of the area remains within an accuracy of up to 10 degrees in the compass angle between validated and processed result. If permanent grassland, field grass, maize and winter rapeseed are excluded at this point, this value increases to around 81 % (Table 3). The influence of the reduced consideration without permanent grassland has already been described earlier in this chapter (Figure 10, bottom row) and Table 4, middle row).

Table 3: Result of the DOP-Analysis: Area of crop-specific deviation by degree in total in hectares. Printed in bold: Particularly high deviants.

Crop (in ha)	Not detected	0 to 5	5 to 10	10 to 20	20 to 30	30 to 50	>50	Share >10
Field Gras (FG)	132.7	34.9	34.2	14.2	46.5	5.3	69.6	**66.3 %**
Grassland (GL)	302.0	7.4	5.0	13.2	22.7	8.4	27.9	**85.4 %**
Maize (M)	322.8	81.4	1.0	102.6	0.0	35.8	82.4	**72.8 %**
Winter Wheat (W)	7.5	1.111.7	167.2	187.0	16.2	62.1	14.9	18.0 %
Winter Rapeseed (R)	6.9	279.4	172.9	177.4	26.4	112.7	49.6	**44.7 %**
Potatoe (P)	123.5	208.1	64.0	41.1	0.0	35.2	16.8	25.5 %

Sugar Beets (SB)	99.0	14.8	0.0	0.0	0.0	0.0	0.0	0.0 %
other Grains (oG)	41.0	494.3	90.3	68.2	23.1	53.0	0.0	19.8 %
other Crops (oC)	169.4	0.0	11.0	0.0	0.0	0.0	2.6	19.1 %
Sum	1.204.8	2.232	545.6	603.7	134.9	312.5	263.8	32.1 %
Sum without GL, FG, M & R	440.4	1828.9	332.5	296.3	39.3	150.3	34.3	19.4 %

In addition to permanent grassland, the other crops mentioned above, arable grass, maize and rapeseed, were excluded from the evaluation for the investigation of the crop type influence on the result studied (Figure 11). With the additional effect of the negative buffer, the highest R^2 in this study were obtained in the DOP evaluation. This was 0.768 (buffer = -10 m) and 0.867 (buffer = -20 m).

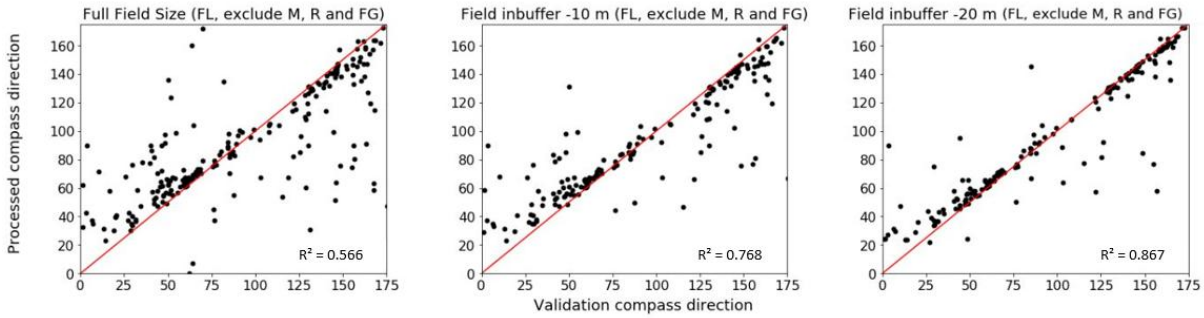

Figure 11: Scatterplots for Farmland (FL) comparing the DOP-validation compass direction to the DOP-processed compass direction for each field which had validation data. Special consideration is paid to edge effects (negative buffer in m) and the selection of particularly suitable crop species (M = Maize, R = Rapeseed, FG = Field Grass) for mapping according to Table 3.

Table 4 summarizes the outcomes of the DOP analysis and highlights the impact of data volume reductions. Implementing reductions not only led to the loss of small areas due to buffering but also significantly reduced the mapped area, particularly with the exclusion of corn and rapeseed. At the stage with the fewest exclusions, 400 fields covering 4.967 hectares were examined, representing all fields for which an LDM could be derived and validation data were available. Validation lines could still be mapped for 519 fields, covering 5.374 hectares out of the 977 fields (5.911 hectares) present in the study area in 2021. Despite including many small fields (median = 1.82 hectares with a mean of 6.1 hectares), 170 fields, accounting for 2.687 hectares or 45.46% of the total possible area, remained in the variant with the highest R^2.

Table 4: Results and properties of the DOP analysis.

Total:	Number of fields in Validation dataset Field Area Sum in ha	519 5.374	Number of fields in AOI Field Area Sum AOI in ha	977 5.911
Land Use Classes		**Buffer = 0 m**	**Buffer = -10 m**	**Buffer = -20 m**
Farmland & Grassland	**Description**	All Agricultural Land, also erosion protecting grassland, turnaround area and field boundaries included	All Agricultural Land, also erosion protecting grassland, turnaround area partly included	All Agricultural Land, also erosion protecting grassland, turnaround area removed

	Number of fields	400	301	276
	Field Area Sum in ha	4.967	4.285	4.086
	R²	0.379	0.526	0.633
Farmland	**Description**	All Agricultural Land, turnaround area and field boundaries included	All Agricultural Land, turnaround area partly included	All Agricultural Land, turnaround area removed
	Number of fields	323	267	255
	Field Area Sum in ha	4.703	4.160	4.002
	R²	0.460	0.622	0.703
Farmland without Maize (M), Rapeseed (R) and Field Grass (FG)	**Description**	Farmland excluding R, M and FG, turnaround area and field boundaries included	Farmland excluding R, M and FG, turnaround area partly included	Farmland excluding R, M and FG, turnaround area removed
	Number of fields	214	177	**170**
	Field Area Sum in ha	3.051	2.718	**2.687**
	R²	0.566	0.783	**0.867**

Figure 12 contrasted for DOP the orientation of the validation lines (a) with those of the processed lines (b). In the result (c) showed in the map image as very heterogeneously distributed.

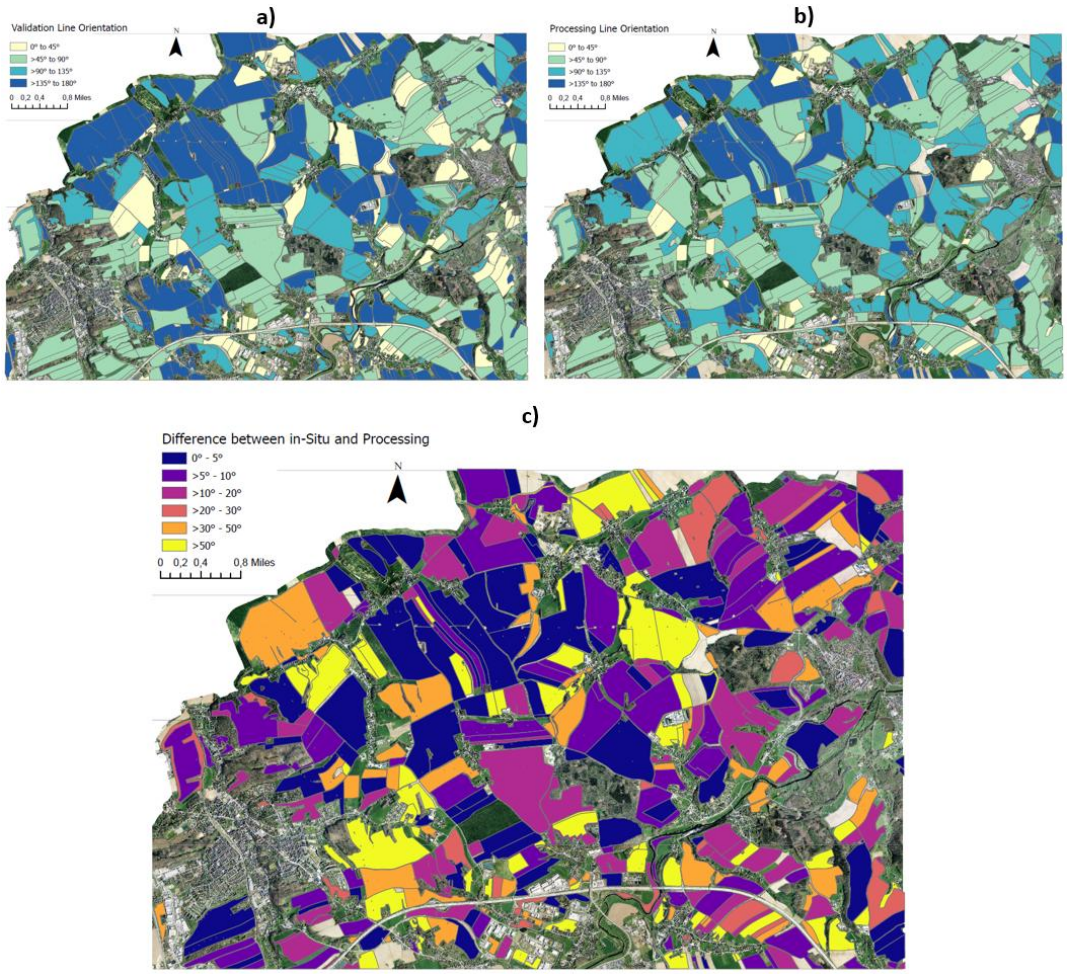

Figure 12: (a) Tillage Direction of the field after evaluation of the DOP validation lines, (b) Tillage Direction of the field after evaluation of the DOP-processing results, (c) Difference between DOP in-situ validation tillage direction and processing tillage direction from well matching results in dark blue to poor matches in yellow.

4.2 Sentinel-2-processing results

Table 5 indicates significant discrepancies between validation and results, particularly for rapeseed and barley, with a large area sum falling within the range of large deviations. The evaluation encompassed all farmland and arable land (R^2 = 0.723, Figure 13 top row left, Table 6 top row left). As observed in the DOP analysis, field grass and permanent grassland were unaffected by this analysis due to a lack of validation data, consistent with previous findings. In contrast, field edge areas in Sentinel-2 did not impact results but showed decreasing matches to the validation dataset with distance (buffer -10 m and buffer -20 m) (Table 5). Winter wheat demonstrated the lowest deviation of 10 compass degrees, while other crop types exhibited deviations of at least 60% in area share, mostly over 80% by more than 10 degrees. Permanent grassland, winter oilseed rape, field grass, and winter rapeseed deviated from validation data by more than 20 compass degrees, with high area percentages. When considering only maize, winter wheat, potatoes, and other crops (mainly legumes) in S-2 records, 73% of plots remained within a maximum deviation of 20°, totaling an area of 1.875 hectares.

Table 5: Result of the Sentinel-2-Analysis: Area of crop-specific deviation by degree in total in hectares. Printed in bold: Particularly high deviants.

Crop (in ha)	Not detected	0 to 5	5 to 10	10 to 20	20 to 30	30 to 50	>50	Share >10	Share >20
Field Gras (FG)	219.31	3.10	27.31	16.99	4.97	223.18	105.77	92.03 %	**87.57 %**
Grassland (GL)	748.05	6.53	0.00	0.00	10.23	1.57	0.00	64.40 %	**64.40 %**
Maize (M)	105.47	1.51	132.38	53.51	47.89	86.10	0.00	58.34 %	41.69 %
Winter Wheat (W)	348.85	613.59	351.57	359.94	161.84	100.89	52.09	41.15 %	19.20 %
Winter Rapeseed (R)	203.84	63.90	29.32	76.15	130.27	147.16	34.71	80.64 %	**64.83 %**
Potatoes (P)	51.41	11.59	64.04	211.10	128.39	35.76	0.00	83.23 %	36.41 %
Sugar Beets (SB)	18.13	19.34	0.00	20.18	43.87	27.31	16.01	84.74 %	**68.81 %**
other Grains (oG)	238.18	51.53	17.98	38.86	163.20	198.20	10.19	85.52 %	**77.42 %**
other Crops (oC) (esp. Legumes (L))	123.79	15.18	4.91	20.61	21.09	46.59	0.00	81.46 %	62.44 %
Sum	2057.04	786.26	627.51	797.35	711.75	866.75	218.76	64.73 %	44.84 %
Sum only M, W, P, other Crops (L)	629.53	641.87	552.90	645.17	359.22	269.33	52.09	52.60 %	27.00 %

Table 6 summarizes the results of the S-2 evaluation and showed the influence of the performed reductions in the amount of data. Buffering had no effect on the number of studied plots, but caused a deterioration of the R^2. From the 997 fields (with 6.065 ha) existing in the study area in 2022, validation lines could still be mapped for 219 fields (with 4.008 ha). In the variant with the highest R^2, 141 fields and thus 1.875 ha or 30.9 % of the possible total area remained for the study. The results of Table 5 showed that

the selection of specific crop types also contributed to maximizing R^2 to 0.833. The relationship between validation lines and processing results can be seen in Figure 13.

Table 6: Results and properties of the Sentinel-2 analysis.

Total:	Number of fields in Validation dataset Field Area Sum in ha	219 4.008	Number of fields in AOI Field Area Sum AOI in ha	997 6.065
Land Use Classes		**Buffer = 0 m**	**Buffer = -10 m**	**Buffer = -20 m**
Farmland & Grassland	**Description**	All Agricultural Land, also erosion protecting grassland, turnaround area and field boundaries included	All Agricultural Land, also erosion protecting grassland, turnaround area partly included	All Agricultural Land, also erosion protecting grassland, turnaround area removed
	Number of fields	219	219	219
	Field Area Sum in ha	4.008	4.008	4.008
	R^2	0.723	0.646	0.651
Farmland	**Description**	All Agricultural Land, turnaround area and field boundaries included	All Agricultural Land, turnaround area partly included	All Agricultural Land, turnaround area removed
	Number of fields	215	215	215
	Field Area Sum in ha	3.990	3.990	3.990
	R^2	0.727	0.646	0.652
Farmland only Wheat (W), Maize (M), Potatoes (P) and Legumes (L)	**Description**	Farmland including mainly W, C, P and L, turnaround area and field boundaries included	Farmland including mainly W, C, P and L, turnaround area partly included	Farmland including mainly W, C, P and L, turnaround area removed
	Number of fields	**141**	141	141
	Field Area Sum in ha	**1.875**	1.875	1.875
	R^2	**0.833**	0.817	0.813

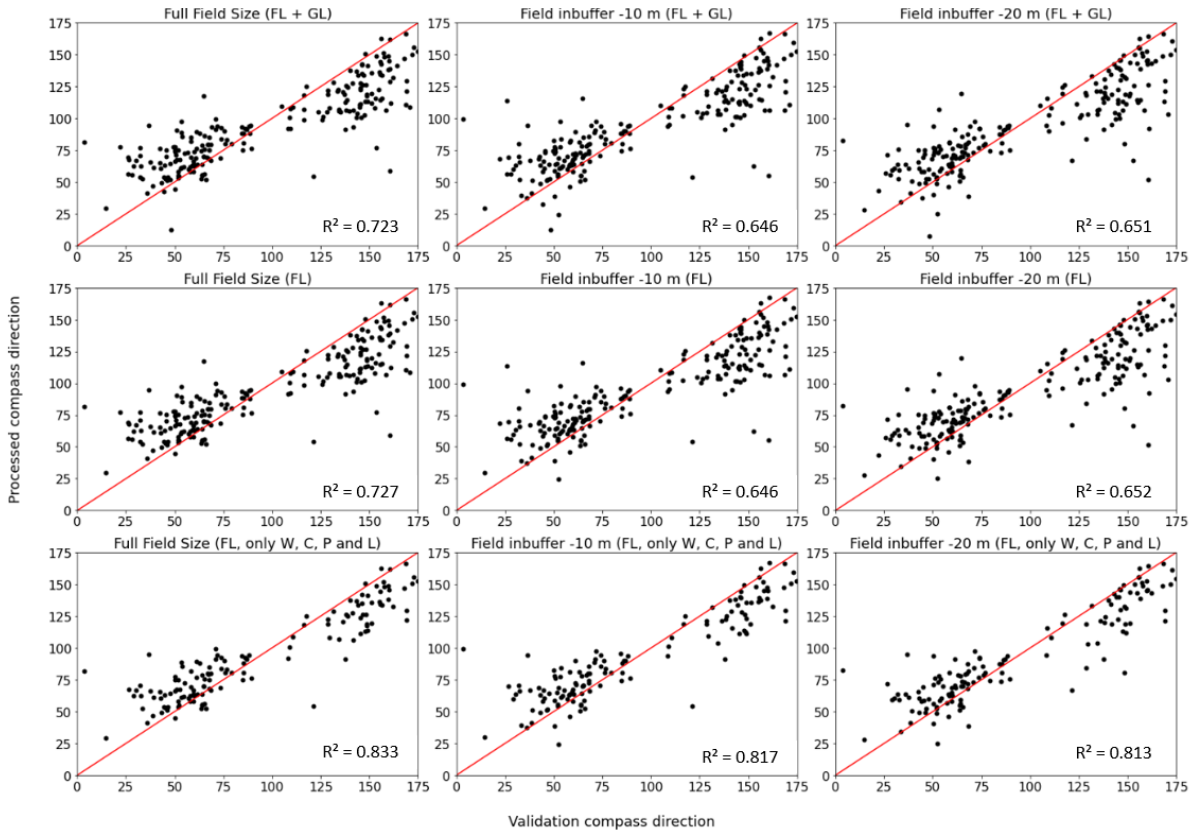

Figure 13: Scatterplots for Farmland (FL) comparing the Sentinel-2-validation compass direction to the Sentinel-2-processed compass direction for each field which had validation data. Special consideration is paid to edge effects (negative buffer in m), the differentiation between farmland (FL) and grassland (GL) and the selection of particularly suitable crop species (W = Wheat, P = Potatoes, C = Corn/Maize and L = Legumes as part of oC) for mapping according to Table 3.

Due to phenology and data source, differences in the quality of the results depending on the crop type became apparent (Table 3 and Table 6). In the Sentinel-2 image from June, for example, maize can already be detected quite well, while this is excluded in an April DOP. Figure 14 contrasted the orientation of the validation lines (a) with those of the processed lines (b) for Sentinel-2 imaging. In the result (c) showed to be very heterogeneously distributed in the map image.

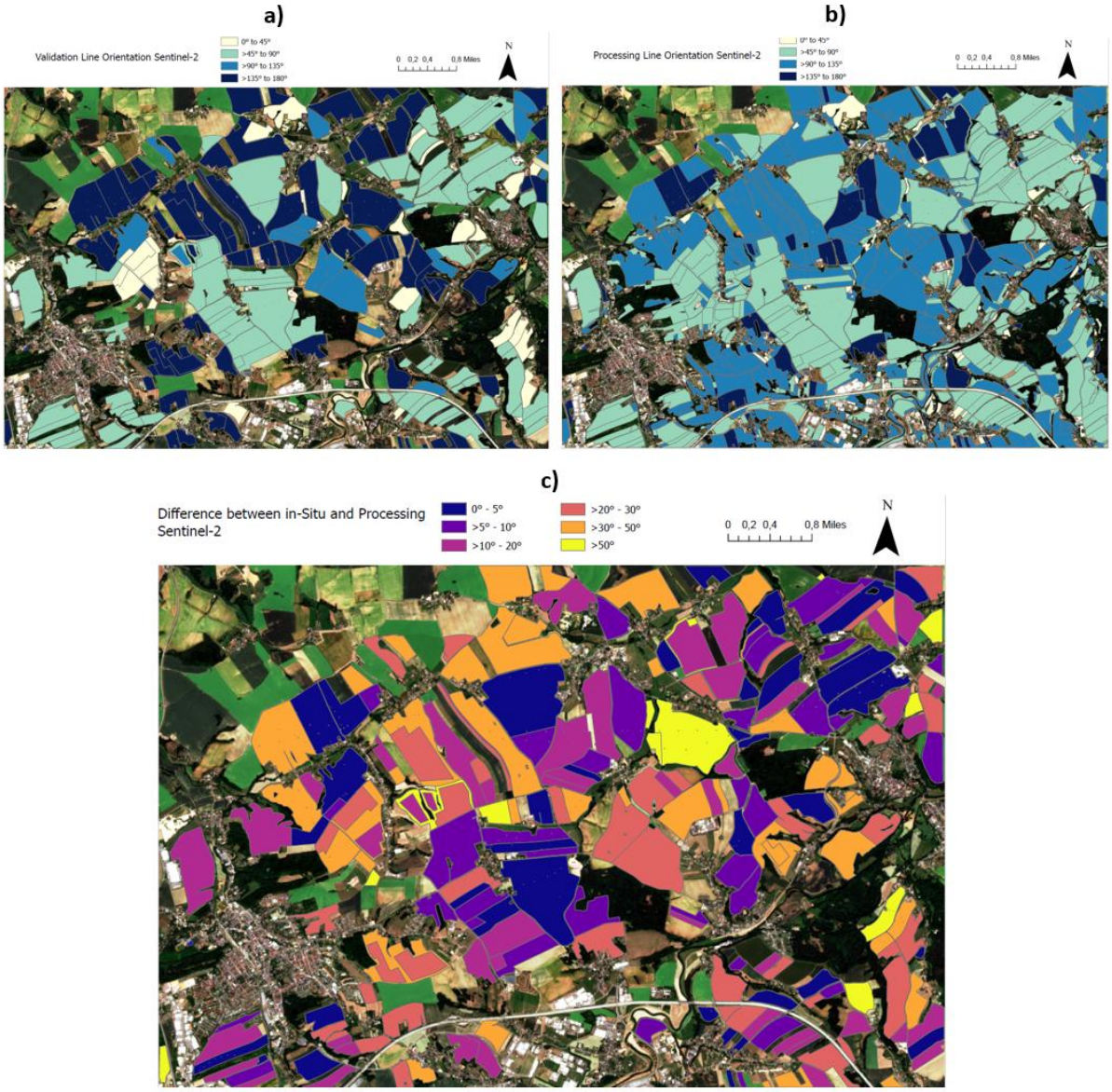

Figure 14: (a) Tillage Direction of the field after evaluation of the Sentinel-2 validation lines, (b) Tillage Direction of the field after evaluation of the Sentinel-2 processing results, (c) Difference between Sentinel-2 in-situ validation tillage directions and processing tillage direction from well matching results in dark blue to poor matches in yellow.

5 Discussion

The results clearly showed that in the DOP application case, buffering into the field and the exclusion of crop species that have not yet grown up phenologically at the time of recording (e.g. maize) or have already grown too densely (e.g. rapeseed) results in a significant increase in the quality of the geodata processing. This reaches up to R^2 = 0.867, in which case 81% of the area then lies within 10 degrees of deviation for validation. Thus, the results of the DOP evaluation are comparable to results from systems comparable in spatial resolution, such as UAV imagery (Fareed & Rehman 2020, Ronchetti et al. 2020, Pang et al. 2020, Bah et al. 2020), although in this study the aspect of area-wide and cross-fruit species analysis at the expense of row

detection is added. Landscape-wide, the results were even comparable to the satellite image analysis of Sicre et al. (2014) , although the single image used here depicted less than 50% of the area in the UG, but as mentioned above there the main cultivation direction could be covered very accurately. Sicre et al. (2014) had also addressed that single surveys, such as the DOP used here, cannot provide area-wide coverage.

Maize plants were still at the very beginning of their season at the time of DOP recording, and therefore tractor tracks could not be formed due to lack of vegetation. These challenges of detecting early stages of plant development have also been noted in other studies (Hassanein et al. 2019). In winter rapeseed, on the other hand, plant development is already so advanced that rows are often already closed to the point that tractor tracks were no longer detectable. Field grass forms a special form of grassland management, as temporary grassland on cropland is assigned to it. Therefore, exclusion of field grass is just as reasonable as exclusion of permanent grassland. Other studies confirm (Goihl 2023) that exclusion of field edges and mixed pixels in Sentinel-2 imagery resulted in significant improvements in the quality of the results because the field interior contained more unaffected information than the field exterior and edge.

A constant reduction of the used results to be taken into account ensure that fewer and fewer areas are accepted in favor of a higher overall agreement. At the end of the examination of the DOP records, the results of less than 50% of the total agricultural area can be determined and used with a high reliability. Fields with excluded crops were no longer available for evaluation, so that within the framework of the agricultural crop rotation and depending on the recording time of the DOP, these areas could only be examined when favorable conditions occur (e.g. cereal cultivation and spring recording of the DOP, Table 4). It became apparent that the steps for DOP must be repeated over several years in order to be able, at least then, to map the croplands over their entire area. Only when this has been done does subsequent indicator development make sense. For the evaluation of DOPs, this means an enormous amount of data and computing power, which must also be estimated several times for the evaluation.

Sicre et al. (2014) achieved in their evaluation for 90% of all surfaces a deviation of maximum 40° while this study for 30% of the total area a deviation of maximum 20° could be determined under the premise of a R^2 of more than 0.83. 66% of all surfaces could be determined at least with a deviation of maximum 30°. Despite the lower spatial

resolution compared to Sicre et al. (2014), significantly more promising accuracies could be calculated overall.

Landscape-wide mapping using DOP or S-2 proved to be a major advantage of the chosen method, which was also cost-effective since free data were used. Unlike the aforementioned studies (Hassanein et al. 2019, Fareed & Rehman 2020, Ronchetti et al. 2020, Pang et al. 2020), the result did not include the individual crop rows accurately surveyed, but only the compass orientation per field. Therefore, as a user of the method, one should not expect to accurately map every crop row from DOP or S-2. As the result proved, this is not even necessary for the chosen use case, since the area-wide analysis is in the foreground and not the precision farming use case.

The evaluation of the Sentinel-2 images yielded an R^2 of 0.833, which represents a similarly high level of accuracy as that observed in the much higher resolution images of the DOPs. However, the variety of crops that can be analyzed is reduced at this point, as the satellite image allows for only a few crops in comparison.

In addition, there is the special case when a field is aligned exactly from north to south. Even small deviations in validation and processing can cause the results of the LDM tool to lie in a high 170 value range, or low range up to e.g. 10. Although the real deviation to each other meant only a few degrees in the compass angle (Figure 6), for the made comparison over a regression is then far over 150 or 160 and can lead accordingly to errors. However, the calculation of the delta (Figure 12c and Figure 14c) between calculation result and validation did not result in such a high deviation in any case (Figures 10, 11, 13).

Sentinel-2 images do not show any advantages by removing edge effects, but it rather causes degradation of the R^2. This should not be surprising since especially smaller fields have only few lines usable for the LDM tool, which are then also eliminated by the removal of the edges. The cascading approach in DOP via individual consideration of edge effects, grassland and cropland, and arable crops had proven successful and can now be used for future application. Therefore, future application to Sentinel-2 imagery should rely primarily on knowledge gained from crop-specific mapping quality. For this, the knowledge base still needs to be extended over several phenological time points. Future research should initially focus on developing an area-wide mosaic of tillage direction using the suitable crops identified in this study via annual Sentinel-2 images. Subsequently, this data set must be integrated with additional information, such as altitude, slope direction, and inclination, to create a comprehensive and

practical indicator. In contrast to DOP, S-2 recordings are temporally high resolution and are available several times over the growing season if conditions are favorable (Sicre et al. 2014).

The limitations of the research are contingent upon the availability of suitable in-situ data, which would have to be obtained at different phenological times and, ideally, with temporally matching remote sensing data. This process is inherently time-consuming, and it could potentially impede the overall progress of the study in years with high cloud cover. The Hough transform method could be employed for the DOPs (Comba et al. 2015, Pérez-Ortiz et al. 2015, Bah et al. 2023) in replacement of manual digitization. Nevertheless, this does not address the issue of collecting in-situ data for the key objective of this study, namely the assessment of S-2 images to ascertain tillage direction. As has been demonstrated, the structures of the tillage direction can be identified with particular efficacy in remote sensing images for specific types of crops. However, there is a further limitation in that information on the cultivated crop type is rarely publicly accessible and available in real time. This information is crucial for an effective and targeted evaluation and must first be obtained. In the absence of this information, the limitation lies in poorer results or a significant amount of effort in post-processing the data. Another challenge arises from the utilization of the "Linear Directional Mean" (LDM) tool. The method employed only utilized the initial and final points along the line to ascertain the direction. However, the lines generated within the workflow are typically composed of numerous points. The result is contingent upon the direction of the initial point; thus, any deviation from this point will result in an erroneous outcome, even if the remaining points are aligned. The use of multiple lines per field and the averaging of results was implemented as a means of counteracting the impact of erroneous outliers. Particularly in the case of automated techniques such as this series of GIS tools, a residual degree of uncertainty persists that cannot be definitively verified through manual inspection and subsequent exclusion based on the extensive number of lines.

Against this background, this study represents a great benefit, since the use of already existing data sources means that no additional aerial flights, such as by UAV, are required. Data in real time, rather than with the aim of creating a data base for subsequent indicator development, is of importance, making this study quite different from previous studies. There is no need for real-time field row detection, for example, to target weeds between rows. This information can then be set to develop indicators

related to relief, slope, shape form (Foski 2019), and runoff trajectories to expand the agricultural water conservation information base. The question must be answered how in the current state the management directions are adjusted to the contour lines and which influencing variables must be considered. A future indicator must match the calculated tillage direction with the current conditions of the runoff paths on site (Voß et al. 2023).

6 Conclusion

By developing and applying a GIS method for evaluating Digital Orthopoto and a Sentinel-2 imagery, this study has succeeded in establishing important bases for determining the management direction of agricultural land for methods based on it. DOP and S-2 imagery achieve a comparable area and accuracy potential. The future application of the considered methods to multitemporal input data has the potential to provide an area-wide source of information if the phenology of arable crops is included. The results themselves can be put to value in the future as a regional indicator to provide information on the management direction of cropland in erosion-prone areas. This overall picture can support environmental, agricultural and nature conservation authorities in their work in the field of water protection and erosion control as a supplementary data source. The indicator allows targeting of stakeholder activities by location, allowing precise implementation of countermeasures in susceptible areas.
However, this will be the content of a forthcoming research and the conclusions reached can only be meaningfully put into value by using additional data sources (elevation models, land cover and land use information, erosion-specific information on arable crops, field shape form). This study presents an important basis for this, especially from the point of view of the use of free data.

Supplementary Materials

No additional material will be provided.

Funding

This research received no external funding.

References

Bah, M.D., Hafiane A., & Canals R. CRowNet (2020). Deep Network for Crop Row Detection in UAV Images. *IEEE Access*, 8, 5189-5200. https://doi.org/10.1109/ACCESS.2019.2960873.

Bah, M.D., Hafiane A., & Canals, R. (2023). Hierarchical graph representation for unsupervised crop row detection in images. *Expert Systems with Applications*, 216. https://doi.org/10.1016/j.eswa.2022.119478.

Brauening A., Schmidt W., & Tenholtern R. (2023). Begrünung von erosionsgefährdeten Abflussbahnen (Greening of erosion-prone runoff paths), 2015. https://publikationen.sachsen.de/bdb/artikel/23739 (accessed on 05.06.2023).

Campos J., García-Ruíz F., & Gil E. (2021). Assessment of Vineyard Canopy Characteristics from Vigour Maps Obtained Using UAV and Satellite Imagery. *Sensors*, 21:2363. https://doi.org/10.3390/s21072363.

Comba L., Gay P., Primicerio J., & Aimonino, D.R. (2015). Vineyard detection from unmanned aerial systems images. *Comput. Electron. Agric*., 114. https://doi.org/10.1016/j.compag.2015.03.011.

Fareed N., & Rehman K. (2020). Integration of Remote Sensing and GIS to Extract Plantation Rows from a Drone-Based Image Point Cloud Digital Surface Model. *ISPRS Int. J. Geo-Inf*., 9:151. https://doi.org/10.3390/ijgi9030151.

Foski M. (2019). Using the parcel shape index to determine arable land division types. *Acta geographica Slovenica*, 59:83. https://doi.org/10.3986/AGS.4574.

Goihl S. (2023). Mapping overwintering grain stubbles using machine-learning methods and image compositions for common agriculture policy-control and water framework directive connected activities. *J. Appl. Rem. Sens*., 17, 014515. https://doi.org/10.1117/1.JRS.17.014515.

Hassanein M., Khedr M., El-Sheimy N. (2019). Crop row detection procedure using low-cost UAV Imagery System. The International Archives of the Photogrammetry, Remote Sensing and Spatial Information Sciences, Volume XLII-2/W13, *2019 ISPRS Geospatial Week 2019*, Enschede, The Netherlands. https://doi.org/10.5194/isprs-archives-XLII-2-W13-349-2019 (10–14 June 2019).

Jia L., Zhao W., Zhai R., An Y., & Pereira P. (2020). Quantifying the effects of contour tillage in controlling water erosion in China: A meta-analysis, *CATENA*, 195. https://doi.org/10.1016/j.catena.2020.104829.

LfULG - Saxon State Office for Environment, Agriculture and Geology (2023). Ostthüringisches Lösshügelland (East Thuringian Loess Hill Country). Available online: https://www.natur.sachsen.de/download/33_Ostthueringisches_Loesshuegelland.pdf (accessed on 24.05.2023)

Lima F., Blanco-Sepúlveda, R., Gómez-Moreno M.L., Dorado J., & Peña J.M. (2021). Mapping tillage direction and contour farming by object-based analysis of UAV images. *Computers and Electronics in Agriculture*, 187:106281. https://doi.org/10.1016/j.compag.2021.106281.

Maetens W., Poesen J., & Vanmaercke M. (2012). How effective are soil conservation techniques in reducing plot runoff and soil loss in Europe and the Mediterranean? *Earth-Science Reviews*, 115. https://doi.org/10.1016/j.earscirev.2012.08.003.

Pang Y., Shi Y., Gao S., Jiang F., Veeranampalayam-Sivakumar A.-N., Thompson L., Luck, J., & Liu, C. (2020). Improved crop row detection with deep neural network for early-season maize stand count in UAV imagery. *Computers and Electronics in Agriculture*, 178:105766. https://doi.org/10.1016/j.compag.2020.105766.

Peña-Barragána J.M., Kelly M., de-Castro A.I., & López-Granados F. (2012). Object-based approach for crop row characterization in UAV images for site-specific weed management. *Proceedings of the 4th GEOBIA*, May 7-9, Rio de Janeiro - Brazil.

Pérez-Ortiz M., Peña J.M., Gutiérrez P.A., Torres-Sánchez J., Hervás-Martínez C., & López-Granados F. (2015). A Weed Monitoring System Using Uav-Imagery and the Hough Transform. *Actas de La Sociedad Española de Malherbologia*, 1.

Plambeck N.O. (2020). Reassessment of the potential risk of soil erosion by water on agricultural land in Germany: Setting the stage for site-appropriate decision-making in soil and water resources management. *Ecological Indicators*, 118. https://doi.org/10.1016/j.ecolind.2020.106732.

Rocha B.M., Ueslei da Fonseca A., Pedrini H., & Soares F. (2022). Automatic detection and evaluation of sugarcane planting rows in aerial images. *Information Processing in Agriculture*. https://doi.org/10.1016/j.inpa.2022.04.003.

Ronchetti G., Mayer A., Facchi A., Ortuani B., & Sona G. (2020). Crop Row Detection through UAV Surveys to Optimize On-Farm Irrigation Management. *Remote. Sens.*, 12:1967. https://doi.org/10.3390/rs12121967.

Santos L.C., Aguiar A.S., Santos F.N., Valente A., & Petry M. (2020). Occupancy Grid and Topological Maps Extraction from Satellite Images for Path Planning in Agricultural Robots. *Robotics*, 9:77, https://doi.org/10.3390/robotics9040077.

Sepuru T.K., & Dube T. (2018). An appraisal on the progress of remote sensing applications in soil erosion mapping and monitoring, *Remote Sensing Applications: Society and Environment*, 1-9. https://doi.org/10.1016/j.rsase.2017.10.005.

Sicre C.M., Baup F., & Fieuzal R. (2014). Determination of the crop row orientations from Formosat-2 multi-temporal and panchromatic images, *ISPRS Journal of Photogrammetry and Remote Sensing*, 94. https://doi.org/10.1016/j.isprsjprs.2014.04.021.

Voß J., Schwan A., Heyne W., & Müller N. (2010). Erosionsschutz in reliefbedingten Abflussbahnen. Entwicklung von Umsetzungsstrategien und -planungen für eine natur- und bodenschutz-gerechte dauerhafte Begrünung von besonders erosionswirksamen Abflussbahnen (Erosion protection in relief-related runoff paths. Development of implementation strategies and planning for permanent greening of particularly erosive runoff paths in accordance with nature and soil conservation requirements). Schriftenreihe des LfULG, 13. https://publikationen.sachsen.de/bdb/artikel/11386 (accessed on 05.06.2023).

Wuepper D., Borrelli P., & Finger R. (2020). Countries and the global rate of soil erosion. *Nat Sustain*, 3. https://doi.org/10.1038/s41893-019-0438-4.